PARAMETRIC APPROACH TO LIFE CYCLE ASSESSMENT

A Dissertation
Presented to
The Academic Faculty

by

Dong-Yeon Lee

In Partial Fulfillment
of the Requirements for the Degree
Doctor of Philosophy in the
School of Civil and Environmental Engineering

Georgia Institute of Technology
May 2016

PARAMETRIC APPROACH TO LIFE CYCLE ASSESSMENT

Approved by:

Dr. Valerie M. Thomas, Advisor
School of Industrial and Systems Engineering
School of Public Policy
School of Civil and Environmental Engineering
Georgia Institute of Technology

Dr. Matthew J. Realff
School of Chemical and Biomolecular Engineering
School of Industrial and Systems Engineering
Georgia Institute of Technology

Dr. Patricia L. Mokhtarian
School of Civil and Environmental Engineering
Georgia Institute of Technology

Dr. Patrick S. McCarthy
School of Economics
Georgia Institute of Technology

Dr. John C. Crittenden
School of Civil and Environmental Engineering
Georgia Institute of Technology

Date Approved: March 30, 2016

ACKNOWLEDGEMENTS

I thank my academic advisor Dr. Valerie M. Thomas for her thoughtful guidance and support throughout my study at Georgia Tech over the last six years. She is a great mentor, researcher, and role model. Her meticulousness, humor, and intelligence-character balance have always inspired me and helped me become a better researcher and person. Numerous other people have also directly and indirectly contributed to this dissertation research as well as my academic endeavor. At Georgia Tech, Dr. Marilyn A. Brown has helped me develop and finish my Master's thesis research which laid a foundation for this dissertation. Dr. Patrick S. McCarthy has also provided me with helpful suggestions and kind encouragements during my research design and implementation. I'm grateful that I've been able to get influenced by Dr. John C. Crittenden, Dr. Matthew J. Realff, and Dr. Patricia Mokhtarian who all have given me excellent directions for the preparation of this dissertation. Each committee member has also helped me identify the core value of my research. In addition to the committee members, I would like to thank my former and current colleagues, including Nathaniel Tindall, Wenman Liu, Rafael Castillo, Dong Gu Choi, James Belanger, Jenna McGrath, Amy Musselman, Caroline Golin, and Paul Kerl for their constructive comments and helpful discussions for my research in general and more specifically for my presentations and manuscripts. Outside of Georgia Tech, I thank Jeff Gonder, Adam Duran, and Robert Prohaska of the National Renewable Energy Laboratory (NREL); Dominik A. Karbowski of the Argonne National Laboratory (ANL); Stan Hadley of the Oak Ridge National

Laboratory (ORNL); and Arvind Thiruvengadam Padmavathy of West Virginia University for their data provision and thoughtful suggestions.

TABLE OF CONTENTS

LIST OF TABLES

LIST OF FIGURES

SUMMARY

Life cycle assessment is a method to evaluate economic and environmental benefits and tradeoffs of technologies, human activities, and systems. Data gaps, variability, uncertainty, and weak generalizability are among the continuing challenges in life cycle assessment. As a way of resolving these issues, a parametric life cycle assessment framework is proposed and demonstrated, using case studies of vehicle electrification and decentralized power generation for buildings. The parametric life cycle assessment involves investigating governing equations; identifying overall relationships between input and output variables; evaluating characteristics and typology of input and output variables; assessing relative importance and contribution of individual input parameters; and developing a parametric form of life cycle assessment models.

For medium- and heavy-duty vehicles electrification, the results from the parametric life cycle assessment indicate that electric vehicles provide positive social benefits for niche applications or locations, regardless of the variations and uncertainties in input conditions including future electric grid evolution and fuel prices changes. Beyond the niche applications or locations, however, electrifying medium- and heavy-duty vehicles is not expected to provide positive net social benefits in the near future, in comparison with conventional technologies powered by petroleum, biofuels, or natural gas. Vehicle operation strategy modifications or a moderate level of electrification such as micro-hybrid technology can provide more immediate benefits.

Using the same parametric LCA approach, life cycle tradeoffs of decentralized power generation technologies for buildings are systematically evaluated, including

natural gas-based hydrogen fuel cell and microturbine technologies. Combined cooling, heating, and power provides numerous benefits including more efficient and stable electricity provision compared to conventional building energy systems. From the life cycle perspective, cogeneration or trigeneration technologies, in particular, microturbines help reduce air emissions and water consumption but at the expense of energy efficiency. Although fuel cell and microturbine technologies tend to move air emissions sources from less-populated locations to population centers, overall air pollution impacts across the U.S. are lower than for conventional systems. Depending on the building types, overall social benefits of these alternative and distributed power production technologies can vary. In general, achieving electric grid independence and improving resilience against power outage requires up to 50% higher valuation of reliable power production.

CHAPTER 1

INTRODUCTION

A parametric life cycle assessment (LCA) approach begins with the investigation of governing equations – Process 1 in Figure 1.1. If analytic (or mathematical) solutions can be found by solving the governing equations, product use phase and life cycle results can be formulated based on those analytic solutions. If not, simulation can be utilized alternatively, which may require data collection beforehand to account for a range of product operating conditions – Process 2 in Figure 1.1. Governing equations also provide a foundation to develop types of variables. Depending on the types, different treatment strategies can be developed to deal with different types of variables. Governing equations also help characterize key variables so that they can be used as explanatory or predictive independent variables afterwards. The basic requirement of satisfactory variable characterization or treatment strategy development is the convergence or dependency of the use phase or life cycle results on the input parameters. In other words, there must be a distinct relationship between the output results and input variables. If not, re-evaluation of governing equations and the variable development process must be repeated until a pattern (of output results) emerges in the identified independent variables. Once such converging relationship is found – Process 3 in Figure 1.1, statistical analysis including linear regression can be utilized, Process 4 in Figure 1.1, to systematically characterize the changing behavior of use phase or life cycle results as functions of input variables. Also, depending on the treatment strategy of variables, correction factors could be included in the statistical model. As a result, a reduced form of parametric LCA model in

functional forms will be achieved – Process 5 in Figure 1.1, which will provide a reasonable level of specificity and carry essential information without having to run complicated simulations or conducting mathematical analysis over and over again.

In the following chapters, I demonstrate the parametric LCA approach with a set of case studies – medium-duty truck electrification (Chapter 2), heavy-duty transit bus electrification (Chapter 3), and combined cooling, heating, and power for buildings (Chapter 4). All case studies follow the same processes illustrated in Figure 1.1.

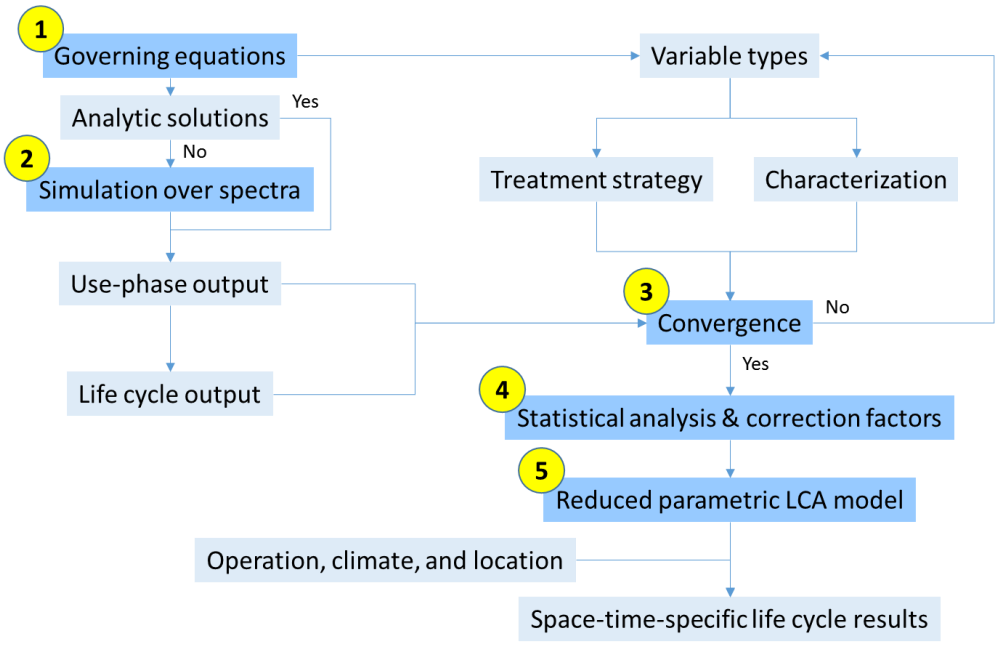

Figure 1.1 Overall Processes for Parametric LCA

CHAPTER 2

MEDIUM-DUTY VEHICLE ELECTRIFICATION

2.1 Chapter Summary

Using a parametric modeling approach, I evaluate economic and environmental life cycle trade-offs of medium-duty electric trucks in comparison with nine non-electric technologies for model year 2015 in the U.S. – conventional internal combustion engine, diesel hybrid electric, and idle reduction technologies with each powered by diesel, biodiesel, or compressed natural gas (CNG). To develop a parametric life cycle assessment model, I modify and integrate the ADVISOR and EPA MOVES models, run vehicle dynamic and emissions simulations, and construct a linear regression-based prediction model using the simulation results. I develop state-by-state hourly marginal electric grid energy consumption, air emissions, and water use factors to assess the impact of electric truck charging load on regional electric grids.

From the overall social life cycle cost standpoint, electric trucks for niche application provide positive net social benefits in many areas of the U.S. However, in the same niche application, idle reduction technology for conventional diesel and biodiesel trucks is also cost-competitive in terms of overall social life cycle cost. For electric trucks to definitely outperform other options in typical operating conditions beyond the niche application, current electric truck capital costs must drop by 30 – 50%; diesel fuel prices must be in the range of 6.5 – 8.1 $/gallon; or carbon emissions reduction must be credited by $300 – $2,000 per metric ton of carbon dioxide. I also find that electric trucks can increase water intensity by 200%.

2.2 Motivation

Today's average U.S. automobiles are about twice as efficient as those in the 1970s (Davis & Diegel 2015). In contrast, average fuel efficiency of current medium-duty trucks weighing 4.5 – 12 metric tons (10,001 – 26,000 pounds) is more or less the same as that of four decades ago (BTS 2015). The new regulations for medium- and heavy-duty vehicles (Federal Register 2015a) will increase fuel efficiency and reduce air emissions in coming years. In terms of overall energy efficiency and reducing environmental impacts of these trucks, alternative medium-duty freight truck technologies such as battery electric (Lee et al. 2013), hybrid-electric (Bachmann et al. 2015), natural gas (Fan et al. 2015), and biodiesel can help.

A number of studies have identified the benefits and limitations of different medium-duty truck (MDT) technologies (Nellums et al. 2003; Delorme and Karbowski 2010; Barnitt 2011; Burton et al. 2013a; Lee et al. 2013; Bachmann et al. 2015). What all these studies indicate is that there are "conditional" trade-offs. For instance, the advantage of the electric-drive technology is maximized in city-type drive cycles (i.e., speed-time profiles or schedules), but the benefit diminishes in high speed driving conditions that are typical for highway or long-haul operations (Lee et al., 2013). On the other hand, what these previous MDT studies are lacking is the prediction capability of life cycle trade-offs varying with input conditions. Whether electric or non-electric MDT life cycle assessment (LCA), most studies rely on average (Fan et al. 2015) or case-specific (Lee et al. 2013; Bachmann et al. 2015) parameters, conditions, and assumptions. It is hard to come by a study that systematically predicts and explains life cycle trade-offs of different MDT technologies with changing input conditions as operationalized variables. Here I develop and propose a parametric LCA for evaluating conditional trade-offs of MDT technologies, focusing on electric trucks.

Our parametric LCA extends conventional LCA and/or previous MDT life cycle studies in that I present LCA results with generic equations, whereas previous life cycle

studies report point estimates, i.e., averages or case-specific results, oftentimes with ranges. Parametric LCA provides four advantages. First, parametric LCA enables systematic prediction of life cycle trade-offs and shows under which conditions electric trucks provide the largest benefits. This can help identify strategic niche applications for electric trucks and assign electric trucks for the most suitable operating conditions (e.g., routes) based on holistic information as to the benefits and trade-offs over a range of operating conditions. Second, parametric LCA reveals to what extent the benefits are robust under numerous conditions and uncertainties. This information can help guide future electric truck technology research, development, and demonstration (RD&D) in the long run. Electric trucks will ultimately have to compete with other truck technologies for general freight transportation operations rather than just for limited or niche applications (e.g., urban delivery). As I sweep through entire input ranges with a parametric LCA approach, I can identify necessary conditions for electric truck benefits to be robust. Third, the parametric approach requires minimal input (e.g., total distance traveled divided by travel time) to evaluate life cycle results and thus alleviates the burden of input and output data availability. Not all truck drivers, fleet operators, or researchers have the capability of collecting, processing, and analyzing individual 1-10 Hz duty cycle (speed-payload-grade-time profile) data and/or running complicated vehicle dynamic and emissions simulations or collecting experimental measurements. Fourth, the parametric LCA explains three things in a predictive manner: How overall energy is consumed – varying with input conditions; why medium-duty (or heavy-duty) electric vehicles show different energy use patterns compared to light-duty electric vehicles; and why this is not the case for non-electric vehicles, that is, almost identical pattern for light-duty and medium-duty vehicles. Explaining “how” (predictive) and “why” (descriptive) as such will eventually help compare and generalize individual MDT life cycle research findings beyond the conditions assumed or tested. Furthermore, compared to previous freight truck LCA studies that focused on carbon footprint (Lee et

al., 2013; Bachmann et al., 2015), I provide a more comprehensive environmental impact assessment (i.e., water and air pollutants emissions) in a parametric manner.

The rationale for a parametric LCA approach is that vehicle energy use and air emissions inherently depend on vehicle dynamics which are a function of drive cycle characteristics (e.g., speed and acceleration), vehicle attributes (e.g., vehicle mass, aerodynamic drag coefficient, etc.), roadway conditions (e.g., road grade), etc. For example, although the exact degree or pattern of the impact can vary with technology, the dependency on drive cycles is universal – all being governed by the laws of physics. That is, most of the time, more severe drive cycles will increase energy consumption and emissions, regardless of vehicle technologies. Numerous studies have shown that vehicle energy use and emissions can be predicted and/or explained with drive cycle characterization parameters. Examples include Watson et al. (1983), Ross (1994), André (2004), Clark et al. (2010), and etc. In other words, once drive cycles are parameterized, vehicle operation performance such as energy consumption and emissions can be represented and predicted as functions of drive cycle parameters. This logic pertains to other input parameters as well. Here I apply this concept to the economic and environmental LCA of medium-duty freight truck technologies, incorporating the following input conditions as predictors: drive cycles, vehicle weight (or payload), road grade, and ambient temperature.

2.3 Life Cycle Assessment Goal and Scope

The goal of my life cycle assessment (LCA) is to compare medium-duty freight truck technologies in terms of cost, energy efficiency, fresh water consumption, and air emissions impacts (i.e., acidification, eutrophication, smog formation, global warming, and monetized human health and ecological damage). As shown in the system boundary diagram in Figure 2.1, my life cycle air emissions inventory includes greenhouse gases (GHGs – CO_2, N_2O, and CH_4), carbon monoxide (CO), ammonia (NH_3), nitrogen oxides (NOx), particulate matter ($PM_{2.5}$ and PM_{10}), sulfur dioxide (SO_2), and volatile organic compounds (VOC). I also account for $PM_{2.5}$ and PM_{10} emissions from tire and brake wear. Once these air emissions are tallied, I assess their midpoint life cycle environmental impacts – climate change, acidification, eutrophication, smog formation, and human health based on TRACI 2.1 (Bare et al. 2002; Bare 2011, 2012) and the 20- and 100-year global warming potential (GWP) from the Fifth Assessment Report (AR5)

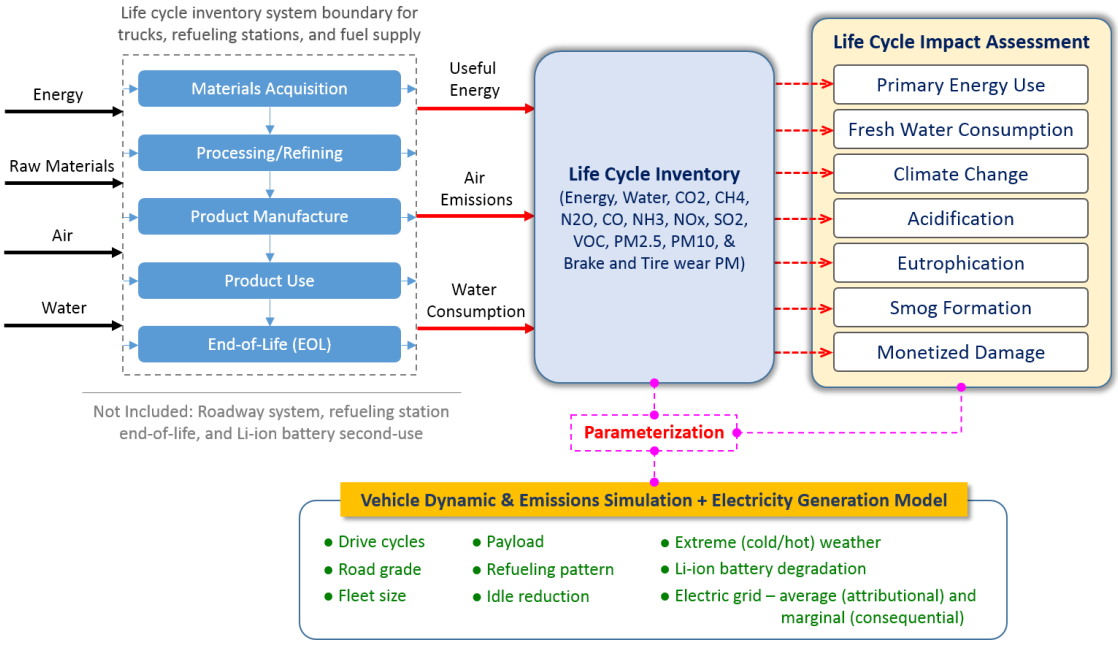

Figure 2.1. Framework and System Boundary Diagram for Medium-Duty Truck Parametric LCA.

of the Intergovernmental Panel on Climate Change (IPCC 2013). As for life cycle water consumption, I present my result in gallons of fresh water used. For endpoint life cycle impact assessment, I utilize APEEP model (Muller 2011) and evaluate monetized air pollutants emissions damage cost combined with social cost of carbon emissions (The White House 2013). The target audience of my LCA includes policy makers, the general public, fleet managers, and LCA researchers. Our study aims to improve understanding of both the promise and limitations of medium-duty truck (MDT) electrification under various operating conditions and in relation to competing truck technologies. The product systems to be compared are 2015 Model Year (MY) medium-duty trucks, specifically, gross vehicle weight rating (GVWR) class 6 (8.8 – 11.8 metric tons or 19,501 – 26,000 lb) goods movement trucks. Table 2.1 summarizes the vehicle specifications. The functional unit is the product of weight of freight moved (payload) and distance traveled (i.e., ton-km). To comply with this definition, whenever I present the results per distance traveled for simplicity, I provide the vehicle weight condition tested so that per-ton-km results can be derived. I compare three different vehicle technologies such as internal combustion engine (ICE), hybrid-electric, and battery electric for four different fuel types such as conventional diesel (or ultra-low sulfur diesel, ULSD), compressed natural gas (CNG), biodiesel (BD), and electricity. Under the Renewable Fuel Standard (RFS), conventional diesel fuel in the U.S. currently contains approximately 3% of biodiesel by volume, and up to 5% of biodiesel blend (or B5) can be called or used as "conventional" diesel without separate biodiesel labeling requirement at the pump. In my analysis, I refer biodiesel to the petroleum diesel blended with 20% of soybean-based biodiesel by fuel volume (or B20). Most of the recent diesel engines and trucks are designed to handle B20, but above that blend level, dedicated biodiesel engine and truck will be needed, which is not included in my analysis.

2.4 Vehicle Production and Refueling Station

For vehicle and parts production and repairs for the truck technologies with specifications in Table 2.1, material-by-material energy use, water consumption, and emissions factors from the GREET 2 model (ANL 2015) were applied to truck material composition data (Gaines et al. 1998) modified to reflect more recent vehicular materials composition (Davis & Diegel 2015). For tires and fluids (e.g., engine oils, transmission oils, coolant, etc.), default values in the GREET 2 model were used with adjustments based on the difference between light-duty vehicles in GREET 2 and medium-duty trucks (e.g., the number of tires, tire size, engine displacement, frontal area, weight, etc.). Compressed natural gas (CNG) cylinders, two Type-3 72-inch cylinders (Freightliner 2014), are not specifically addressed in the GREET 2 model. For this, I assume a 50-50 share of aluminum (for a metal liner) and carbon fiber (for an overwrap) materials (Luxfer 2013). I use EIO-LCA to analyze the energy efficiency, water use, and emissions from the refueling stations construction and operation (CMU GDI 2008), based on the parameters in Table 2.1 and the following section. Lee et al. (2013) used a similar method, combining process-based and EIO-LCA approaches, oftentimes called a hybrid LCA.

Table 2.1. Modeled Truck Specifications

	Diesel	Biodiesel (BD20)	Diesel or Biodiesel Hybrid	CNG	CNG Hybrid	Electric
Model year	2015					
Vehicle weight class	6					
Manufacturer	Freightliner					SEV
Gross vehicle weight (ton)	11.8 (curb weight + payload capacity)					
Overall size (m)	8.8 (length) x 2.2 (width) x 2.8 (height)					
Curb weight (kg)	7700	7700	7980	7960	8240	6830
Payload cap. (kg)	4100	4100	3820	3840	3560	4970
Engine model & power (kW)	Cummins ISB 6.7L (186 kW)			Cummins ISL G250 (186 kW)		-
Aftertreatment system	Diesel Particulate Filter (DPF) and Selective Catalytic Reduction (SCR)			Three-Way Catalyst (TWC)		-
Electric motor power (kW)	-	-	44 kW Induction	-	44 kW Induction	120 kW PMSM
Transmission	6-speed Allison 2100 HS		6-speed Eaton Fuller	6-speed Allison 2100 HS	6-speed Eaton Fuller	Single-gear reduction
Traction battery capacity (kWh)	-	-	1.9 kWh (Hitachi Li-ion)	-	1.9 kWh (Hitachi Li-ion)	80 or 120 kWh (Li-ion)
Fuel tank	Single aluminum tank (50 DGE, diesel gallon equivalent)			2 Type-3 Cylinders (17 DGE)		-
Refueling option	Gas station			CNG station		AC Level 2 15kW
Refueling station cost ($)	-			141,000 per truck for 10 fleet; 43,000 per truck for 50 fleet		7,000
Tire (6 pieces/truck)	Michelin 215 75R17.5					
Capital cost ($)	75,000	75,000	115,000	105,000	145,000	150,000 - 180,000
Battery pack specific cost ($/kWh)	-	-	See SI – Section 7	-	-	See SI – Section 7
Maintenance cost ($/mile)	0.2	0.2	0.16	0.22	0.22	0.14

Vehicle and parts specifications: (Freightliner 2014; Kenworth 2014; Eaton 2014; SEV 2014; Allison Transmission 2015; Cummins 2015). Cost data sources: (Fairley 2011; Sankey et al. 2011; Deal 2012; ATRI 2013; ANL 2013; Lee et al. 2013, Gibson and Adamson 2013; WVU 2014).

2.5 Cost

I include purchase cost without incentives, maintenance and repairs cost, fuel cost, and additional internal combustion engine (ICE) emissions-related cost (e.g., aftertreatment fluid cost). I also account for air emissions damage cost as mentioned earlier. All monetary values are in constant 2015 dollars. Purchase prices for model year 2015 class 6 freight trucks are $75,000, $115,000, and $105,000 for diesel, hybrid, and CNG models, respectively (Deal 2012; ANL 2013). The electric truck with an 80 kWh battery costs $150,000 and the one with a 120 kWh battery costs $180,000 (SEV 2014). Maintenance and repair costs are $0.2/mile for diesel, 0.16 for hybrid, 0.22 for CNG, and 0.14 for electric (ANL 2013; ATRI 2013). For hybrid and electric trucks, I assume three battery replacements over a vehicle's operating lifetime. The first replacement will be covered by manufacturer warranty and the remaining two will cost fleet operators. Future battery price is expected to go down to $250/kWh by 2020 (Fairley 2011; Sankey et al. 2011; Gibson and Adamson 2013). CNG refueling station costs about $141,000 per truck for the fleet of 10 natural gas trucks and $43,000 for the fleet of 50 trucks (WVU 2014). Electric vehicle supply equipment (EVSE) cost per truck is around $7,000 (Lee et al. 2013). For current fuel prices, I use state-by-state monthly data (AAA 2015; EIA 2015a). For future fuel prices evolutions, I use EIA's three fuel price projections (baseline, high, and low) for petroleum diesel, CNG, and electricity (EIA 2015b). It has been reported that approximately two regenerations of a diesel particulate filter (DPF) are required per week totaling a half an hour of down time and an additional 0.4 gallon of fuel used per week (CARB 2008). Selective catalytic reduction (SCR) for NOx emission control consumes urea with approximately 3% of the diesel fuel gallon burnt, at a cost of $4/gallon. A residual value is not included in my calculation, because my previous study (Lee et al. 2013) shows the residual value is not significant. I assume vehicle lifetime as 560,000 km (or 350,000 miles) (Huai et al., 2006) over a 20-year time horizon (2015 – 2035).

2.6 Fuel Supply and Electric Grid (Average & Marginal)

Upstream energy, water, and emissions factors associated with petroleum diesel, soybean-based biodiesel, and natural gas fuel production, transmission, and distribution were taken from the GREET 1 model (ANL 2015). GREET model assumes about 1% of fugitive methane emissions for natural gas. I also consider 5% emissions case, based on the literature (Howarth et al. 2011; Schwietzke et al. 2014; Camuzeau et al. 2015). I assume about 75% carbon uptake credit for soybean-based biodiesel production (Wang et al. 2011). I use GREET factors for power plant construction and operation as well as power generation fuel supply. For on-site energy consumption, water use, and air emissions in power plants, I use EPA CEM's hourly data (EPA 2016a) augmented with EPA NEI database (EPA 2015a). This enables us to account for heterogeneity in energy efficiency and air emissions of different power plants in different locations and times. I estimate water withdrawal and consumption factors for thermo-electric power plants based on EIA data (EIA 2015c) for 2013. I aggregate individual boiler-level data to cooling systems and power plants, with differentiation by fuel type, prime mover, water source type (e.g., surface, ground, fresh, saline, etc.), and cooling system type (e.g., once-through, recirculating, dry, hybrid, etc.) for each state.

I model state-by-state hourly power generation with a simplified load-filling approach. I take 8760-hour power load profiles (FERC 2015) and fill with actual hourly fossil fuel generation data (EPA 2016a) and renewable power generation (NREL 2015; EIA 2015c). I then convert these generation results to consumption-based hourly electricity mix, based on the methodology proposed by Marriott and Matthews (2005) and inter-state electricity trade data (EIA 2015c), as follows:

$$E_{Gen_{s,h}} = \frac{\sum_f^{N_{s,F}} \left(P_{s,h,f} \cdot E_{s,h,f}\right)}{\sum_f^{N_{s,F}} P_{s,h,f}} \tag{2.1}$$

$$E_{Cons_{s,h}} = \frac{\left(P_{s,h} \cdot E_{s,h}\right) - \left(\sum_e^{N_{s,E}} P_{s_{e,h}} \cdot E_{s_{e,h}}\right) + \left(\sum_i^{N_{s,I}} P_{s_{i,h}} \cdot E_{s_{i,h}}\right)}{P_{s,h} - \sum_e^{N_{s,E}} P_{s_{e,h}} + \sum_i^{N_{s,I}} P_{s_{i,h}}} \tag{2.2}$$

where $E_{Gen_{s,h}}$ and $E_{Cons_{s,h}}$ are energy use, water intensity, and air emissions factors for the s-th state and h-th hour for power generation and consumption, respectively; $P_{s,h,f}$ and $E_{s,h,f}$ are power generation and energy use, water intensity, and air emissions for the s-th state, h-th hour, and f-th fuel type; $P_{s_{e,h}}$ and $P_{s_{i,h}}$ are the export to the e-th state (s_e) and the import from the i-th state (s_i) in the h-th hour; and $N_{s,F}$, $N_{s,E}$, and $N_{s,I}$ are the total number of fuel types, exporters, and importers for the s-th state, respectively. Although the equations Eqs. (2.1) and (2.2) are used for state-level results, whenever possible, I aggregate the input data based on individual boilers and/or generators.

Based on the same data sources and Siler-Evans et al.'s methodology (2012), I estimate hourly marginal electric grid efficiency, air emissions, and water consumption (see Figure 2.2 for example). This information constitutes average and marginal 8760-hour power consumption characteristics for 2014. For future years, I use state-by-state carbon emissions reduction goals in the clean power plan (CPP) (Federal Register 2015b). For this assessment, I divide all power generating units into three separate groups: zero emitting units (ZEU), U.S. Clean Power Plan (CPP) target units (CPPTU), and non-CPPTU. I estimate carbon emissions factors for 2030 as follows:

$$CEF_{Total,2014} = \frac{CO_{2_{Total,2014}}}{G} \tag{2.3}$$

$$CEF_{Total,2030} = \frac{1}{G} \cdot [G_{CPPTU} \cdot CEF_{CPPTU} \cdot (1 - \alpha) + G_{Non-CPPTU} \cdot CEF_{Non-CPPTU}] \tag{2.4}$$

$$\gamma = \frac{CEF_{Total,2030}}{CEF_{Total,2014}} \tag{2.5}$$

$$EF_{LC,2030} = EF_{Infra} + EF_{FS} + (\gamma \cdot EF_{Gen}) \tag{2.6}$$

where $CO_{2_{Total,2014}}$ is total (direct and on-site) carbon dioxide emissions (kg); G is total power generation (kWh); $CEF_{Total,2014}$ and $CEF_{Total,2030}$ are overall carbon emission factors for 2014 and 2030; G_{CPPTU}, $G_{Non-CPPTU}$, CEF_{CPPTU}, and $CEF_{Non-CPPTU}$ are power generation and carbon emissions factors for CPPTU and Non-CPPTU; α is the CPP carbon emissions reduction target; $EF_{LC,2030}$ is life cycle energy use and emissions

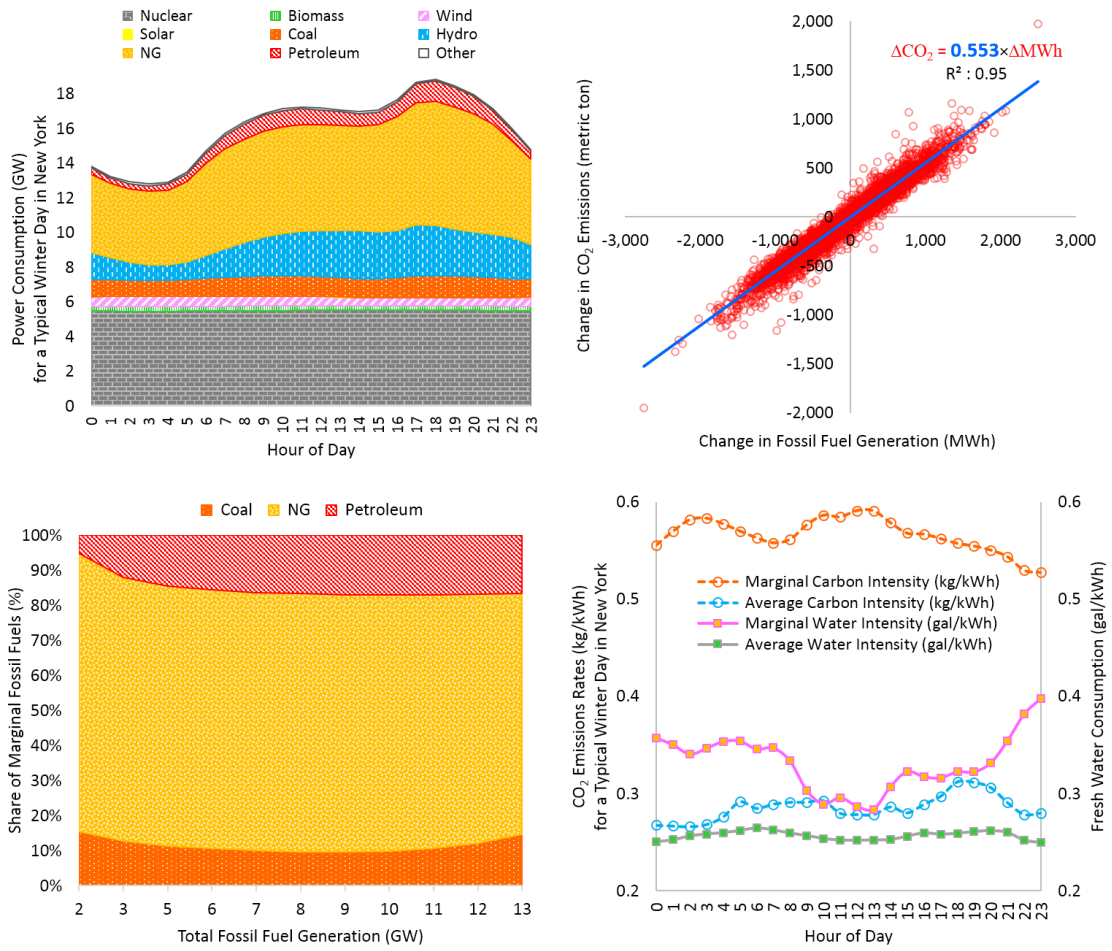

Figure 2.2. Example of hourly average and marginal emissions rates for the state of New York in winter in 2014. Power consumption fuel mix (top left); Marginal carbon dioxide emissions based on 8760-hour (a whole year) marginal power consumption (top right); Relationship between marginal fossil fuel mix and total fossil fuel generation as a proxy of overall power demand (bottom left); Comparison between on-site (not life cycle) average and marginal hourly carbon dioxide emissions and fresh water consumption (bottom right).

factors for 2030; EF_{Infra}, EF_{FS}, and EF_{Gen} are energy use and emissions factors for 2014 infrastructure, fuel supply, and generation (or on-site), respectively. Note that CEF_{ZEU} is zero and thus not included in Eq. (2.4) and that the CPP carbon emissions reduction only applies to direct (or on-site) emissions in Eq. (2.6). Given the complexity of water consumption for power generation, carbon emissions reduction may not be directly

related to water use reduction. For simplicity, however, I apply the same method above for water consumption for future years' power generation and consumption.

2.7 Vehicle Dynamic Simulation and Integration with VSP-based Emissions Model

For vehicle operation energy consumption, I use ADVISOR (ImagineMade, 2014), a vehicle dynamic simulator. Compared to a simpler tractive energy-based modeling approach (Davis and Figliozzi, 2013; LaClair 2012), the vehicle dynamic simulation software accounts for non-linear behavior of vehicle components (e.g., non-constant efficiency of internal combustion engine, traction battery, etc.). Also, the vehicle dynamic simulator is helpful for reducing potential biases (i.e., over- or under-estimation), as the software accounts for physical limits of vehicle performance (e.g., top speed, maximum payload, drive cycle traceability, etc.). U.S. EPA specifically sets allowable range of traceability (following requested vehicle speed) (40 CFR part 1066). Based on this requirement, I filter simulation results and use only those that pass the traceability test.

For the tail-pipe emissions analysis, I utilize MOVES (EPA, 2014a), a modal emissions model based on emissions data stratification by statistical or deductive definition of vehicle operating modes. MOVES is built upon the concept of vehicle specific power (VSP), the instantaneous tractive power per unit mass of the vehicle, proposed by Jimenez (1999). VSP is oftentimes called scaled tractive power (STP). MOVES has numerous disadvantages and issues. Examples include lack of transparency of input data, mismatch with real-world vehicle test results, time lag in data collection and implementation for more recent model years, no consideration of variations in vehicle specifications or physical capacity (e.g., traceability), and etc. For CNG vehicles, MOVES provides emissions factors only for transit buses. I take the ratios between the emissions factors for diesel and CNG buses and apply them to diesel trucks and get CNG truck factors. Before doing so, as shown in Figure 2.3, I adjust CNG bus emissions factors based on vehicle test data (Yoon et al. 2013; WVU 2014) to reflect recent

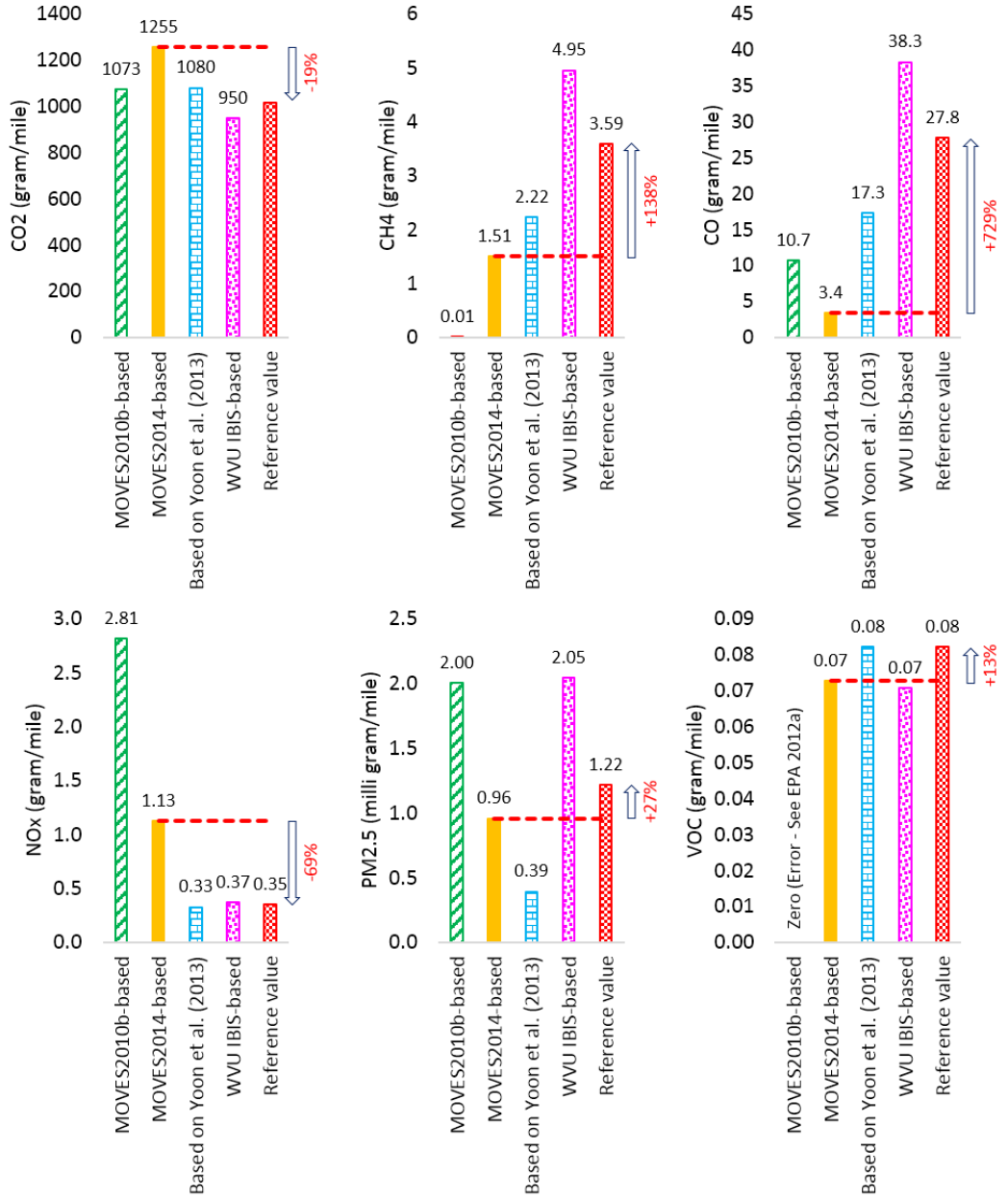

Figure 2.3. Adjustment factors for MOVES2014-based tail-pipe emissions rates for CNG medium-duty truck. Two sets of vehicle test data (Yoon et al. 2013; WVU 2014) for EPA Heavy-Duty Urban Dynamometer Driving Schedule (HD-UDDS) were used for reference (average of the two data sets). All test vehicles were equipped with stoichiometric engine and TWC aftertreatment system. For MOVES2010 erroneous data and bugs (e.g., zero VOC rates), see EPA materials (2012a, 2012b).

advances in CNG vehicles such as stoichiometric engine equipped with three-way catalyst (TWC) system. MOVES also provides no emissions factors for hybrid vehicles. For hybrid and idle reduction technologies, I build my own map-based emissions

modeling approach based on ADVISOR internal combustion engine model and MOVES emissions factors for conventional vehicles. More detailed description is provided in Appendix A. Figure 2.4 shows an example of my integrated vehicle dynamic and emissions simulations based on ADVISOR and MOVES. Following the hybrid-electric vehicle test guidelines proposed by Wayne et al. (2004) and to minimize bias, I make sure that the final state of charge (SOC) at the end of each drive cycle (e.g., 62.5% in Figure 2.4) is the same as the initial SOC at the beginning of the drive cycle.

2.8 Life-Cycle Inventory Parameterization

To identify the underlying relationship between input parameters (e.g., vehicle operation conditions) and output results (e.g., energy consumption), I run simulations (see Figure 2.4 for example) thousands of times with different input conditions for each technology and construct a sample space upon which I can develop a statistical relationship between input and output variables. I use hundreds of drive cycles collected from publicly-available sources – the ARTEMIS project (ARTEMIS 2006), the NGSIM program (FHWA 2004), ADVISOR (ImagineMade 2014), MOVES (EPA 2014a), and TSDC (NREL 2014a). Part of the results is shown in Figure 2.5, where each data point represents an aggregated result of an individual simulation (for example, Figure 2.4). Although not all of the drive cycles collected are medium-duty truck-specific and only some of them are real-world, they are still useful to build the spectra of possible driving conditions (Duran and Walkowicz 2013). Note that I distinguish drive cycle and duty cycle: Drive cycle is a speed-time profile, whereas duty cycle refers to time profile of speed as well as vehicle weight and/or road grade. Drive cycles can be characterized by parameters such as average trip/cycle speed, average driving speed, number of stops, maximum speed, positive kinetic energy (PKE), product of speed and acceleration, vehicle specific power (VSP), kinetic intensity (KI), aerodynamic speed, characteristic acceleration, and etc. (Watson et al. 1983; EPA 1993; Jimenez 1999; EPA 2003; O'Keefe et al. 2007; Lascurain 2008; Lascurain et al. 2012; Burton et al. 2013a, 2013b). Energy consumption and emissions can be similar for completely different drive cycles, if they share common characteristics (O'Keefe et al. 2007; Lascurain 2008; Clark et al. 2010; Lascurain et al. 2012; Burton et al. 2013a; LaClair et al. 2014). These studies support my parametric approach for the prediction of energy use and emissions based on statistical parameterization of input conditions. Figure 2.5 shows that on an operation-only (not full life cycle basis), electric vehicles use less energy than diesel or CNG vehicles. This is not

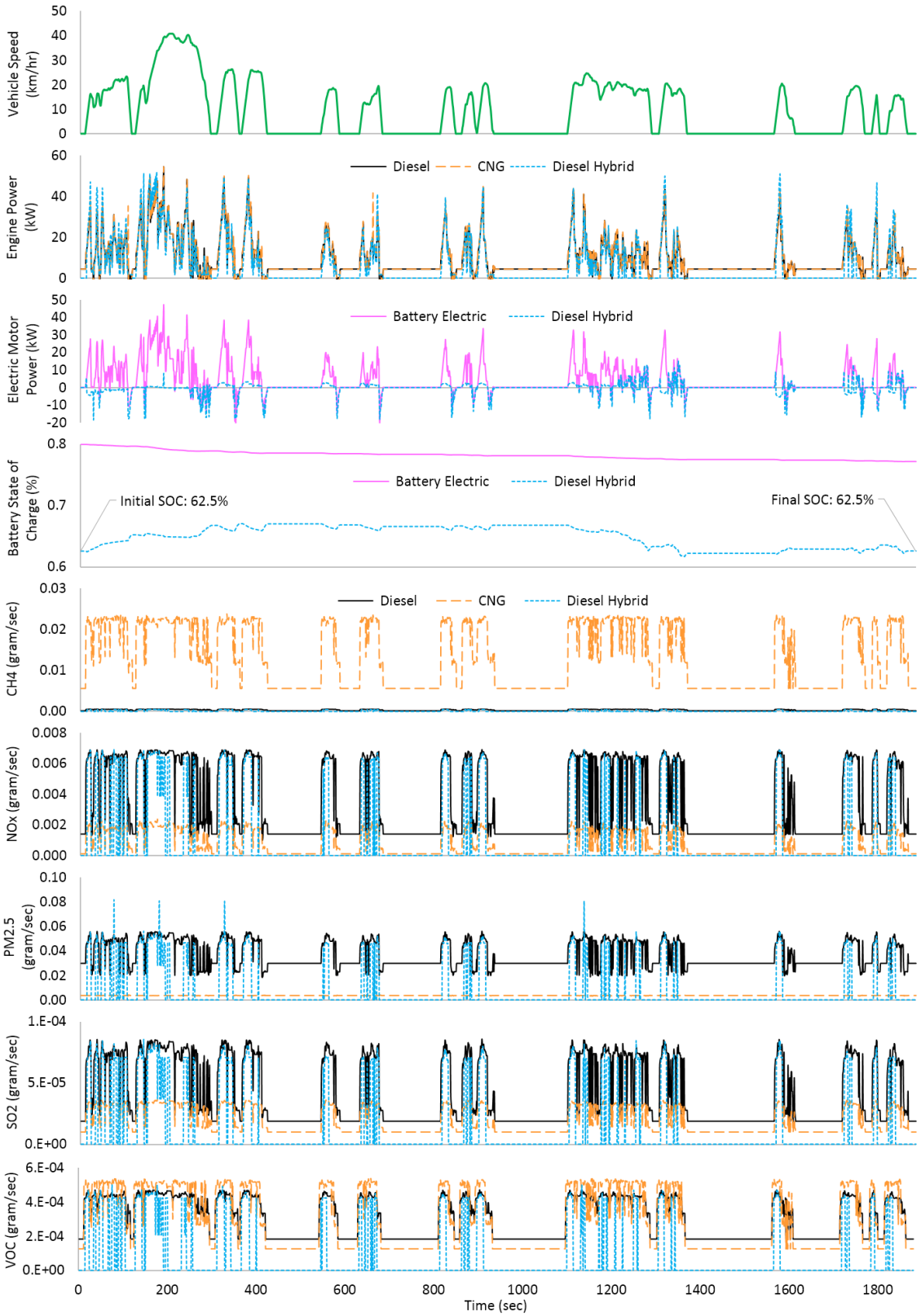

Figure 2.4. Vehicle dynamic and emissions simulation – example results for a part (first 1880 seconds) of Hybrid Truck Users Forum Class 6 Parcel Delivery Driving Schedule (HTUF-6PDDS).

surprising, considering the relative efficiency advantage of electric-drive systems (converting 60% of the electric energy from the grid to useful work) over the internal combustion engine (about 20%) (DOE, 2014). Also, electric trucks emit no tail-pipe GHGs.

Among the numerous duty cycle characterization parameters, I choose average trip speed, positive kinetic energy, vehicle weight, payload, ambient temperature, and road grade. As shown in Figure 2.5, average trip speed has a close relationship with energy consumption of non-electric trucks. However, I find that average trip speed or positive kinetic energy (or PKE) (Watson et al. 1983) are not very effective in explaining the variability of electric trucks' energy use (Figure 2.6). Therefore, I modify the concept of PKE and define weighted PKE (WPKE), as follows:

$$WPKE = \frac{\sum_{i=0}^{T-1} m_i({V_{i+1}}^2 - {V_i}^2)}{\int_0^T V dt} \text{ for } V_{i+1} > V_i \quad (2.7)$$

where m_i and V_i are vehicle weight and speed for the i-th moment (second) of total time duration (T) of the given trip. The newly-defined WPKE can account for medium- and heavy-duty vehicles' dominant kinetic energy in total vehicle energy consumption as wells as a mass change over the freight delivery route.

Although average trip/cycle speed does not have a universal effect as such, other variables do. For example, regardless of vehicle technologies, more hilly roads and/or more extreme climate conditions will universally lead to increased energy use with different degrees of impact (sensitivities) that vary with different vehicle technologies. As shown in Figure 2.7, based on the vehicle dynamic simulation, I develop scaling factors as a function of road grade for each of the technologies to avoid the biases of averages and extremes. Regarding recoverable energy for electric trucks during downhill driving, there are three aspects to note: First, the recoverable energy level depends on the initial state of charge of traction battery. If the battery is fully charged (hypothetically), no regenerative braking energy can be saved. Second, because of the second law of

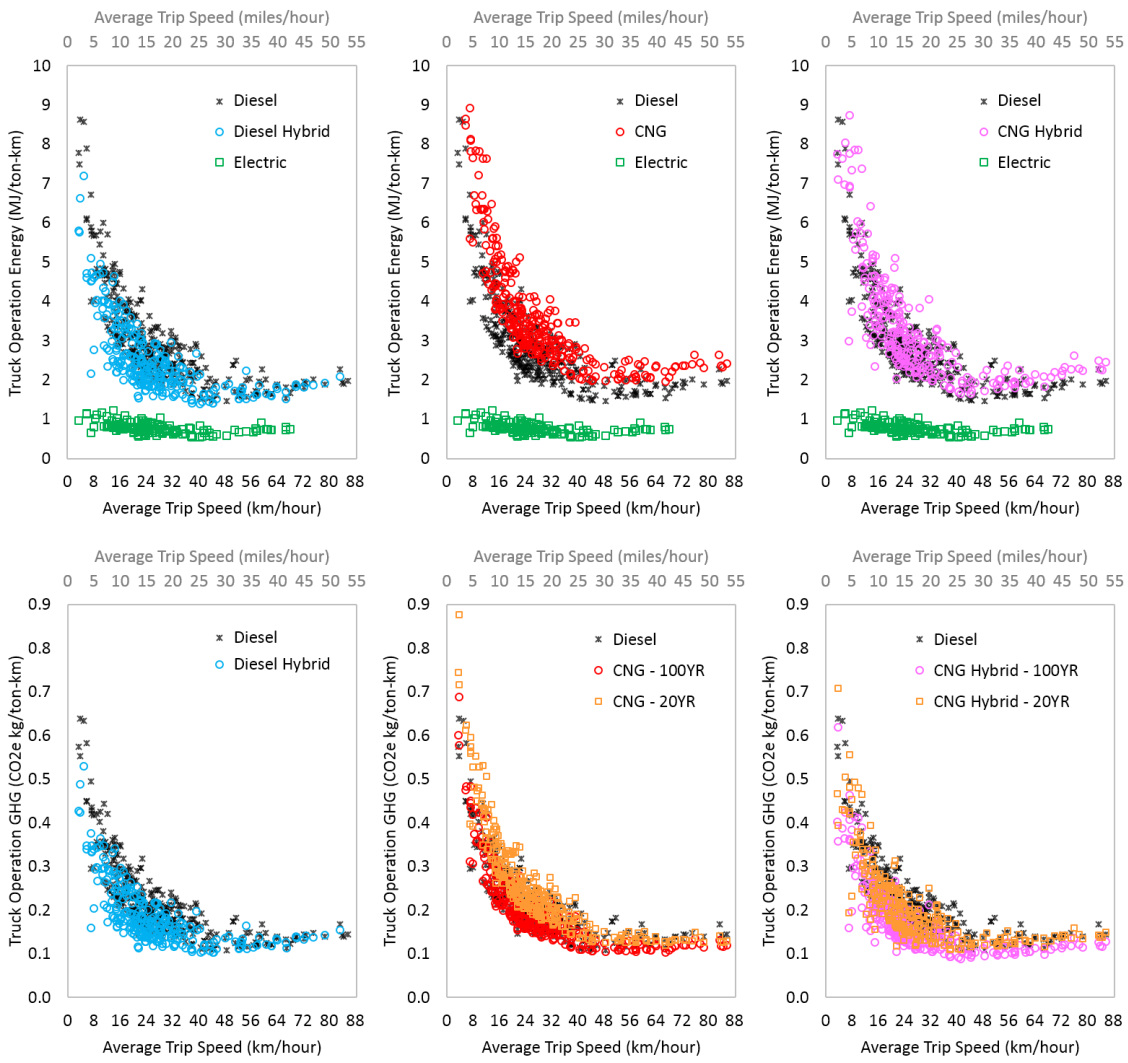

Figure 2.5. Use phase energy consumption and tail-pipe greenhouse gas emissions for medium-duty freight truck – moving a ton of payload per unit distance. Energy use for the electric truck refers to the input (purchased) utility AC electricity to Level 2 EVSE, that is, energy consumed by the external charger. CNG 20-YR and 100-YR refer to the time horizon of the global warming potential. Tail-pipe GHG emissions from the electric vehicle are not shown; see Figure 2.10 for life cycle emissions results.

thermodynamics, recovered energy in downhill driving is always smaller than total braking energy consumed on the wheels. Third, despite the limitations of recoverable energy and irreversibility as such, even without regenerative braking, downhill driving requires less overall traction energy than that for level-ground or uphill driving, owing to

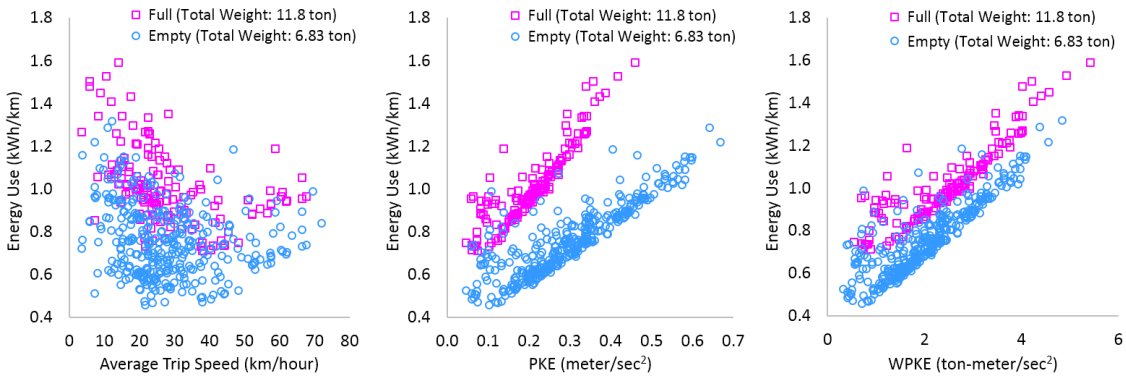

Figure 2.6. Relationship between energy use for electric truck operation and kinematic (i.e., average trip speed and PKE) and kinetic (e.g., WPKE) variables.

the gravitational acceleration effect, as is the same for non-electric trucks. That's why we see asymmetric patterns in Figure 2.7.

I develop similar scaling factors for climate condition impact (Figure 2.8), using the electric vehicle test data as well as EPA MOVES and IBIS models (ANL 2014; EPA 2014a; WVU 2014). This type of correction factors can also be found in sensitivity analyses – see Noel and Wayson (2012) for example. I use county-by-county hourly climate condition profiles and integrate them with the scaling factors, as shown in the example in Figure 2.8. Cold or hot climates increase energy consumption for both diesel and electric trucks, but non-electric trucks exhibit a different pattern from their electric counterpart. Non-electric trucks consume more energy for air-conditioning and removing the waste heat while overcoming the hot ambient temperature. In winter time, the energy consumption becomes lower, owing to the waste heat of the engine available for cabin heating, but can increase again as the climate condition becomes more extreme. However, climate condition does not always explain the overall impact, because of the confounding effect of fuel prices, specifically due to monthly fuel prices variations. As illustrated in Figure 2.8, diesel fuel prices decreased from 2014 to 2015, while CNG prices were relatively steady, and shows a direct relationship with seasonal temperature variations. Electricity tends to be more expensive in summer than in winter. Therefore, in

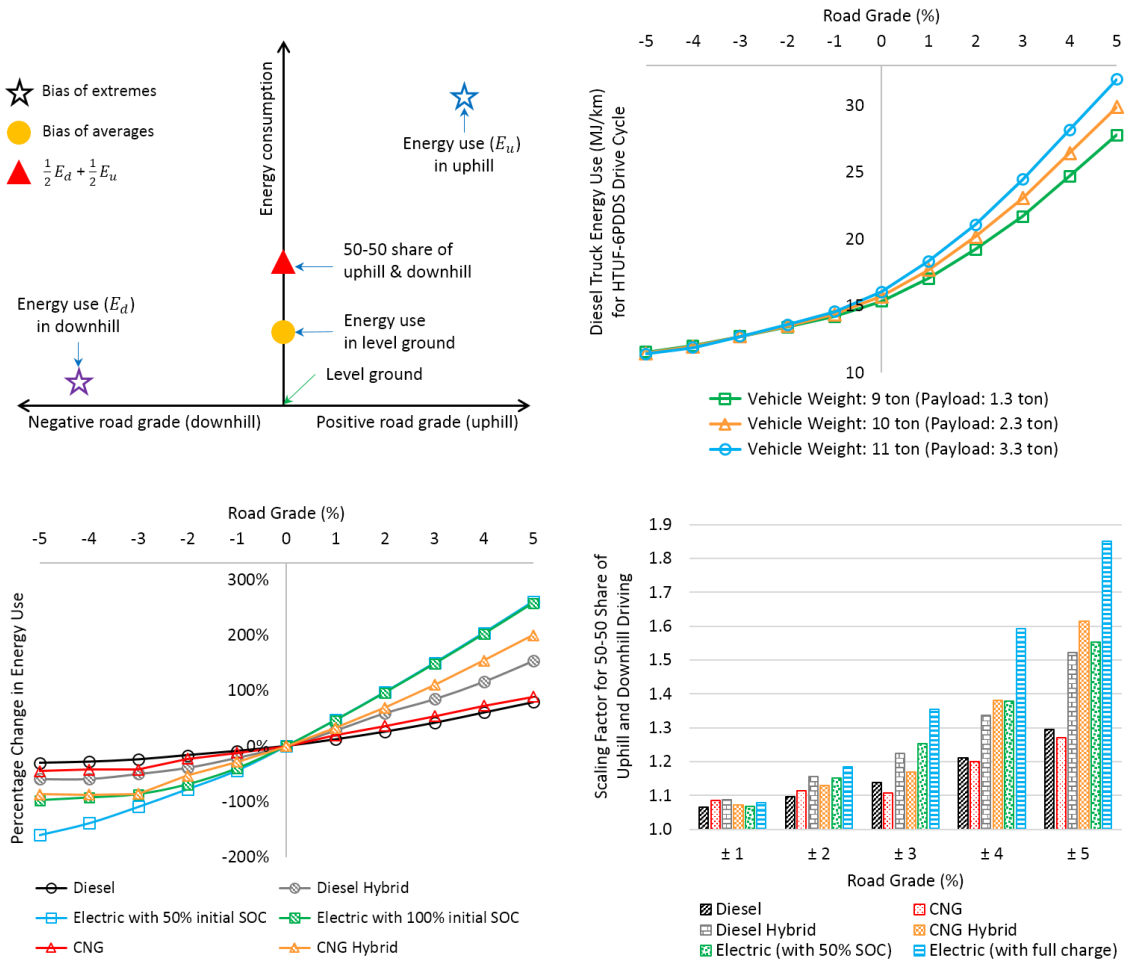

Figure 2.7. Energy consumption impact of road grade, based on the result for local drayage drive cycle (Thiruvengadam et al. 2015). Biases of averages and extremes (top left); Asymmetric impact of road grade for diesel truck (top right); Percentage change in energy use for different truck technologies (bottom left); Scaling factors (weighted averages of uphill and downhill) for different technologies and road grades.

Los Angeles, with a mild winter, higher summer electricity prices have larger impact than climate conditions, leading to higher fueling cost in summer than in winter. This is not the case for New York area, where a cold winter results in higher fuel costs during the winter time even though there are higher electricity rates during summer.

Based on the parameterization discussed above along with vehicle dynamic and simulation results, I develop the following generic life cycle inventory prediction models, written as the product of powers:

$$\hat{Y} = \exp(\hat{\beta}_0) \cdot \prod_{i=1}^{I} [\exp(X_i)]^{\hat{\beta}_i} \cdot \prod_{j=1}^{J} X_j^{\hat{\beta}_j} \cdot \prod_{k=1}^{K} \left[\exp\left(\frac{1}{X_k}\right)\right]^{\hat{\beta}_k} \quad (2.8)$$

where $\hat{Y}$'s are life cycle results (e.g., energy consumption, air emissions, smog formation,

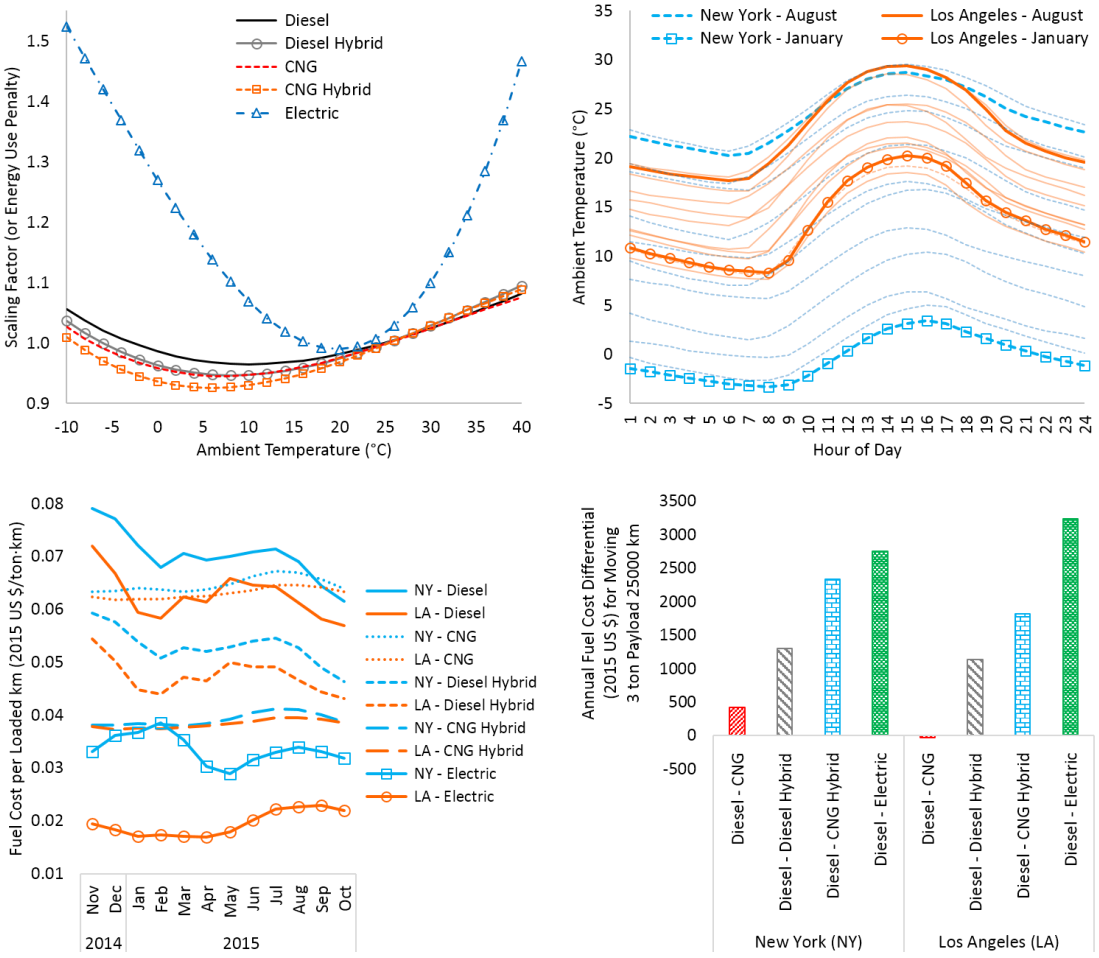

Figure 2.8. Impact of local climate condition and seasonal electricity prices variation. Scaling factor function for temperature variation (top left); Average hourly temperature profiles for 12 months in two select metropolitan areas – New York and Los Angeles (top right); Fuel cost with both temperature (6 am – 9 pm average) effect and monthly fuel prices variations accounted for (bottom left); Annual fuel cost differential relative to conventional diesel trucks (bottom right).

etc.); X's are independent variables (or predictors) (e.g., average trip speed, payload, WPKE, etc.); and $\hat{\beta}$'s are the multiple linear regression parameters estimated based on the ordinary least squares method. On top of these generic models, scaling factors for road grade and climate condition can be multiplied. Due to data availability, I apply county-by-county hourly climate profiles without road grade, but the scaling factors I developed can be used when the high-resolution road grade data coupled with drive cycles become available. Using the generic models in Eq. (2.8), the complicated vehicle dynamic and emissions simulations do not need to be run. Instead, one can simply plug the characterization values into Eq. (2.8). For this calculation, I utilize the National Renewable Energy Laboratory's Fleet DNA project data (Walkowicz et al. 2014) for 1,520 samples of medium-duty truck activity records across the U.S (Figure 2.9). The data are based on vehicle routes and duty cycle characterization parameters, which matches the parametric modeling framework. I also incorporate EPA SmartWay data

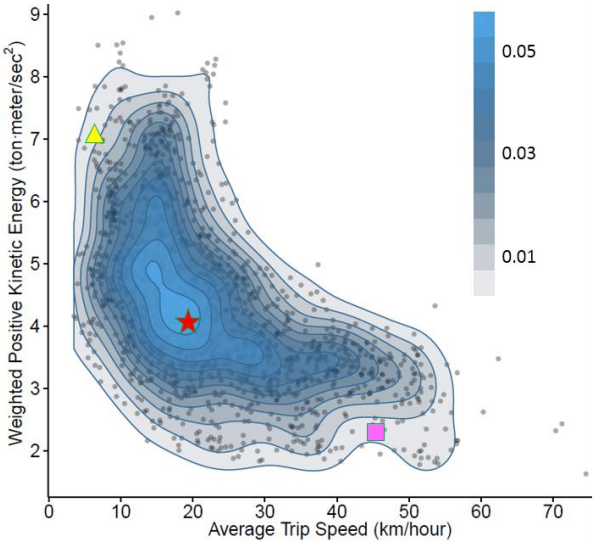

Conditions	Average trip speed (km/hour)	WPKE (ton·meter/sec²)
The most severe	7.9	7.1
Average	19.7	4.1
The least severe	46.7	2.4

Figure 2.9. Probability density for statistical operating condition of medium-duty freight trucks – adapted based on the data from the NREL Fleet DNA project (1,527 samples) and EPA SmartWay program. The most severe, average, and the least severe conditions refer to the combinations of 5-, 50-, and 95-th percentiles in the two-dimensional probability density domain.

(EPA 2015b) for statistical distribution of vehicle weight and real-world electric truck charging profiles (Duran et al. 2014).

2.9 Parametric Prediction of Life Cycle Inventory and Impact Assessment Results

Figure 2.10 shows the life cycle inventory results for vehicle and parts production. Despite the lighter curb weight and lack of diesel engine, bulky multi-speed transmission, and after-treatment systems, the electric truck is generally worse than the other technologies, mostly because of the secondary (or traction) battery packs. This contrasts with the operation-level-only comparison, in which the electric truck outperforms the other competing technologies in terms of energy use per unit distance traveled (Figure 2.5).

For electric trucks, neither operational nor life cycle energy show a strong dependency on average trip speed, unlike non-electric trucks. This distinctly different pattern between electric and non-electric trucks is not observed in light-duty vehicles (Figure 2.11). To explain this difference, based on the vehicle dynamic simulations of light- and medium-duty vehicles, I break down life cycle energy consumption into individual components (Figure 2.11). Note that the modeled light-duty vehicle is based on the Toyota Corolla and that the electric grid I used for the results shown in Figure 2.11 is based on the U.S. national average for illustration; the overall relationship is also seen in other cases. I find two factors are in play. First, as shown in Figure 2.11, for both light- and medium-duty non-electric vehicles, the energy associated with the internal combustion engine dominates overall life cycle energy consumption, which varies with average trip speed. Second, among the operation-level energy use components, useful work accounts for the largest portion for electric trucks, which varies with positive kinetic energy (not average trip speed) – see Appendix A. In contrast, other energy use components including aerodynamic drag and electric motors are more dominant than useful work for light-duty electric vehicles, which all vary with average trip speed. For these reasons, both light- and medium-duty non-electric vehicles show a changing pattern

directly related to average trip speed, which also is seen for light-duty electric vehicles. However, this is not the case for medium-duty electric vehicles for which the changing

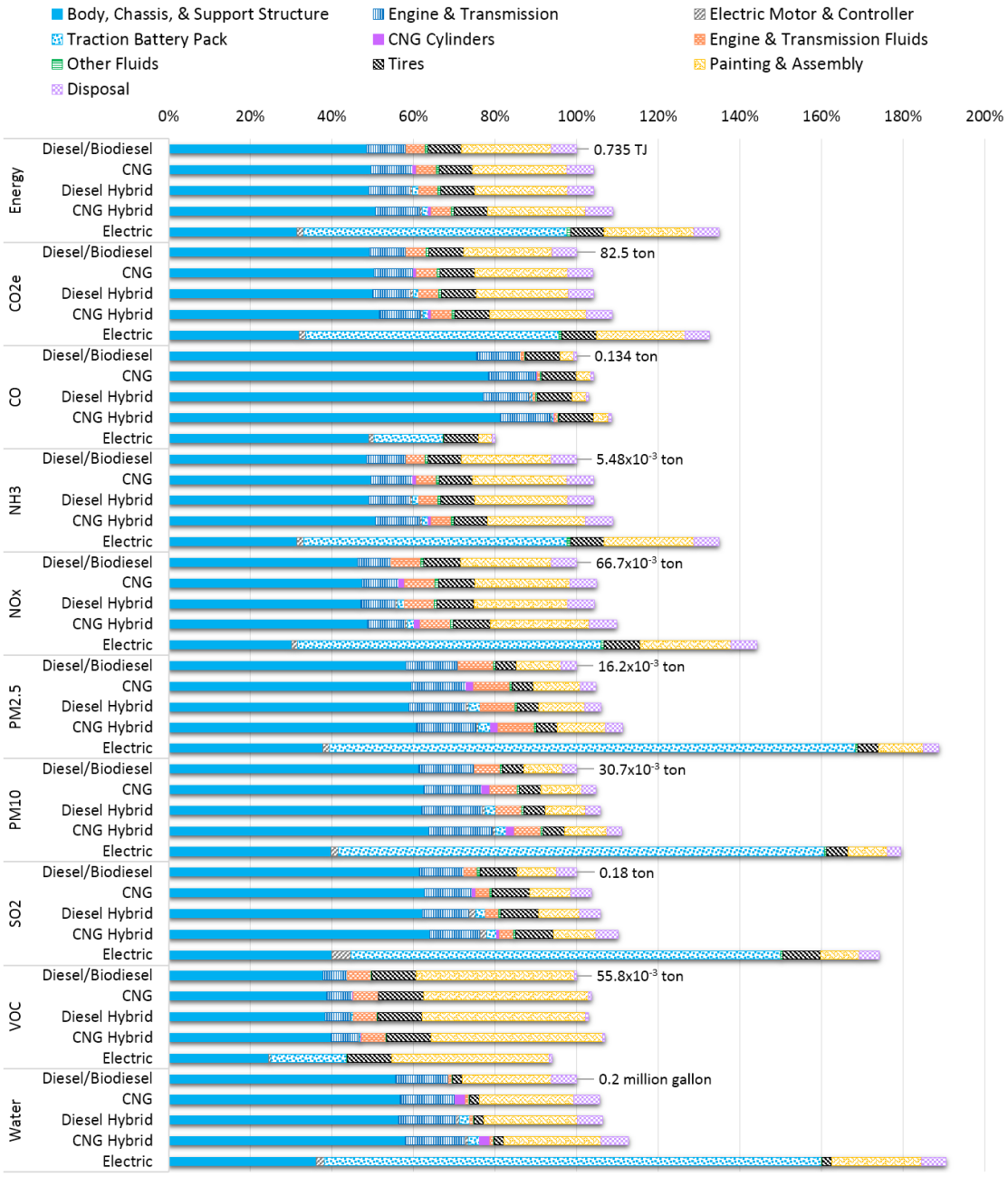

Figure 2.10. Medium-duty freight truck and parts production inventory (per truck and for truck lifetime) in percentage with the diesel truck as reference (100%). Detailed data are provided in Appendix A.

pattern of life cycle results depend on positive kinetic energy rather than average trip speed. In Figure 2.11, note that because of the differences in top speed of light- and medium-duty vehicles as well as electric and non-electric trucks, the horizontal axes are different.

As discussed earlier, both life cycle inventory and impact assessment results can be evaluated with a parametric modeling approach. Table 2.2 and Table 2.3 show linear regression-based parametric models for life cycle energy use and greenhouse gas emissions, respectively. For electric trucks, I only show the two select U.S. states for simplicity, for minimum and maximum cases as of 2015 in the U.S. These predictive models explain 91 to 98% of the variability of life cycle results. Parameters for other life cycle results can be found in the Appendix A. Figure 2.12 is a graphical illustration of the predictive models in the average trip speed domain, for half-loaded vehicle weight condition (see Table 2.1 for payload and vehicle weight information). Because of the lack of dependency of electric trucks on average trip speed, I show constant values for electric trucks as references, based on the average PKE value from the Fleet DNA project (Walkowicz et al. 2014). The minimum for electric trucks is for the daytime charging case for the state with the least value for each impact category, whereas maximum refers to the nighttime charging case for the state with the largest values.

As shown in Figure 2.12, CNG trucks show the highest life cycle energy consumption across the board. Although CNG trucks have lower tail-pipe GHG emissions than their diesel counterpart, CNG trucks emit more GHGs for fuel supply-chain, vehicle and parts production, and infrastructure installation, which leads to very similar overall GHG emissions to that of diesel trucks in the case of 1% fugitive methane emissions. However, in the 5% fugitive methane emissions case, CNG trucks, whether conventional or hybrid, are the most carbon-intensive technologies in terms of both 100- and 20-year global warming potential impacts. Other than smog (ground-level ozone) formation impact, CNG trucks do not provide life cycle benefits over diesel trucks. The

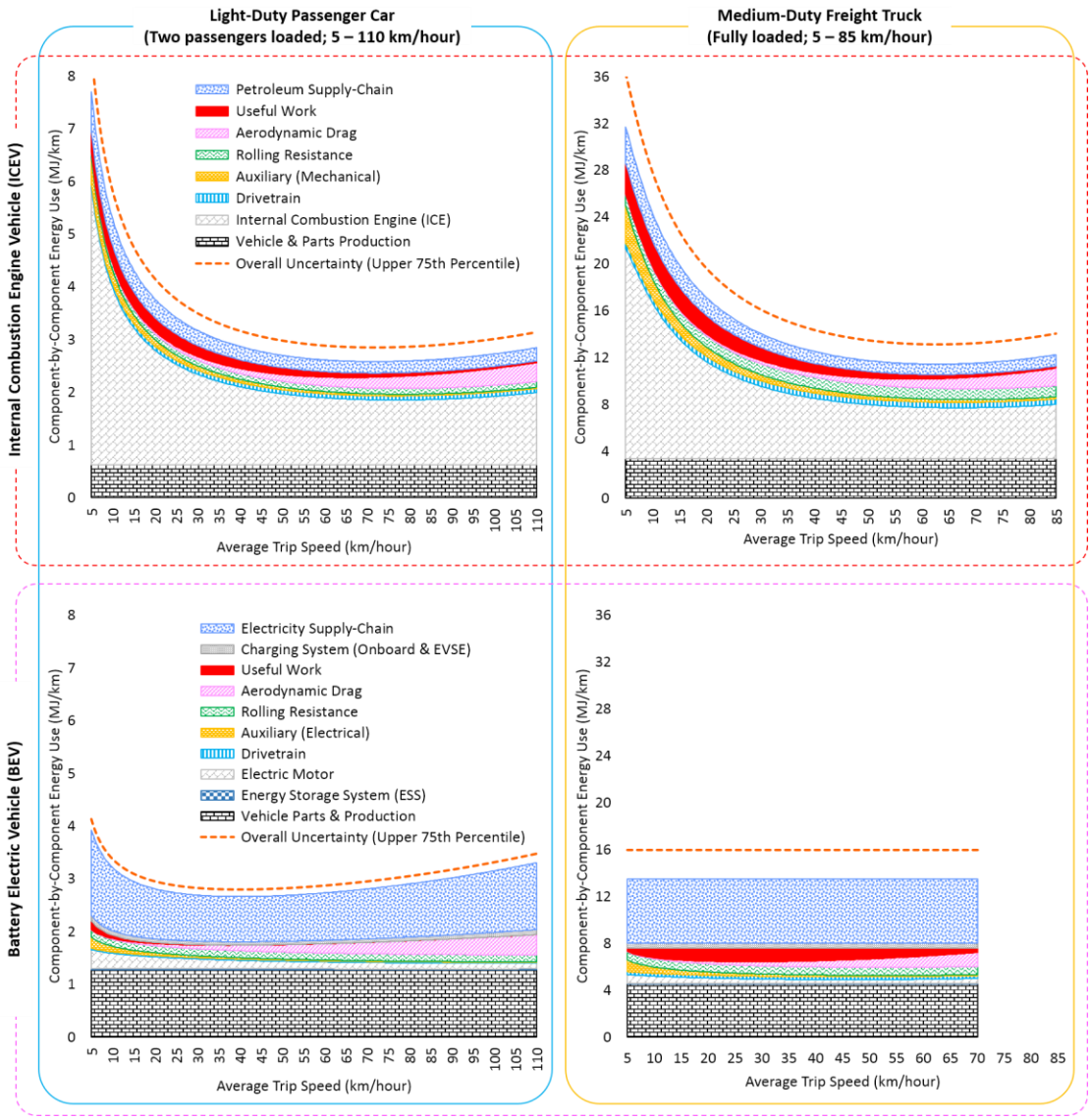

Figure 2.11. Parametric structure of life cycle energy consumption and its variation with different technologies (i.e., internal combustion engine vs. battery electric) and different vehicle weight classes and/or types (i.e., light-duty passenger cars vs. medium-duty freight trucks).

20% biodiesel option (BD20) is the most water-intensive and electric trucks generally consume more (fresh) water than diesel or CNG trucks. Other than water use impact, electric truck's overall life cycle environmental impacts are similar to or slightly higher than those of diesel trucks. Electric and hybrid (diesel and biodiesel) trucks are the most efficient and least GHG-emitting in general. As Lee et al. (2013) showed, the more

severe the drive cycle is (Figure 2.9), the higher the advantage of electrification becomes. The same tendency can be found for idle reduction technologies. At lower average trip speed conditions, the reduction potential is higher for life cycle energy use, air emissions, and water consumption impacts. For average trip (or drive cycle) speed and statistics (e.g., average trip speed and positive kinetic energy), please see Appendix A.

I pick two extreme cases, the most and least severe operating conditions in Figure 2.10, and show state-by-state results in Figure 2.13. Here the most severe condition refers to the 95^{th} percentile of average trip speed and 5^{th} percentile of WPKE in Figure 2.10, and the least refers to the combination of severe 5^{th} and 95^{th} percentiles of average trip speed and WPKE, respectively. The operating condition severity is directly related to the overall energy intensity. As opposed to the constant values in Figure 2.12, now as I account for WPKE in addition to average trip speed, I have more accurate life cycle results for electric trucks, as shown in Tables 2.2 and 2.3. I present only conventional diesel and diesel-powered hybrid trucks as reference technologies to compare with electric trucks, because CNG and other (non-electric) truck technologies emit similar or higher GHGs, although CNG shows slightly lower life cycle water-intensity (Figure 2.12). Biodiesel (B20) trucks consume far more water than the other technologies (Figure 2.12). In most of the states, whether the most or least severe conditions, electric trucks provide GHG emissions reduction benefits, although electric trucks almost always consume more fresh water than diesel-powered technologies over the life cycle. Considering the results in Figure 2.13 are based on marginal nighttime electric grid, which tends to have higher carbon-intensity than average or daytime electric grid, I can say that the GHG emissions reduction benefits are robust.

Another thing to note in Figure 2.13 is the complexity of carbon-water-intensity of thermo-electric power generation and resulting trade-offs of electric trucks. Simply put, the state emitting the least amount of GHGs is not necessarily the place where water

Table 2.2. Life cycle inventory (LCI) prediction model for energy consumption – see Appendix A for other life cycle inventory and impact prediction models.

Predictors	**Dependent variable**: $\hat{Y}$, **Life cycle energy use (MJ/km) per truck**							
	$\log(\hat{Y}) = \hat{\beta}_0 + \hat{\beta}_0 m_p + \hat{\beta}_2 WPKE + \hat{\beta}_3 \overline{V}_{trip} + \hat{\beta}_4 \overline{V}_{trip}^{-1} + \hat{\beta}_5 \log(\overline{V}_{trip}) + \hat{\beta}_6 \overline{V}_{trip}^{2}$							
	Conventional ICE			**Hybrid Electric**			**Battery Electric**	
	Diesel	BD20	CNG	Diesel	BD20	CNG	CA	CT
	Coefficients $\hat{\beta}_i$ and t-statistic (in parenthesis)							
$\hat{\beta}_0$	2.33 (117.6)	2.38 (119.3)	3.52 (61.9)	1.671 (170.4)	1.72 (173.6)	3.29 (82.9)	1.548 (193)	1.84 (209)
$\hat{\beta}_1$	1.33×10^{-2} (12.9)	1.35×10^{-2} (12.9)	1.28×10^{-2} (12.6)	1.79×10^{-2} (10.8)	1.8×10^{-2} (10.8)	3.64×10^{-2} (17.03)	3.06×10^{-2} (31.1)	3.31×10^{-2} (30.7)
$\hat{\beta}_2$	0.1188 (66.3)	0.1194 (66.1)	0.108 (58.2)	0.153 (55.1)	0.154 (55)	0.122 (34.6)	0.192 (66.9)	0.208 (66.2)
$\hat{\beta}_3$	-1.59×10^{-2} (-21.8)	-1.61×10^{-2} (-21.8)						
$\hat{\beta}_4$	3.27 (30.3)	3.27 (30.1)	1.74 (10.1)	3.91 (38.7)	3.94 (38.6)			
$\hat{\beta}_5$			-0.396 (-25.3)			-0.397 (-34.1)		
$\hat{\beta}_6$	1.57×10^{-4} (21.6)	1.58×10^{-4} (21.5)	7.09×10^{-5} (22.6)	3.73×10^{-5} (13.38)	3.75×10^{-5} (13.31)	9.31×10^{-5} (22.5)	7.66×10^{-5} (28.6)	8.34×10^{-5} (28.5)
Adj. R^2	0.97	0.97	0.98	0.94	0.94	0.91	0.94	0.94
F-stat.	5485	5446	6416	2465	2452	1684	2348	2296
N_{obs}	725	725	680	624	624	645	489	489

m: total vehicle weight (metric ton) = sum of curb weight m_c (metric ton) and payload m_p (metric ton), $\overline{V}_{trip}$: average trip speed (km/hour) = total distance traveled divided by total trip time taken, $WPKE$: ($m \cdot PKE$) weighted positive kinetic energy (ton·meter/sec^2), and N_{obs}: the number of observations (or samples).

For battery electric, I here show the results for two select cases – minimum (daytime charging in California (CA) and nighttime charging in Connecticut (CT), based on consumption-based marginal electric grid. Other states fall between the two (minimum and maximum).

On top of this generic prediction equation, correction factors may be applied (multiplied) for road grade (Figure 2.7) and/or temperature (Figure 2.8).

intensity is the lowest. Nuclear generating units don't emit direct greenhouse gases, but depending on cooling system type and water source type, fresh water consumption can vary widely. For example, plant Vogtle in Georgia draws fresh water from the Savannah River for its recirculating cooling system, consuming 0.8 gallons of fresh water per kWh

Table 2.3. Life cycle inventory (LCI) prediction model for greenhouse gas emissions (with 100-year horizon) – see Appendix A for other life cycle inventory and impact prediction models.

Predictors	**Dependent variable**: $\hat{Y}$, **Life cycle GHG-100YR emissions (gram/km) per truck**							
	$\log(\hat{Y}) = \hat{\beta}_0 + \hat{\beta}_1 m_p + \hat{\beta}_2 WPKE + \hat{\beta}_3 \bar{V}_{trip} + \hat{\beta}_4 {\bar{V}_{trip}}^{-1} + \hat{\beta}_5 \log(\bar{V}_{trip}) + \hat{\beta}_6 {\bar{V}_{trip}}^{2}$							
	Conventional ICE			**Hybrid Electric**			**Battery Electric**	
	Diesel	BD20	CNG	Diesel	BD20	CNG	VT	ND
	Coefficients $\hat{\beta}_i$ and t-statistic (in parenthesis)							
$\hat{\beta}_0$	6.68 (334)	6.67 (333)	7.81 (151.5)	6 (605)	6 (604)	7.44 (192)	4.87 (4215)	6.205 (683)
$\hat{\beta}_1$	$1.35\text{x}10^{-2}$ (12.9)	$1.35\text{x}10^{-2}$ (12.9)	$1.28\text{x}10^{-2}$ (13.9)	$1.81\text{x}10^{-2}$ (10.8)	$1.8\text{x}10^{-2}$ (10.8)	$3.55\text{x}10^{-2}$ (17.01)	$4.6\text{x}10^{-3}$ (32.5)	$3.4\text{x}10^{-2}$ (30.5)
$\hat{\beta}_2$	0.1194 (65.9)	0.119 (65.9)	0.0997 (59.2)	0.154 (55)	0.154 (55)	0.1197 (34.8)	0.0282 (68.6)	0.213 (66)
$\hat{\beta}_3$	$-1.62\text{x}10^{-2}$ (-21.9)	$-1.62\text{x}10^{-2}$ (-21.9)						
$\hat{\beta}_4$	3.28 (30.1)	3.28 (30)	1.623 (10.4)	3.94 (38.6)	3.94 (38.6)			
$\hat{\beta}_5$			-4.09 (-28.9)			-0.379 (-33.3)		
$\hat{\beta}_6$	$1.59\text{x}10^{-4}$ (21.6)	$1.59\text{x}10^{-4}$ (21.6)	$6.28\text{x}10^{-5}$ (22.1)	$3.75\text{x}10^{-5}$ (13.3)	$3.75\text{x}10^{-5}$ (13.3)	$8.84\text{x}10^{-5}$ (21.9)	$1.08\text{x}10^{-5}$ (28.1)	$8.58\text{x}10^{-5}$ (28.45)
Adj. R^2	0.97	0.97	0.98	0.94	0.94	0.91	0.94	0.93
F-stat.	5455	5462	7854	2450	2452	1668	2506	2278
N_{obs}	725	725	680	624	624	645	489	489

m: total vehicle weight (metric ton) = sum of curb weight m_c (metric ton) and payload m_p (metric ton), $\bar{V}_{trip}$: average trip speed (km/hour) = total distance traveled divided by total trip time taken, $WPKE$: ($m \cdot PKE$) weighted positive kinetic energy (ton·meter/sec^2), and N_{obs}: the number of observations (or samples).

For battery electric, I here show the results for two select cases – minimum (daytime charging in Vermont (VT) and nighttime charging in North Dakota (ND), based on consumption-based marginal electric grid. Other states fall between the two (minimum and maximum).

On top of this generic prediction equation, correction factors may be applied (multiplied) for road grade (Figure 2.7) and/or temperature (Figure 2.8).

of electricity generated. Plant St. Lucie in Florida is also a nuclear power plant, but it draws saline water from the Atlantic Ocean for its once-through cooling system, consuming 0 gallons of fresh water. In other words, despite its lower carbon-intensity advantage, nuclear power plants can add to regional water stress. In contrast, coal power plants certainly emit direct greenhouse gas emissions, but there are wide variations of water-intensity. For example, the coal power plant Bowen in Georgia draws fresh water

from the Etowah River for its four recirculating cooling systems, consuming 0.4 gallons of fresh water on average per kWh of electricity generated. However, the coal power plant C R Huntley in New York draws fresh water from Niagara River for its once-through cooling system, with substantially lower fresh water consumption.

I estimate both direct (or total cost of ownership, TCO) and indirect cost (i.e., monetized air emissions damage), based on the cost data discussed earlier and predictive life cycle inventory models presented above. I look at three cases in the average trip speed and PKE domain in Figure 2.10 – the most severe, average, and the least severe conditions. As mentioned above, the most severe condition favors electric trucks, which confirms Lee et al.'s (2013) findings. For overall social life cycle cost calculation, I take the following method:

$$SLCC_{c,t} = TCO_{c,t} + \sum_{i=0}^{20} \frac{\left(SCC_{t,i} \cdot CE_{t,i}\right) + \left(AEDC_{c,t,i} \cdot APE_{c,t,i}\right)}{(1+d)^i} \quad (2.9)$$

where $SLCC_{c,t}$ and $TCO_{c,t}$ refer to social life cycle cost (SLCC) and total cost of ownership (TCO) (see Lee et al. 2013) for the t-th technology in c-th county in the continental U.S., respectively; $SCC_{t,i}$ and $CE_{t,i}$ are social cost of carbon (SCC) and carbon emissions (CE) for the i-th year and t-th technology, respectively; $AEDC_{c,t,i}$ and $APE_{c,t,i}$ are air emissions damage cost (AEDC) and air pollutants emissions (APE) for the i-th year and t-th technology in c-th county, respectively; and d is discount rate for the time value of money. I find that electric trucks are not cost-effective in both average and least severe operating conditions and that conventional diesel is the most cost-effective across the country, mostly owing to the low diesel fuel prices as of 2015. In Figure 2.14, I show only the results for the most severe condition, based on Monte Carlo simulations with a range of cost parameters (see Appendix A). The results are based on nighttime charging and marginal electric grid. The overall cost (SLCC) difference between average and marginal electric grid cases, mostly owing to air emissions damage differential, ranges from 1 – 5%. Based on the $SLCC_{c,t}$, I pick the most cost-effective

truck technology in each county. If I exclude idle reduction option, the truck technology choice is biodiesel (B20) hybrid or battery electric. Even under the current low diesel fuel price condition, for niche application, battery electric trucks provide positive net social benefits in many areas. Once I include the idle reduction option, however, 33% of the counties that favored electric trucks and 100% of the counties that favored B20 hybrid trucks will now favor idle reduction as the most cost-effective technology, which shows the disruptive effect of idle reduction technology. This finding is in part due to the operating condition tested (the most severe) for which idle reduction can have the largest benefit (see Figure 2.12). For average and least severe operating conditions, biodiesel (B20, without idle reduction) and B20 hybrid provides the largest net social benefit, respectively.

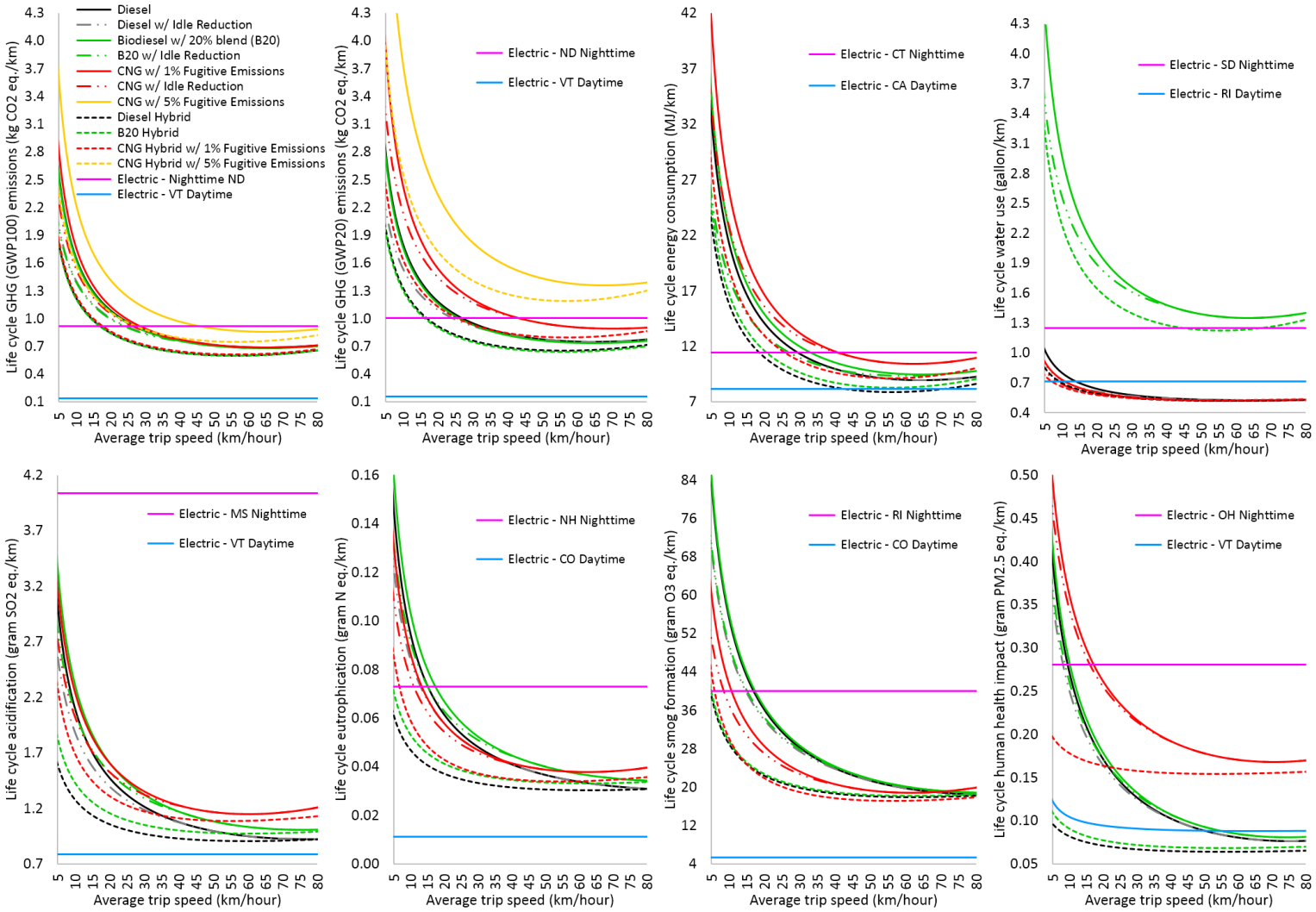

Figure 2.12. Parametric prediction of life cycle impact assessment (LCIA) results. Electric for two states with minimum and maximum values.

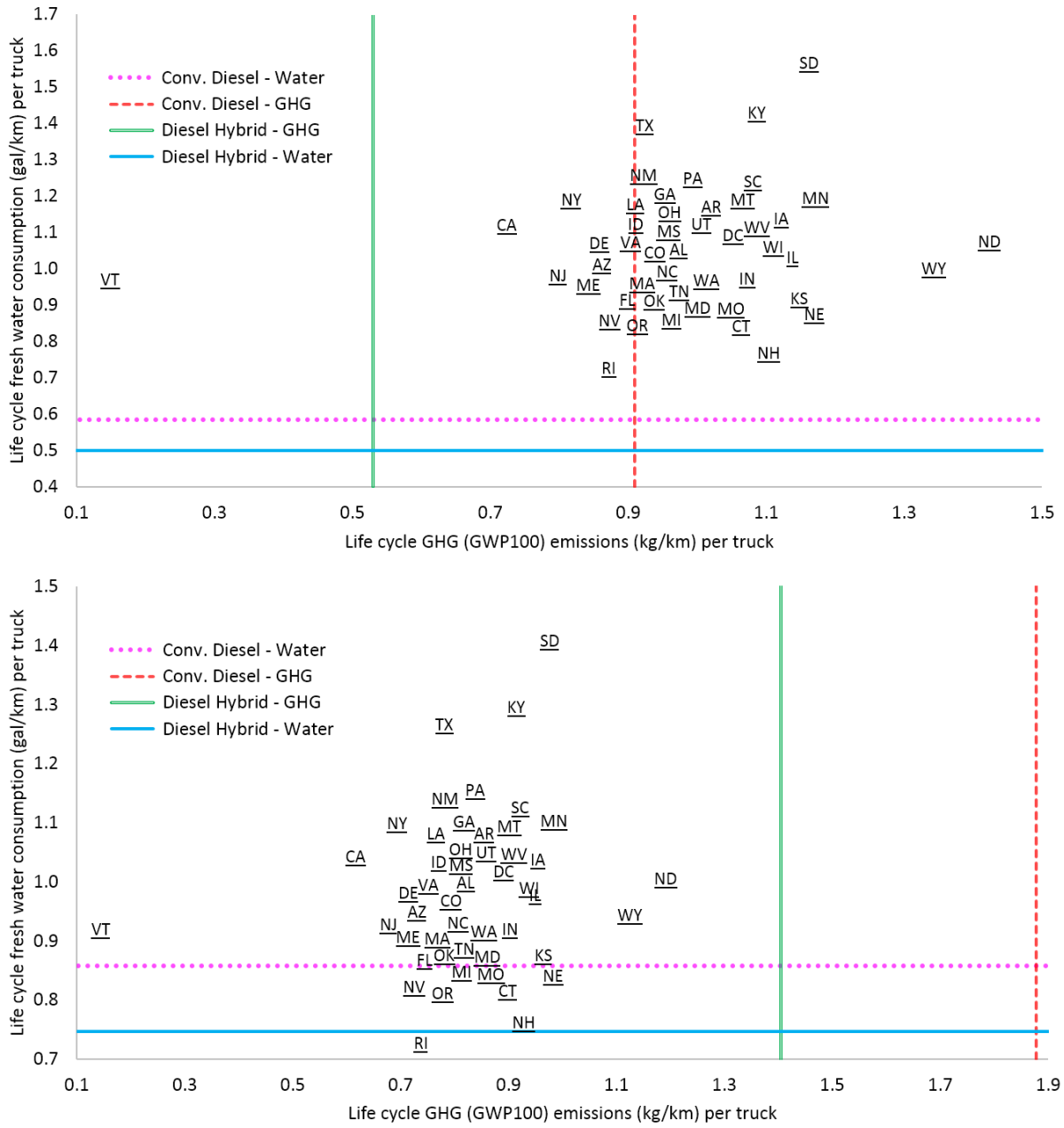

Figure 2.13. Life cycle greenhouse gas (GWP100) emissions and fresh water consumption comparison between electric (marginal electric grid and nighttime charging) and two select non-electric (conventional diesel and hybrid-electric diesel) technologies – for the least severe operating condition (top) and for the most severe (bottom), based on the Fleet DNA truck operation statistics (see Fig. 2.10).

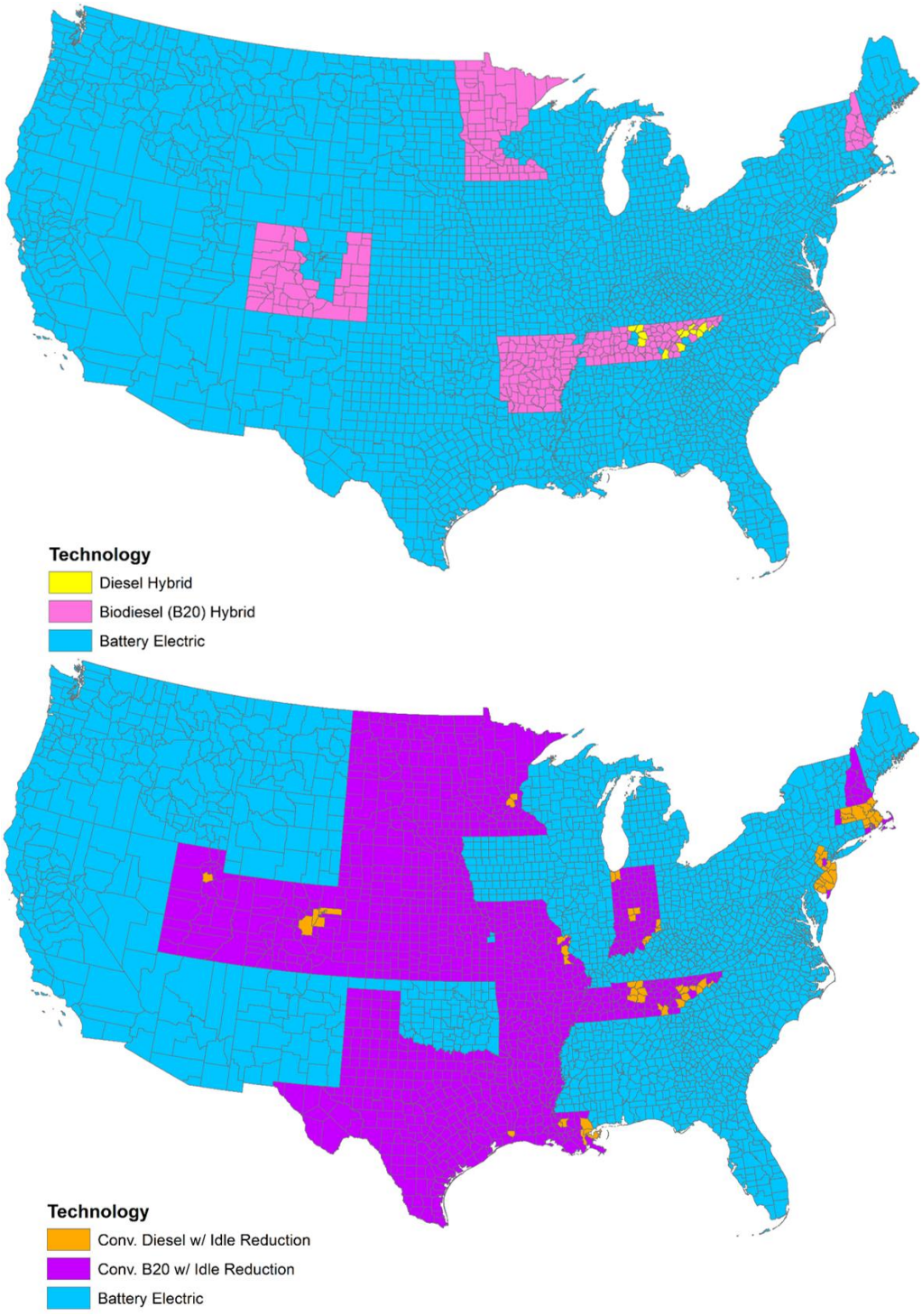

Figure 2.14. Spatial analysis of 2015 social life cycle cost (sum of total cost ownership and monetized life cycle air emissions impacts) for most severe truck operating condition (see Figure 2.10) – the best application (or sweet spot) for electric trucks – excluding (top) and including (bottom) the idle reduction option, based on Monte Carlo simulation using real-world truck activity data.

2.10 Necessary Conditions for Robust Benefits from Truck Electrification

The future is hard to predict. Nevertheless, successful medium-duty truck electrification requires electric trucks to be able to compete cost-effectively in major freight truck applications (e.g., typical or average operating conditions) beyond the niche market (e.g., the most severe operating conditions). Relying on Monte Carlo simulations based on the cost analysis and the predictive LCA models above, I sweep through entire domain of average trip speed and WPKE in Figure 2.10 and identify which conditions are necessary for electric trucks to become cost-effective. In doing so, I simultaneously vary key input cost parameters (e.g., capital cost, fuel prices, etc.). Testing the entire spectrum of operating condition characteristics as such is possible mainly because of the functionality of the parametric LCA approach with which I can see not only the trade-offs but also the robustness of competing technologies over the entire range of input variables. Furthermore, without detailed duty cycle data, my model enables the estimation of life cycle results with only a few variables of publicly-available truck operating statistics (e.g., NREL Fleet DNA project and EPA SmartWay). For simplicity, I define a niche application (for electric trucks) as the 5^{th} percentile in the cost-effectiveness probability domain between electric and non-electric technologies. Major market or application refers to 50^{th} percentile in the same domain. I exclude higher percentile cases, because my analysis indicates that it is very unlikely that electric trucks can compete against non-electric trucks in those conditions (e.g., long-haul and/or highway).

Figure 2.15 shows necessary conditions for electric trucks to be cost-effective and the advantage to be robust against B20 with idle reduction and conventional internal combustion engine technologies. Note that B20 with idle reduction is the second most cost-effective technology next to battery electric in niche application (Figure 2.14).

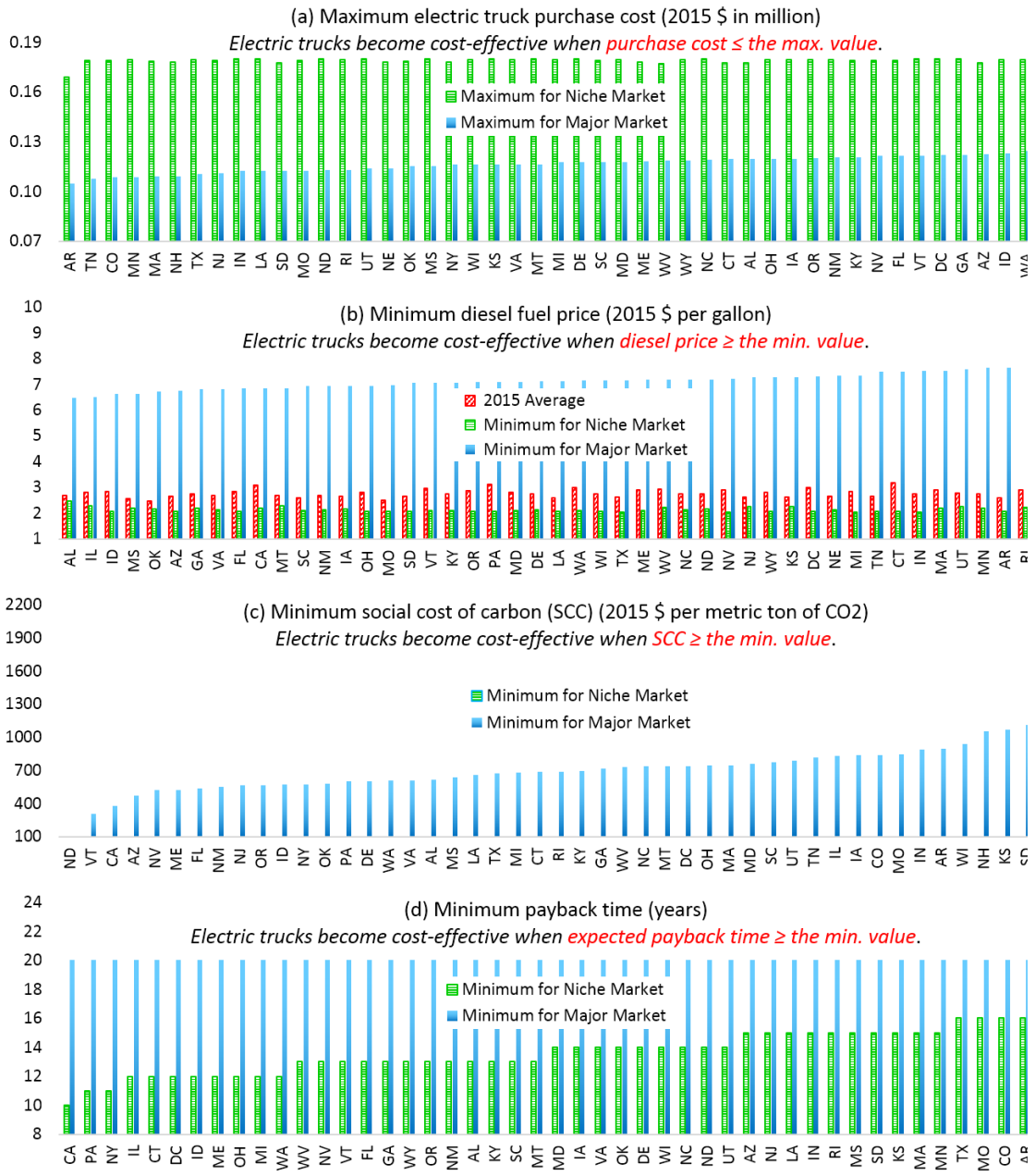

Figure 2.15. Necessary conditions for electrifying medium-duty freight trucks to be cost-effective, and for the advantage to be robust for a niche and major market penetration: (a) maximum electric truck capital cost; (b) minimum diesel fuel price; (c) minimum carbon price; (d) minimum payback time. Missing values in (c) indicate that electric trucks are cost-effective even without giving credits with social cost carbon. The analysis is based on Monte Carlo simulation using the parametric life cycle model, hourly temperature profiles, hourly marginal electricity consumption characteristics, statistical distribution of operating conditions (Figure 2.10).

Conventional internal combustion engine trucks powered by biodiesel (B20) is the most cost-effective technology in average operating conditions. More than 90% of the counties favor B20 in terms of social life cycle cost. Figure 2.15 shows that maximum capital cost of electric trucks ranges from $170,000 to $180,000 for niche market and from $105,000 to $130,000 for major market. This confirms that electric trucks are cost-competitive and robust for niche market, even under 2015 electric truck prices ($150,000 - $180,000 for the largest and heaviest model – see Table 2.1). However, to penetrate major market, electric truck capital costs must fall by about half or 30% at least, varying by region. In terms of fuel prices, it is required that 2015-2030 average diesel fuel prices are in the range of 2 – 2.5 $/gallon for the cost-effectiveness of electric trucks to be robust in the niche market application. This required range is lower than the 2015 average price in all the states, which means current low diesel fuel prices do not negate the cost-effectiveness of electrification in niche applications. However, more drastic conditions are needed for major market application robustness, that is, 6.5 – 8.1 $/gallon. This result implies that within reasonably expected diesel fuel prices in the future, electric trucks' cost-effectiveness is not robust in terms of the major market adoption potential. According to the result of minimum required social cost of carbon (SCC), carbon emissions reduction benefit of electric trucks does not sufficiently compensate the lack of cost-effectiveness either in niche or major market. To be robust in the major truck market, giving credits to carbon emissions reduction for electric trucks, the SCC must be higher than $300 – 2,000 $/metric ton of CO_2, which is significantly higher than the typically-used SCC of $30 – 60. Although not shown, according to my calculations, the maximum discount rate required ranges from 14% to 19% for the niche market, which is similar to or higher than the range of 5% - 15% that is typically used. This finding means that the cost-effectiveness of electric trucks in the niche market is robust. There exist no positive discount rate solutions for major market application, confirming that electric trucks are less likely to be cost-effective in that application. This result can be inferred by the fact

that the necessary maximum capital cost for major market (Figure 2.15 – a) is below the normal range for an electric truck ($0.15 – 0.18 million dollars). The electric trucks' robustness in cost-effectiveness for niche application is conditional on the expected payback time ranging from 11 – 20 years. If the desired payback time is less than 10 years, it is very unlikely that an electric trucks can be cost-competitive in comparison with non-electric trucks. Lastly, given the wide range of variability of necessary conditions between regions, my analysis shows that policy incentives to promote electric trucks could be region-specific. For example, if electric trucks are to be adopted for a major market application in Massachusetts, about $40,000 – $70,000 incentives or tax credits for electric truck purchases may be needed to compensate the expensive upfront capital cost, whereas $20,000 – $50,000 will be needed in California.

CHAPTER 3

HEAVY-DUTY VEHICLE ELECTRIFICATION

3.1 Chapter Summary

Variability and data gaps are among the continuing challenges for life cycle assessment (LCA). The economic and environmental life cycle performance of an industrial product or its use are inherently functions of the variables and parameters associated with product attributes, use profiles, and external environmental characteristics. Therefore, much of the variations of LCA results can be explained and/or predicted by modeling over the ranges of input values or by using functional forms. This is different from uncertainty and/or sensitivity analysis which shows the influence of each or group of input variables but doesn't explain or improve the lack of generalizability of LCA results.

Using transit bus electrification as a case study, I characterize and parameterize variable inputs and then treat them as variables in LCA so that results can be presented in functional forms or spectra. This shows how LCA results change in relation to input variables, and improves the generalizability of the assessment. Also, a parametric LCA modeling approach helps not only identify the potential bias of averages and extremes but also reveal data and future research needs for LCA in general.

3.2 Motivation

Variability – lack of consensus in data and results – is recognized as one of the unresolved challenges of life cycle assessment (LCA) (Reap et al. 2008a, 2008b; Masanet et al. 2013). Relying on commonly-used values can reduce variability at the risk of suppressing important variations. Alternatively, variability can be reduced through case-specific studies, for example, tailored to individual product operating conditions, as in comparative LCAs of transportation vehicles and fuels (Raykin et al. 2012a, 2012b; Karabasoglu and Michalek 2013; Lee et al. 2013; Taptich and Horvath 2014). Sources of variability and their effect on LCA outcomes have regularly been identified and evaluated (Kennedy et al. 1997; Huijbregts 1998; Lloyd and Ries 2007; Venkatesh et al. 2011a, 2011b; Hauck et al. 2014). Even so, the extent to which LCA results can be applied to conditions other than the ones studied is unclear. To fill this research gap, I show here a parametric LCA modeling approach: when the variation in parameters can be quantified and/or the relationship between key input variables and LCA output can be identified, the results can be developed as a function of the variables. This parametric approach not only can address the generalizability issue but also can help avoid biases of averages or extremes by revealing the changing patterns of the LCA results over the ranges of the variables. Furthermore, the parametric approach can improve descriptive and predictive power of conventional LCA and therefore alleviate the data gap challenge (Steinmann et al. 2014) and identify the data needs.

3.3 Rationale for Parametric Modeling Approach

Typical life cycle assessment (LCA) is based on an aggregation structure of linear combination of individual life cycle components, as follows:

$$e_{LC} = e_{PROD} + (1 + \tau_{FSC}) \cdot e_{OP} + e_{NFOM} + e_{INFRA} + e_{EOL} \quad (3.1)$$

where e is energy (MJ/mile) or air emissions (gram/mile) inventory or impacts per distance traveled (VMT) for life cycle (LC), product production (PROD), operation (OP), non-fuel operation and maintenance (NFOM), infrastructure (INFRA), and end-of-life (EOL); and τ_{FSC} is fuel supply chain (FSC) factors – inverse of FSC efficiency (η_{FSC}), $\frac{1}{\eta_{FSC}}$, for energy and FSC emissions factor (gram/MJ), EF_{FSC}, for air emissions. Most of the time, life cycle results (e_{LC}) are presented as point estimates (averages or case-specific) with ranges. However, as the results are inherently functions of input conditions and the aggregation is based on linear combination, once individual life cycle components in Eq. (3.1) are parameterized and the aggregated results converge to a certain pattern, the final results can also be presented in functional forms. Additionally, industrial products including mechanical systems (e.g., vehicles) have relatively clear deterministic properties/characteristics unlike socio-economic phenomena that oftentimes have no clear cause-and-effect relationship. Having deterministic relationship between input and output factors as such is another enabling element for the parametric LCA approach.

3.4 Transit Bus Electrification Case Study

In this study, I demonstrate the parametric modeling approach through a case study of transit bus electrification. I assess life cycle primary energy efficiency as well as greenhouse gases (CO_2, CH_4, and N_2O) and air pollutants (CO, NOx, PM2.5, PM10, SO_2, and VOC) emissions of various types of electric buses in comparison with conventional diesel, diesel hybrid-electric, and natural gas buses. More specifically, I evaluate three non-electric bus technologies: diesel (DB), diesel hybrid-electric (DHEB), and compressed natural gas (CNGB), and four electric bus system architectures: conventional battery electric (BEB), BEB with an on-route overhead DC rapid charging system (BEB-ORC), BEB-ORC with lightweight body (BEB-ORC-LW), and electric trolley (ETB) buses. For the demonstration of the parametric approach, I focus on the vehicle operation phase (e_{OP}). Vehicle operation is known to be the largest variability component in overall life cycle results. Additionally, as shown in the second term in the right side of Eq. (3.1), vehicle operation (often called tank-to-wheel) energy also determines upstream fuel supply chain (or well-to-tank) energy consumption and emissions results, which further increases the importance of vehicle operation phase (e_{OP}) in overall life cycle results. I limit my analysis to model year 2015 buses over 2015 – 2027 (12 years) time horizon.

3.5 Governing Equations

Parameterization of vehicle operation energy use and emissions output begins with the identification of overall relationship and pattern between the input and output values. Also, it is crucial to evaluate relative importance of contributing factors in overall energy consumption or emissions so that the results can be parameterized with important key input variables. Eq. (3.2) shows a normalization by VMT and scaling factors (SF, 10^{-6} for energy and 1 for emissions) for the results from Eqs. (3.3) and (3.4) that are simplified governing equations for energy consumption (J) and emissions (gram) for vehicle operation phase.

$$e_{OP} = \frac{SF \cdot e'_{OP}}{VMT(=\int_0^T V_m dt)} \tag{3.2}$$

$$\begin{aligned} e'_{OP,Energy} = {} & \frac{1}{\eta_{RF}}\frac{1}{\eta_{DT}}\int_0^T \frac{C_{tr}}{\eta_{ESS}\eta_{PM}}(F_{inertia} + F_{res})V dt \\ & + \frac{1}{\eta_{RF}}\int_0^T \frac{1}{\eta_{ESS}\eta_{PM,accessory}} P_{accessory} dt \\ & + \overline{EI}_{coasting} T_{coasting} + \overline{EI}_{braking} T_{braking} + \overline{EI}_{idling} T_{idling} \\ & - \eta_{DT}\int_0^T \eta_{ESS}\eta_{PM}\gamma_{reg} C_{br} \left|(F_{inertia} + F_{res})V + P_{braking,ICE} + P_{braking,friction}\right| dt \end{aligned} \tag{3.3}$$

$$\begin{aligned} e'_{OP,Emissions} = {} & \int_0^T \left[\left(1 - \frac{ER_{AFT}}{100}\right) EMF + \overline{EMI}_{wear,tire}|_{V>0}\right] dt \\ & + \left(1 - \frac{\overline{ER}_{AFT,coasting}}{100}\right) \overline{EMF}_{coasting} T_{coasting} \\ & + \left[\left(1 - \frac{\overline{ER}_{AFT,braking}}{100}\right) \overline{EMF}_{braking} + \overline{EMI}_{wear,braking}\right] T_{braking} \\ & + \left(1 - \frac{\overline{ER}_{AFT,idling}}{100}\right) \overline{EMF}_{idling} T_{idling} \end{aligned} \tag{3.4}$$

Similar to life cycle results in Eq. (3.1), vehicle operation results in Eqs. (3.3) and (3.4) are the aggregated effect of contributing input parameters, including vehicle properties (e.g., vehicle configuration, mass, frontal area, rolling coefficient, etc.), driving characteristics (e.g., acceleration, speed, braking, idling, etc.), and environmental conditions (e.g., road surface condition, ambient temperature, road grade, etc.). More

specifically, vehicle operation energy is a combined result of propelling the vehicle ($F_{inertia}$); overcoming resistance force (F_{res}) related to rolling, slope climbing, and aerodynamic drag; providing accessory load ($P_{accessory}$); coasting ($EI_{coasting}$), braking ($EI_{braking}$), and idling (EI_{idling}); and recuperating energy by regenerative braking shown in the third integral term in Eq. (3.3). Likewise, two of the key input parameters in Eq. (3.4), after-treatment emissions reduction efficiency (ER_{AFT}) and engine output emissions factors (EMF), are all functions of $F_{inertia}$ and F_{res} as shown in Eqs. (3.5) – (3.7).

$$ER_{AFT} = p(L) \tag{3.5}$$

$$EMF = q(L) \tag{3.6}$$

$$\begin{aligned} L = \frac{1}{\eta_{DT}\eta_{ESS}\eta_{PM}}\left[C_{tr}(F_{inertia} + F_{res})V + \frac{\eta_{PM}}{\eta_{PM,accessory}}P_{accessory}\right] \\ - \eta_{DT}\eta_{ESS}\eta_{PM}\gamma_{regen}C_{br}\left|(F_{inertia} + F_{res})V + P_{braking,ICE} + P_{braking,friction}\right| \end{aligned} \tag{3.7}$$

All these contributing factors ($F_{inertia}$, F_{res}, ER_{AFT}, EMF, etc.) are essentially functions of the duty cycle variables as in Eqs. (3.8) – (3.10). More specifically, vehicle mass (m), speed (V), acceleration (a), and road grade (θ) affect virtually every component in the governing equations for operation phase energy consumption and emissions results in Eqs. (3.3) and (3.4).

$$F_{inertia} = ma = (m_{curb} + m_{PX})a \tag{3.8}$$

$$F_{res} = C_{rr}mgcos\theta + \frac{1}{2}\rho AC_D V^2 + mgsin\theta \tag{3.9}$$

$$\theta = tan^{-1}\left(\frac{\%\ slope}{100}\right) = tan^{-1}\left(\frac{\Delta h}{s}\right) \tag{3.10}$$

Also, duty cycle factors determine the driving regime – traction in Eq. (3.11), braking in Eq. (3.12), coasting ($F_{inertia} = F_{res}$), or idling ($e'_{OP,Energy} > 0$ when $V = 0$).

$$C_{tr} = \begin{cases} 1, & (F_{inertia} + F_{res}) > 0 \\ 0, & otherwise \end{cases} \quad (3.11)$$

$$C_{br} = \begin{cases} 1, & \left(F_{res} + F_{braking,ICE} + F_{braking,friction}\right) < -F_{inertia} \\ 0, & otherwise \end{cases} \quad (3.12)$$

Having said that, it is not surprising that the duty cycle factors explain large portion of the variations in energy use and emissions output values. In addition to the duty cycle variables, factors associated with the characteristics (e.g., efficiency, η_{PM}) of prime movers – internal combustion engine (ICE) or electric motor – are among the key components in the governing equation for energy, Eq. (3.3). Likewise, prime mover-related factors (e.g., engine output emissions, EFM) along with after-treatment systems are the important parameters in the emissions governing equation, Eq. (3.4).

3.6 Direct Operation Phase Energy and Emissions Simulation

When identifying the relationships between input parameters and output values for energy use and emissions, the best approach would be finding analytic solutions to the governing equations in Eqs. (3.3) and (3.4). However, because of the non-linearity and interactions between the terms, it is difficult to derive analytic solutions for Eqs. (3.3) and (3.4). For example, the prime mover efficiency (η_{PM}) is a function of $F_{inertia}$, F_{res}, powertrain control algorithm, and other input parameters. For this reason, instead of analytic approach, I rely on vehicle dynamic and emissions simulation to estimate the energy consumption and air emissions. More precisely, I collect data from the vehicle dynamic and emissions simulations to construct a sample space and derive overall relationship between the input and output.

I use West Virginia University's Integrated Bus Information System (IBIS) as the primary data source for fuel consumption and tail-pipe emissions for DB, DHEB, and CNGB (Wayne et al. 2011; FTA 2013). IBIS provides only certain level of specificity. I complement IBIS with Motor Vehicle Emission Simulator (MOVES) model (EPA 2014a) for more detailed analysis (e.g., vehicle weight, road grade, and hot/cold conditions, etc.). Note that I use MOVES only as a secondary data source to avoid the inaccuracy issues (FTA 2013), errors (EPA 2012b), and lack of transparency of the statistical black-box model of MOVES. Comparable to the Altoona proving ground test results (LTI 2013), the IBIS data are based on thousands of dynamometer and in-use vehicle test results archived in publicly-available place and therefore more verifiable and reliable. As a benchmark, I also use energy consumption and emissions standards from the recent heavy-duty vehicle regulations (Phase I and proposed Phase II) and regulatory impact assessments (EPA 2011; Federal Register 2011; Federal Register 2013; EPA 2015c; Federal Register 2015a). For electric buses, I utilize the Advanced Vehicle Simulator (ADVISOR), an open source vehicle dynamic simulation software (ImagineMade 2014). I adopt a variety of drive cycles collected from publicly available

sources (ARTEMIS 2006; EPA 2014a; ImagineMade 2014) and simulate them in ADVISOR and MOVES.

3.7 Explanatory Variables

As briefly mentioned earlier, parametric modeling approach relies on the convergence of the life cycle results. This in turn requires that a set of input variables explains a significant portion and structure of the changing relationship (or pattern) of the results conditional on the input parameters. To identify the appropriate set of explanatory input variables as such, I evaluate the contribution of individual input components in Eqs. (3.3) and (3.4) in terms of the variability of overall energy use and emissions results. Not only absolute (or gross) contribution of individual components but also relative importance between them in overall energy consumption or emissions determine the relationship and pattern of changing life cycle results with respect to the input parameters. Figure 3.1 shows some of vehicle operation energy consumption components for diesel (DB) and electric (BEB-ORC-LW) buses – two technologies at both ends of the electrification spectrum. For both non-electric and electric buses, prime mover efficiency has a close relationship with average trip speed ($\bar{V}_{trip}$ in miles/hour, as opposed to V_t in meter/sec) defined in Eq. (3.13), as do aerodynamic resistances. Rolling resistances in MJ/mile are almost constant, varying only with vehicle weight (empty or full). To explain rolling resistance energy-related variability, vehicle weight will be an essential parameter. In contrast, neither the inertia term (or useful work) in Eq. (3.8) nor recuperated energy from regenerative braking can be effectively explained by $\bar{V}_{trip}$. For this, based on the inertia-related energy equation in Eq. (3.14), I modify Watson et al.'s (1983) positive kinetic energy (PKE) concept and define weighted PKE (WPKE) as in Eq. (3.15). In Eq. (3.14) – (3.15), vehicle mass at time t (m_t) is the sum of curb weight and passenger loading weight, and N_T is the unit-less length (total duration) of the trip, which has the same value as T but no unit. Dividing the summation of vehicle mass (m_t) by N_T is trip (or cycle) average vehicle mass ($\bar{m}$). As shown in Figure 3.1, whether non-electric and

electric technologies, WPKE can effectively explain the changing behavior of useful work and recovered energy.

$$\bar{V}_{trip} = \frac{2.24 \sum_{t=1}^{T} V_t}{T} \tag{3.13}$$

$$E_{inertia} = \int_0^D (ma)ds = \int_0^T mVdV \approx \frac{1}{2}\sum_{t=1}^{T} m_{t-1}\left({V_t}^2 - {V_{t-1}}^2\right)\Big|_{V_t > V_{t-1}} \tag{3.14}$$

$$\begin{aligned} WPKE &= \frac{\sum_{t=1}^{T} m_{t-1}\left({V_t}^2 - {V_{t-1}}^2\right)\Big|_{V_t > V_{t-1}}}{\int_0^T Vdt} \\ &\approx \frac{\left(\sum_{t=1}^{T} m_{t-1}\right)\left[\sum_{t=1}^{T}\left({V_t}^2 - {V_{t-1}}^2\right)\Big|_{V_t > V_{t-1}}\right]}{1000 \times N_T \int_0^T Vdt} \end{aligned} \tag{3.15}$$

Another important implication in Figure 3.1 is that prime mover characteristics is the most influential factor for non-electric buses, as is useful work for electric buses. Engine loss accounts for over 60% of overall operation energy use, whereas electric motor's portion is about 10%. The share of useful work for diesel bus is around 7%, but it takes 40% of energy for electric bus on average. Rolling energy accounts for approximately 40% of energy use for electric buses, but the variability is very small, which makes useful work the largest variability factor. From the parameterization standpoint, given the significance of prime mover characteristics for non-electric buses, it is natural to choose average trip speed as a key explanatory variable. This complies with previous studies (Chester et al. 2010; Delgado et al. 2011; Wayne et al. 2011; EPA 2012c; FHWA 2013; FTA 2013; Lajunen 2014) that showed the close relationship between average trip speed and energy use and emissions. For electric buses, since useful work is the largest contributor of energy consumption and its variability (and thus emissions) in general, WPKE becomes the most important explanatory variable.

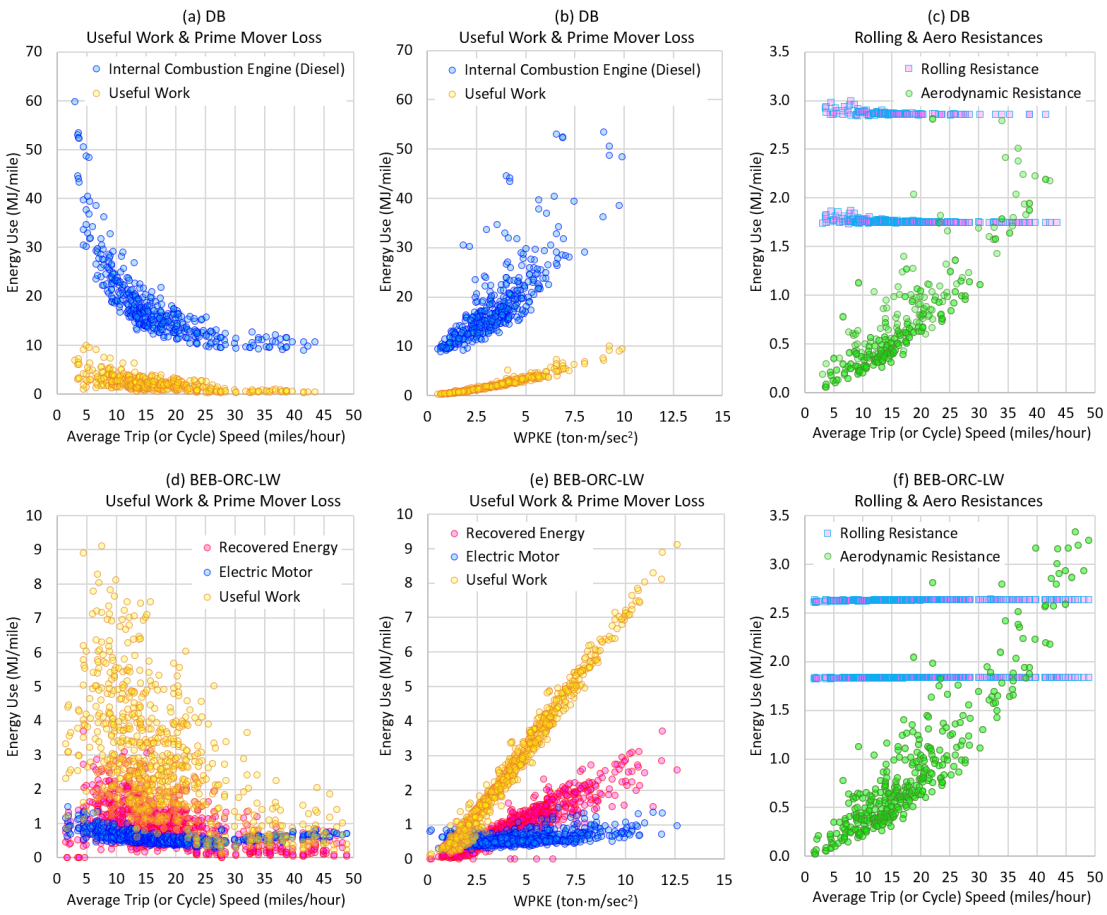

Figure 3.1. Component-by-component vehicle operation energy use samples for diesel (DB) and battery electric with on-route rapid charging system and lightweight body (BEB-ORC-LW) buses: Useful work, prime mover energy loss, and recovered energy in the spectrum of average trip speed (a and d) and WPKE (b and e); rolling and aerodynamic resistance energy loss (c and f).

3.8 Indirect Energy Use and Emissions

Energy use and emissions from the upstream fuel supply chain for petroleum diesel and natural gas are based on data from GREET (ANL 2015). GREET was also used for the power plant construction and electricity generation fuels supply chain inventory. For vehicle maintenance and repairs inventory, I use the EIO-LCA database (CMU GDI 2008). As for energy consumption and emissions from power plant operation, I develop a state-by-state electricity consumption fuel mix and emissions model to incorporate spatial and temporal heterogeneity. For this, I use data from the U.S. Energy Information Administration's Annual Energy Outlook and Electric Power Monthly; and the U.S. Environmental Protection Agency's Emissions & Generation Resource Integrated Database (eGRID); and Continuous Emissions Monitoring System (EIA 2015b, 2015c; EPA 2016a, 2016b). Using the methods proposed by Siler-Evans et al. (2012) and Marriott and Matthews (2005), I also estimate air emissions for marginal electricity consumption. Both average and marginal air emissions for electricity consumption are shown in Figure 3.2. I take the result for Year 2014 as a baseline and project future years' emissions reduction potentials based on the Clean Power Plan (Federal Register 2015b).

I use material composition data for diesel-powered city buses manufactured by Volvo (Pusenius et al. 2005) and Mercedes-Benz (Ally and Pryor 2008). I disaggregate the data for vehicle parts (e.g., body and chassis, powertrain, transmission, tires, fluids, and etc.), based on the bus specifications and vehicle parts' material input information from GREET (ANL 2015). I adjust the body and chassis data for my target vehicles based on vehicle specifications, and the result is used as a common platform across the bus technologies in consideration. I aggregate all the other remaining vehicle parts including

fluids for each of the technologies to complete the inventory for vehicle production, maintenance, and end-of-life (EOL). More detailed information for bus and parts and inventory results can be found in Appendix B.

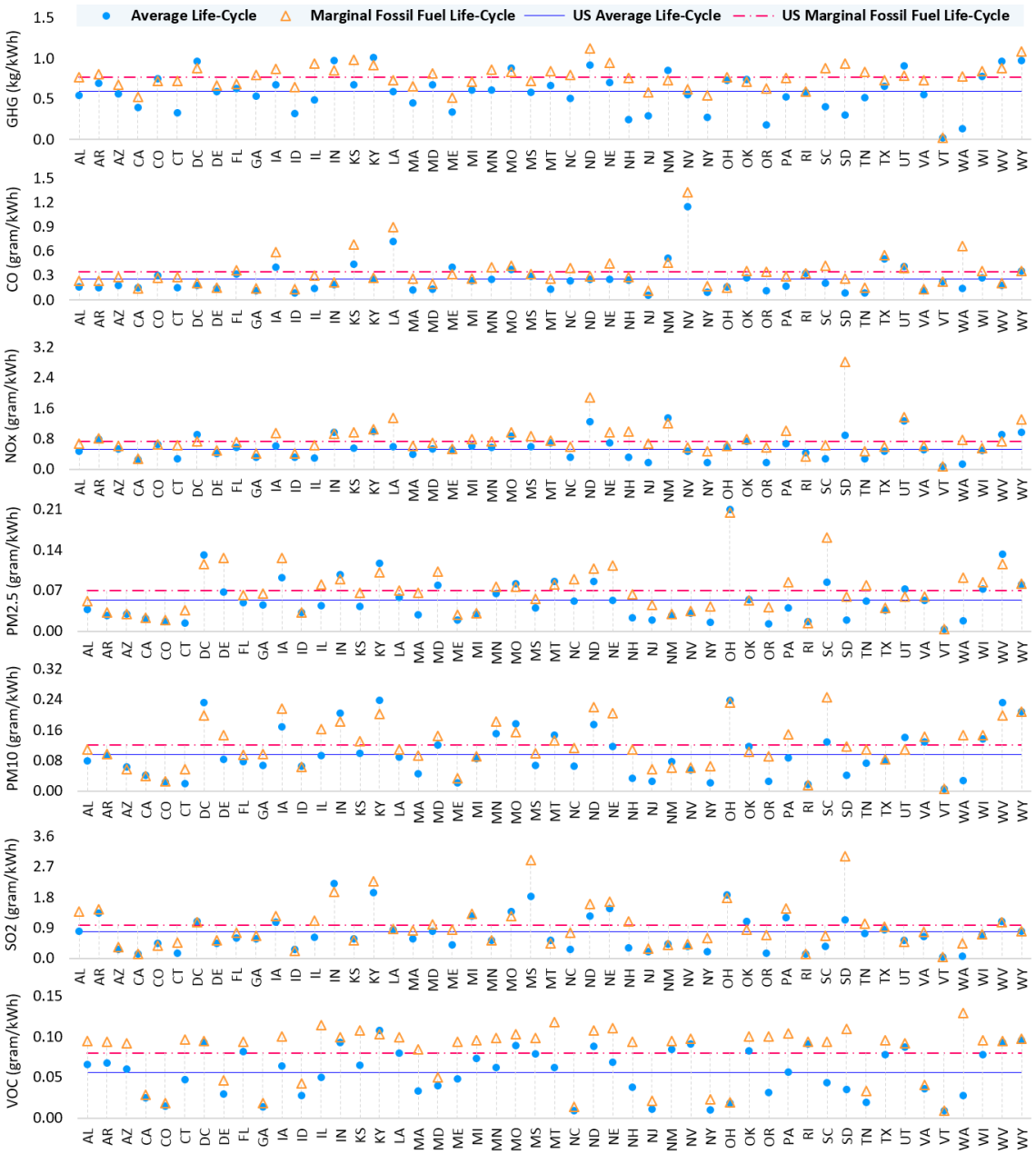

Figure 3.2. Annual average (Year 2014) life cycle emissions per unit electricity consumed (or life-cycle power consumption emissions) for average and marginal electric grid in the contiguous U.S.

Natural gas, battery electric (with or without on-route rapid charging), and electric trolley buses all require a dedicated energy supply infrastructure to refuel and operate vehicles. When it comes to the infrastructure, lock-in effects and economies of scale are among the most important factors. The latter is directly related to vehicle fleet size for which I use the non-linear marginal infrastructure cost reported in IBIS for CNGB. In principle, BEBs can be charged on layover, overnight, or whenever possible. Given the large battery capacity (320 kWh) and corresponding range, however, I assume that BEB fleet operators will charge the BEBs once a day with the BEB manufacturer's 324 kW fast charger system so the battery lifetime can be maximized (Bullis 2011). In the case of the BEB-ORC, to have a comparable operating range to BEB, two ORC (300 kW) stations, one in the depot and the other on route will be needed, which can be shared by the fleet of 10 – 20 BEB-ORC's without service disruptions (De Filippo et al. 2014). I assume that the fleet of 10 ETBs serve a 24-mile route with the requirement of 12 miles of a two-way overhead wire system, in which each ETB is deployed to the route five or more times a day (Proterra 2009; KCM 2011). Environmental impact associated with the refueling infrastructure are normalized on a per-vehicle basis. I adopt the EIO-LCA database (CMU GDI 2008) to analyze the economy-wide impact of refueling infrastructure construction and operation.

3.9 Spatio-temporal Heterogeneity

In addition to the electric grid characteristics discussed above, I consider spatial and temporal variations in climatic condition, road grade, and fuel properties. Both climatic condition (e.g., ambient temperature and relative humidity) and road grade are cyclic parameters which fluctuate from moment to moment and from route to route. However, over a long span of time, road grade leads to rather universal (not cyclic) effect on energy consumption and emissions regardless of technologies – stiffer road grade resulting in higher level of energy consumption and emissions as can be seen in Eqs. (3.3) – (3.10). I don't correlate road grade with city, county, or region, which otherwise is misleading, because road grade varies not only between but also within those geographical boundaries. In other words, road grade depends on individual routes rather than geographical boundaries. Sometimes, road grade is juxtaposed with drive cycle, most of the time assuming that the two are independent. However, doing so can introduce significant biases. For example, each additional 1% constant uphill road grade reduces the top speed of transit buses by roughly 10 miles/hour (i.e., +4% corresponding to about 40 miles/hour reduction), compared to 65-70 miles/hour maximum speed on level ground. Note that road grade also limits maximum achievable acceleration. Because the time derivative of the left side of Eq. (3.3) is fixed/rated at maximum power, increasing road grade will affect/constrain other parameters (e.g., speed, acceleration, etc.), which is another reason why juxtaposing road grade and drive cycle is not a fair and realistic analysis. Also, it is crucial to consider not only uphill condition but also downhill portion of the trip to more accurately account for round-trip characteristics of vehicles. In case of electric buses, other complications may occur. For example, depending on the initial state of charge of traction battery which is not very repeatable or controllable, the impact of road grade on the energy consumption can be very different. For these reasons, I rather exclude road grade in my model, although I evaluate road grade impact of different technologies in Appendix B. For climatic conditions, I take county-by-county hourly data

for 12 months from MOVES model and average them for the typical transit bus operating duration – 7 am to 10 pm, because picking the hottest/coldest day and hottest/coldest hour can result in bias of extremes. Fuel properties for diesel or natural gas fuels across the country are assumed to be identical based on the MOVES data (EPA 2014a). MOVES provides location-specific emissions rates for DB and CNGB, but those variations are purely climate-dependent, because MOVES doesn't differentiate the diesel and natural gas fuel properties between locations, especially for inventory year 2014 and later.

3.10 Linear Regression

Governing equations mentioned earlier indicate that duty cycle variables and prime mover factors determine vehicle operation and fuel supply-chain energy use and emissions as well as overall life cycle results. Duty cycle factors are "cyclic" by nature. For instance, speed, passenger loading, and climatic conditions are all cyclic (fluctuating) within each trip. However, what really matters from the LCA perspective is an aggregate effect of those contributing factors. Although passenger loading may be cyclic within a trip, overall effect is universal across technologies, that is, higher passenger loading level leading to higher energy consumption and emissions. All things considered, I identified average trip speed ($\bar{V}_{trip}$), vehicle weight ($\bar{m}$) in metric ton, and weighted positive kinetic energy ($WPKE$) as key variables that can explain the variability patterns. For example, $\bar{V}_{trip}$ explains much of the variability associated with ICE characteristics and aerodynamic resistance; $\bar{m}$ rolling resistance; and $WPKE$ useful work (or kinetic energy). I also considered a variety of kinematic duty cycle characterization parameters (e.g., average positive acceleration, number of accelerations, standard deviation of speed, average product of speed and acceleration, etc.) but found that the three variables ($\bar{V}_{trip}$, $\bar{m}$, and $WPKE$) are enough to explain more than 90% variability of life cycle results. Adding more variables would increase specificity, but increasing precision and/or complexity doesn't always lead to more accurate results. Among the three key variables I identified, $\bar{V}_{trip}$ and $\bar{m}$ are intuitive, easy to understand, and widely used. WPKE is by definition, as in Eq. (3.15), directly related to kinetic energy which in turn has much to do with driving behavior. More specifically, for the same average trip speed which is a proxy for transportation productivity or efficiency (distance and/or passengers moved per unit of time), higher WPKE means more aggressive driving or vice versa. Based on the data and key explanatory variables discussed thus far, I employ a linear regression

method and develop a set of functions/equations for estimating life cycle inventory (LCI) for energy consumption and air emissions.

Figure 3.3 graphically illustrates my basic parametric model, for which some quantitative regression results (equations) are presented in Table 2.1, which are all based on the generic equation of Eq. (3.16):

$$\hat{Y}_{i,t} = exp\left[\hat{\varphi}_{0_{i,t}} + \hat{\varphi}_{1_{i,t}}\bar{V}_{trip} + \hat{\varphi}_{2_{i,t}}\frac{1}{\bar{V}_{trip}} + \hat{\varphi}_{3_{i,t}}\,log\left(\bar{V}_{trip}\right) + \hat{\varphi}_{4_{i,t}}\bar{V}_{trip}{}^{2} + \hat{\varphi}_{5_{i,t}}\bar{m} + \hat{\varphi}_{6_{i,t}}WPKE\right] \tag{3.16}$$

where $\hat{Y}_{i,t}$ is estimated results for the i-th LCI (energy consumption and air emissions) and t-th technology (DB, CNGB, DHEB, BEB, BEB-ORC, BEB-ORC-LW, and ETB), and $\hat{\varphi}$'s are estimated parameters. Lines (or curves) in Figure 3.3 show average patterns that can be estimated with only average trip speed. Light shades are for the variability caused by passenger loading variation. Dark shades are for the impact (on top of the passenger loading) of driving behavior variation

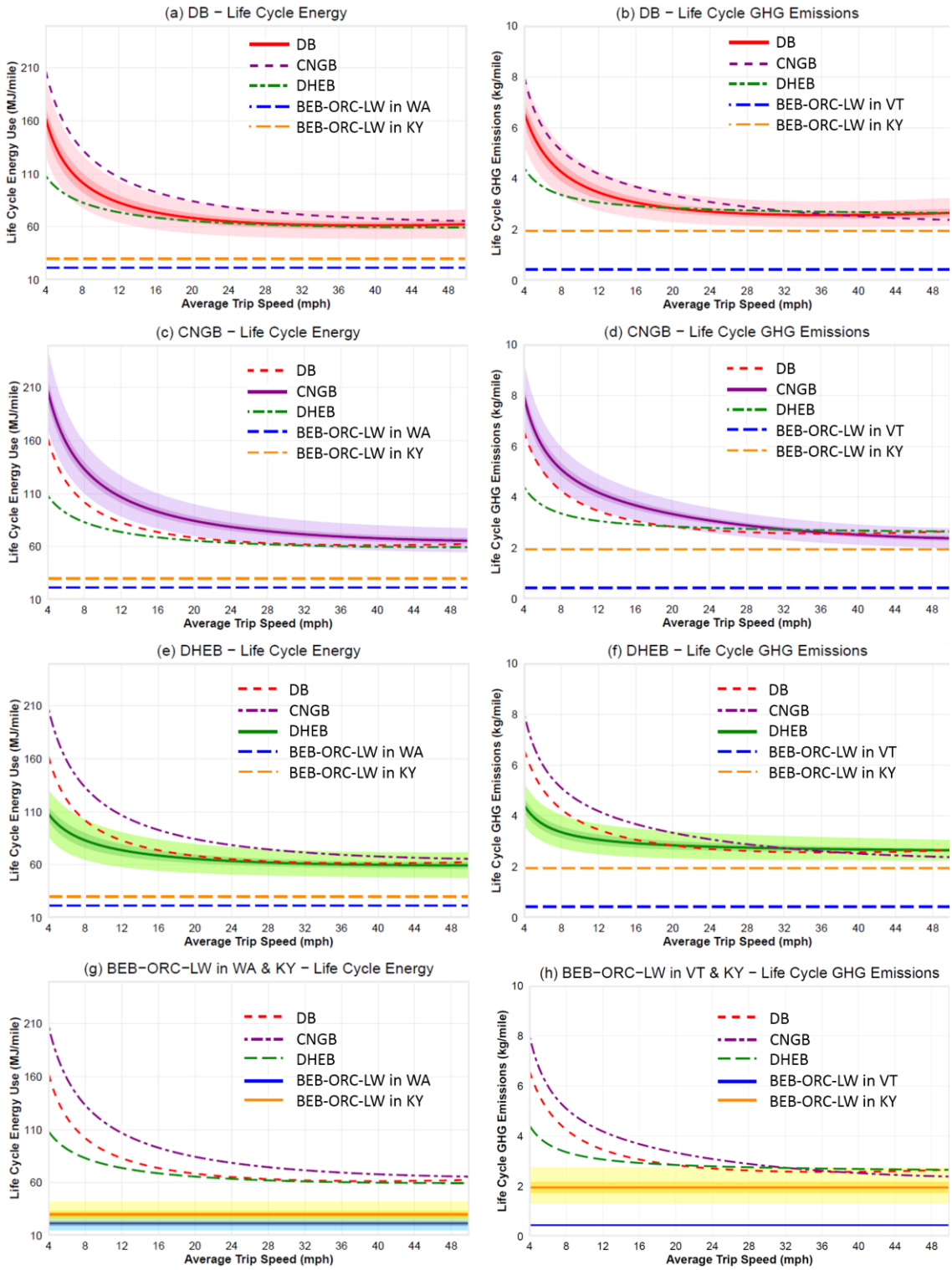

Figure 3.3. Life cycle energy use and GHG emissions – lines: average, dark shades: variation related to passenger loading, and light shades: variation associated with driving behavior.

Table 3.1. Linear regression models for life cycle energy use and GHG emissions

$\hat{\varphi}_j's$ for Energy (MJ/mile)	DB	CNGB	DHEB	BEB-ORC-LW (WA)	BEB-ORC-LW (KY)
Intercept	3.63	4.68	3.6	2.4	2.65
$\bar{V}_{trip}$					
$\bar{V}_{trip}^{-1}$	3.35	1.63	1.55		
log($\bar{V}_{trip}$)		-0.23			
$\bar{V}_{trip}^{2}$	$7.9\text{x}10^{-5}$	$6.93\text{x}10^{-5}$	$7.2\text{x}10^{-5}$	$1.62\text{x}10^{-4}$	$1.8\text{x}10^{-4}$
$\bar{m}$	$1.16\text{x}10^{-2}$	$9.46\text{x}10^{-3}$	$1.66\text{x}10^{-2}$	$1.78\text{x}10^{-2}$	$2\text{x}10^{-2}$
WPKE	$7.5\text{x}10^{-2}$	$6.04\text{x}10^{-2}$	$6.7\text{x}10^{-2}$	$6.97\text{x}10^{-2}$	$7.76\text{x}10^{-2}$
Adj. R^2	0.97	0.98	0.95	0.91	0.91
F-statistic	3243	3380	1962	2625	2567

$\hat{\varphi}_j's$ for GHG (kg/mile)	DB	CNGB	DHEB	BEB-ORC-LW (VT)	BEB-ORC-LW (KY)
Intercept	7.53	7.96	7.42	6.13	6.83
$\bar{V}_{trip}$	$-8.7\text{x}10^{-3}$				
$\bar{V}_{trip}^{-1}$	2.9	2.5	1.4		
log($\bar{V}_{trip}$)		$-8.2\text{x}10^{-2}$			
$\bar{V}_{trip}^{2}$	$2.24\text{x}10^{-4}$	$-6.9\text{x}10^{-5}$	$1.04\text{x}10^{-4}$	$8.08\text{x}10^{-5}$	$1.79\text{x}10^{-4}$
$\bar{m}$	$1.06\text{x}10^{-2}$	$8.65\text{x}10^{-3}$	$1.44\text{x}10^{-2}$	$8.7\text{x}10^{-3}$	$2\text{x}10^{-2}$
WPKE	$6.86\text{x}10^{-2}$	$5.6\text{x}10^{-2}$	$5.72\text{x}10^{-2}$	$3.54\text{x}10^{-2}$	$7.7\text{x}10^{-2}$
Adj. R^2	0.97	0.98	0.94	0.92	0.91
F-statistic	2841	3723	1434	2795	2571

All parameter estimates presented are statistically significant at a 5% significance level.

that leads to deviation from the average lines. For other results than energy use and GHG emissions in Figure 3.3 and Table 3.1, please see Appendix B. Note that I take a log-transformation of the dependent variables to comply with the normality assumption in linear regression. Also, I adopt different forms of the variable $\bar{V}_{trip}$ for better results. These modified terms of $\bar{V}_{trip}$ are correlated with $\bar{V}_{trip}$, but I draw implications based on only $\bar{V}_{trip}$. The three primary variables ($\bar{m}$, $\bar{V}_{trip}$, and $WPKE$) are not correlated one another. As Table 3.1 indicates, the parametric model explains a reasonable amount of variability in life cycle results.

3.11 Assessing Variability

I evaluate the impact of individual variability factors, based on the parametric LCA model. I first estimate constant terms such as vehicle production, infrastructure, non-fuel operation and maintenance, and base (minimum) value of well-to-wheel (direct operation plus fuel supply chain) inventory. I then vary values of input parameters and see how much the results change along with the direction (increase or decrease). The variables I considered include average trip speed (from 50 to 5 miles/hour), driving behavior, passenger loading (from 1 to 40), climatic conditions (VT for non-electric as an example), fleet size (from 40 to 10), electric bus configuration (conventional battery electric to electric trolley), electric bus light-weighting (difference between BEB and BEB-ORC-LW), average to marginal (daytime) electric grid, and daytime to nighttime marginal electric grid. Figure 3.4 illustrates the results for life cycle GHG (GWP100), NOx, and PM2.5 emissions. Average trip speed as well as fuel supply chain components cause the largest variability for GHG emissions of non-electric buses. Overall structure of variability impacts change significantly between geographical areas for electric buses, mainly because of the electricity source variations. Vehicle production and electric bus configuration accounts for the largest variability in Vermont (VT), but driving behavior, climatic conditions, and marginal electric grid characteristics comprise most of the variability in Kentucky (KY). In both Vermont and Kentucky, reducing electric bus weight decreases GHG emissions. On the other hand, marginal electric grid leads to an increase of GHG emissions in Vermont, whereas the opposite pattern is observed in Kentucky because of the transition from coal-based average power generation to firing

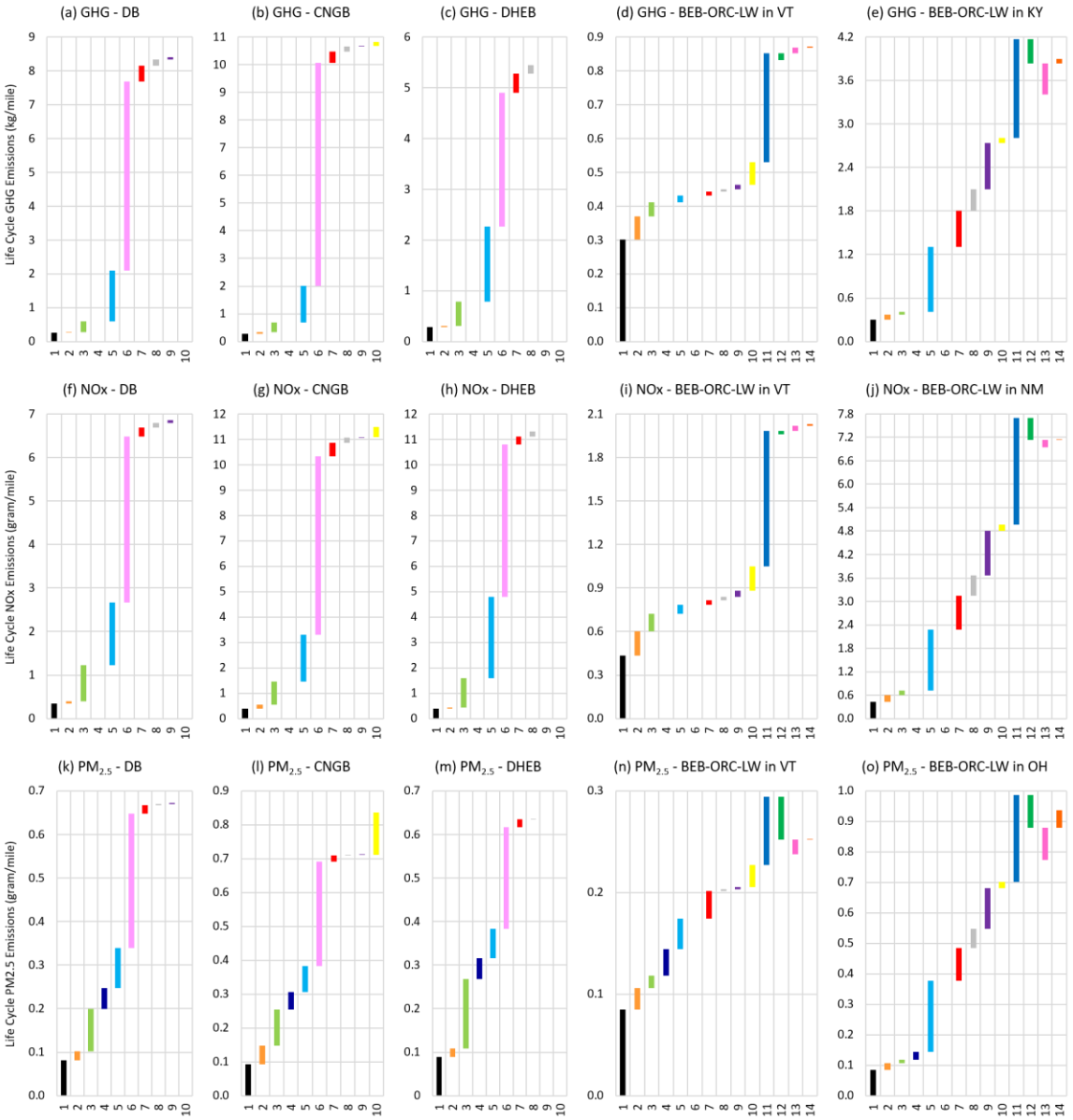

Figure 3.4. Individual variability impacts on top of *base* values (1: production, 2: infrastructure, 3: non-fuel operation and maintenance), using the parametric modeling approach. Horizontal axes – 4: tire and brake wear particulate matters, 5: remaining well-to-wheel *base* value, 6: average trip speed, 7: driving behavior, 8: passenger loading (1 to 40), 9: climatic conditions (VT for non-electric), 10: fleet size (40 to 10), 11: electric bus configuration (BEB to ETB), 12: electric bus light-weighting (BEB to BEB-ORC-LW), 13: average to marginal (daytime) electric grid, 14: daytime to nighttime marginal electric grid.

natural gas (less carbon-intensive than coal) for marginal electricity generation. NOx emissions show similar patterns to GHG emissions. However, PM2.5 emissions

variability reveals somewhat different phenomena. Direct tail-pipe PM2.5 emissions for non-electric buses takes a very small portion in overall well-to-wheel emissions (items 4, 5, and 6 combined), because tail-pipe PM emissions have been reduced dramatically over the years by regulations. Tire and brake wear (item 4) or upstream fuel supply chain emissions (most of the items 5 and 6) are approximately 250% (500% combined) larger than tail-pipe PM2.5 emissions. Unlike GHG and NOx, the variability stemming from tail-pipe emissions is very small, and vehicle production, non-fuel operation and maintenance, and fuel supply chain are the largest sources of variability. The large portion of the average trip speed impact (item 6) is mostly due to not tail-pipe but vehicle operation energy consumption varying with average trip speed and resulting in upstream emissions from the fuel supply chain. This has an important implication in terms of data needs for addressing variability. Depending on the air emission inventory categories (e.g., GHG, NOx, PM2.5, VOC, etc.), focus is to be put on different data and thus different industry sectors, for example, tail-pipe (or vehicle operation) for GHG and fuel supply chain (e.g., natural gas production) for PM2.5.

Variability impact is oftentimes complicated by the choice of functional unit, for example, vehicle miles traveled (VMT) (Figure 3.3) or passenger miles traveled (PMT, a product of VMT and the number of passengers transported) (Figure 3.5). The (marginal) impact of vehicle weight and/or passenger loading can be seen in Figure 3.5, for which the calculation is based on the following equation:

$$e_{LC_{PMT,t}} = \frac{SF \cdot \left(N_V \cdot e_{LC_{Empty,t}} + \Delta e_{LC_{PX,t}} \cdot N_{PX}\right)}{VMT_{LT} \cdot N_{PX}} \tag{3.17}$$

where $e_{LC_{PMT,t}}$ is life cycle inventory of energy consumption or air emissions, the same as Eq. (3.1) if multiplied by N_{PX}, to transport a passenger a mile with the t-th bus technology, VMT_{LT} is lifetime vehicle miles traveled (VMT), N_{PX} is the number of passengers loaded (ranging from 1 to 80), N_V is the number of buses required to transport

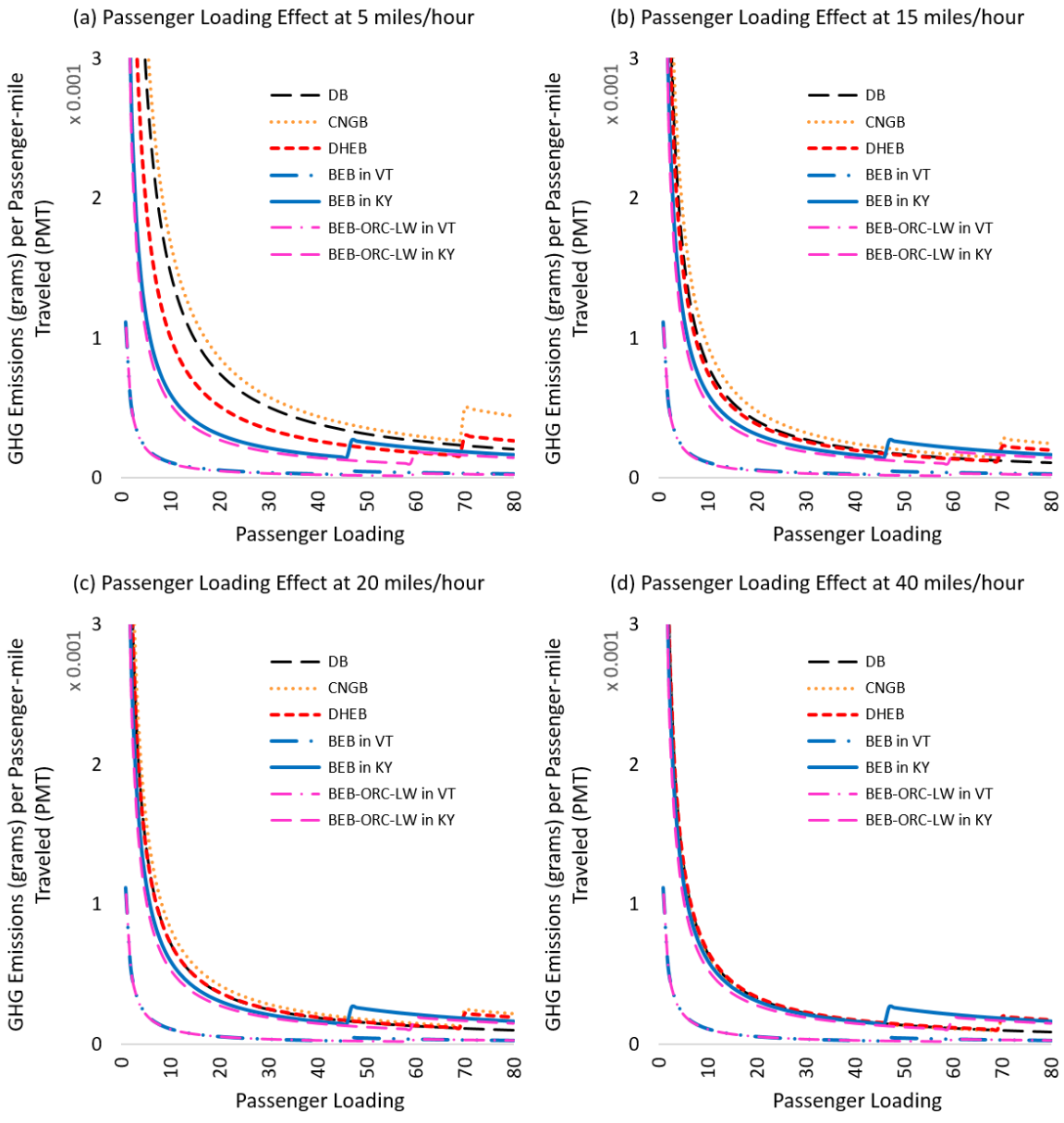

Figure 3.5. Parametric analysis of passenger loading effect on life cycle GHG emissions for four different average trip conditions (5, 15, 20, and 40 miles/hour).

N_{PX} (1 for $N_{PX} \leq N_{Cap_t}$, 2 otherwise) , N_{Cap_t} is passenger loading capacity for the t-th technology, $e_{LC_{Empty,t}}$ is life cycle inventory for empty ($N_{PX} = 0$) condition, and $\Delta e_{LC_{PX,t}}$ is incremental life cycle inventory due to unit increase of passenger loading for the t-th technology. The importance of PMT tends to be over-emphasized because of the suppressing effect of PMT in communicating the life cycle results. Adding one more passenger doesn't significantly increase the energy consumption or emissions on a VMT basis. More importantly, positive or negative change in passenger loading leads to universal effect on energy use and emissions (increase for positive change and vice versa), regardless of vehicle technologies or configurations. This relatively small and universal marginal effect, however, is magnified as the passenger loading is used in denominator for PMT-based life cycle results. PMT is a certainly important functional unit for transportation LCA, but lack of knowledge on passenger loading is not to limit the LCA thereof. Rather, simplification (dividing average life cycle results by PMT) provides reasonable estimates, as long as PMT-based parametric life cycle results are presented or passenger loading condition is specified as well as VMT-based results. It is also crucial to show or acknowledge different capabilities (e.g., maximum speed, passenger loading capacity, grade climbing ability, etc.) of different technologies being compared. Otherwise, the LCA results can be misleading or unfair. In fact, passenger loading is more about criticality than exact number of passengers, especially in terms of comparing different technology options. As shown in Figure 3.5, even when not knowing exact passenger loading condition, the parametric LCA approach enables an easy evaluation of the effectiveness of improving ridership (increasing passenger loading) in comparison with switching from non-electric to electric bus technologies. In case of 5 miles/hour average trip speed, improving ridership is less effective than switching to electric buses for reducing GHG intensity for the same PMT. However, the comparison changes drastically for higher level of passenger transportation demand, because electric

buses have a lower passenger loading capacity than non-electric counterparts, as can be seen in Figure 3.5-(b) and (c). However, in medium- to high-speed operation in Kentucky, ridership improvement is much more effective way of achieving GHG emissions reduction. Carrying more passengers leads to increased energy consumption and emissions per unit distance traveled but is still much more efficient way of reducing emissions than switching to electric buses, in part because the marginal penalty in energy use and emissions are smaller than the gain in passenger transportation efficiency.

3.12 Uncertainty

In addition to variability, uncertainty can make LCA studies less generalizable. For example, there is no consensus with regards to tail-pipe or upstream fugitive methane (CH4) emissions for CNG buses. Depending on the assumptions of CH4 emissions, the results can change drastically, because CH4 is about 30 times more potent GHG than CO2. When input values are highly uncertain, break-even analysis can be informative, which can easily be conducted based on my parametric LCA model. Tail-pipe CH4 emissions of CNGB used to be over 80 times of those of DB, although the most recent heavy-duty vehicle regulations require CNGB's tail-pipe methane emissions to be the same as DB's. So, the possible range of the tail-pipe CH4 emissions ratio between CNGB and DB is 1 to 80. And I test 1 – 10% fugitive methane emissions range for CNG production. As shown earlier, GHG emissions of CNGB and DB vary in the average trip speed spectrum, which means that the break-even methane emissions will also vary accordingly. As shown at the top of Figure 3.6, higher average trip speed increases break-even methane emissions. Per 100-year global warming potential (GWP), at 50 miles/hour average trip speed, CNGB will have lower GHG emissions than DB up to 4% fugitive emissions level. Because the break-even methane emissions depend on average trip speed as such, I conduct 2-dimensional break-even analysis, testing tail-pipe and upstream fugitive CH4 emissions simultaneously. Now, the break-even value is the average trip speed. The bottom of Figure 3.6 indicates that 5% fugitive emissions will make CNGB GHG emissions always higher than DB, no matter what the tail-pipe methane emissions are. In other words, even if CNGB's tail-pipe methane emissions pair with DB, CNGB's life cycle GHG emissions will not become lower than DB unless the fugitive methane emissions are reduced. Another important implication of Figure 3.6 is that reductions in both tail-pipe and fugitive methane emissions would not result in lower GHG emissions for CNGB compared to DB, especially for low to medium speed range. Lower GHG emissions benefits of CNGB's will be limited for high-speed operating conditions even

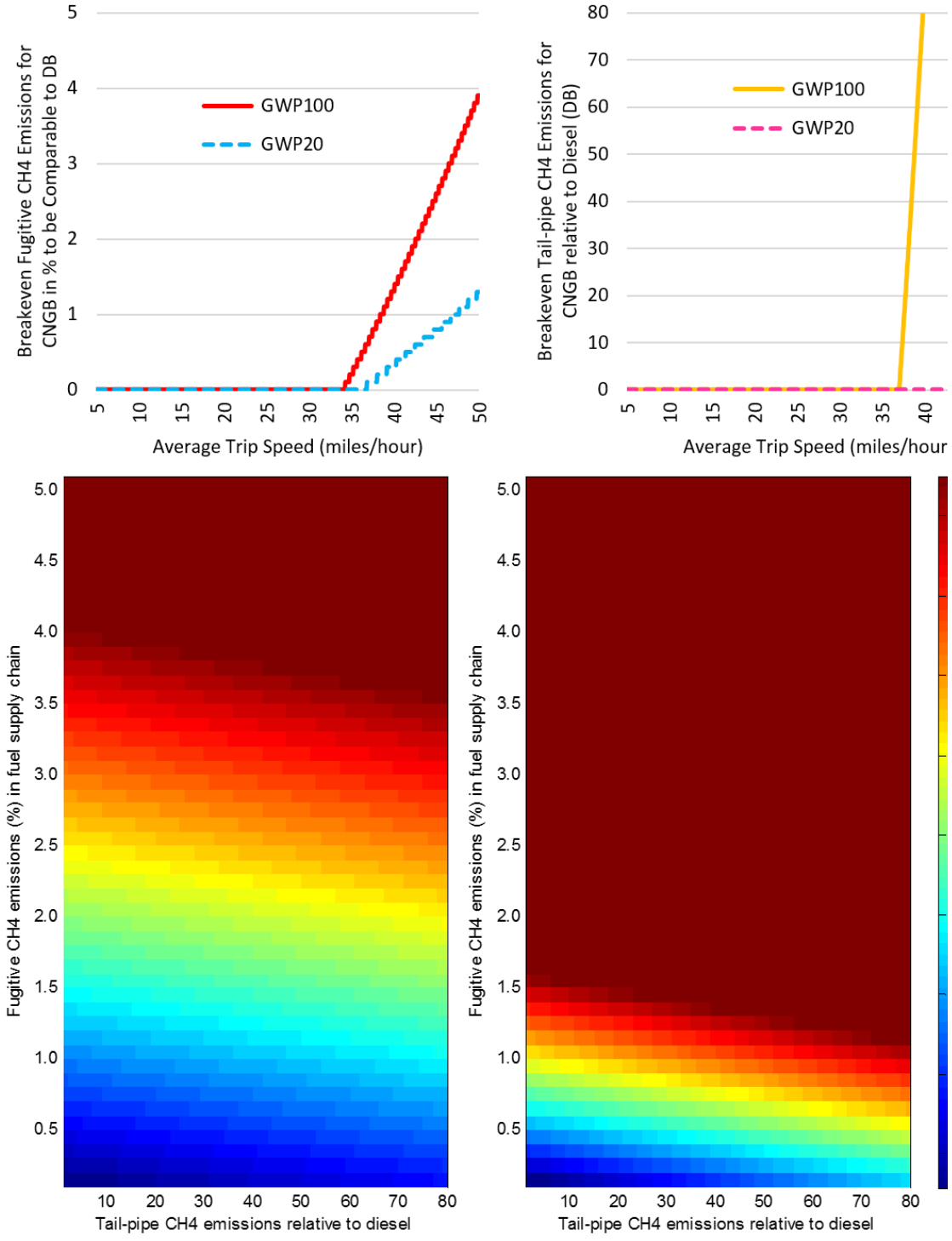

Figure 3.6. Parametric breakeven analysis for fuel supply chain fugitive CH4 emissions and tail-pipe CH4 emissions for CNGB relative to DB. Top: 1-dimensional breakeven analysis, bottom: 2-dimensional analysis for GWP100 (left) and GWP20 (right) cases.

with significant reductions in tail-pipe and/or fugitive methane emissions. Multiple factors are in play here. Despite the lower CO2 intensity of natural gas fuel compared to petroleum diesel, lower operation efficiency, heavier weight, and new infrastructure requirement of CNGB in comparison with DB have a penalizing effect on life cycle GHG emissions. Despite the data gaps and uncertainty regarding methane emissions, as demonstrated here with the parametric break-even analysis, once variability and its impact can be incorporated methodologically, uncertainty and data gaps could in part addressed simultaneously. This exemplifies why the methodological approaches to variability are important. Along with uncertainty, variability lies at the center of the generalizability issue, but the most urgent and important step to take is to understand what is causing the variability, most importantly, not by a case-by-case but by generic methodological approach.

CHAPTER 4

COMBINED COOLING, HEATING, AND POWER FOR BUILDINGS

4.1 Chapter Summary

Life cycle assessment is a method to evaluate economic and environmental benefits and tradeoffs of technologies, human activities, and systems. Data gaps, variability, uncertainty, and weak generalizability are among the continuing challenges in life cycle assessment. As a way of resolving these issues, a parametric life cycle assessment framework is proposed and demonstrated, using the case study of decentralized power generation for buildings. The parametric life cycle assessment involves investigating governing equations; identifying overall relationships between input and output variables; evaluating characteristics and typology of input and output variables; assessing relative importance and contribution of individual input parameters based on simulation or statistical analysis; and developing a parametric form of life cycle assessment models.

I show the parametric life cycle assessment approach can systematically and effectively explain and predict more than 90% of variability in the life cycle trade-offs of combined cooling, heating, and power technologies such as microturbines and fuel cells with the building energy demand characteristics as input variables. I also propose a decoupled modeling strategy for the parametric life cycle assessment, particularly for the application of decentralized power generation technology analysis. Our results indicate that microturbines or fuel cells can reduce environmental impacts such as air emissions and water consumption, but those technologies are generally not cost-effective in comparison with conventional building energy systems. Decentralized power generation will be inherently fuel switching (from centrally-generated electricity to natural gas) and move the emissions sources from the central power plants to population centers. The cost

that customers must bear to achieve 100% electric grid independence by relying on natural gas or other fuels will be 50% higher than the cost they currently pay for the energy services.

4.2 Motivation

Conventional residential and commercial buildings in the U.S. rely on energy from natural gas and electric grids to meet the thermal and electric energy demand. For typical building energy systems, thermal energy is supplied from on-site combustion of natural gas, and electrical energy is delivered from electricity generation in centralized power plants. One of the disadvantages of this conventional building energy system architecture is a mismatch of waste heat streams in central power plants and thermal energy needs in buildings in dispersed locations. As an alternative, on-site or decentralized electricity production enables the direct utilization of the waste heat from the power generation process, improving overall energy efficiency. On-site power generation as such also provides increased energy self-sufficiency and resilience against power outage of centralized electric grid. One promising technology for decentralized building energy systems is combined cooling, heating, and power (CCHP) which is also called combined heat and power (CHP) when there is no cooling component in the system.

CHP/CCHP systems are comprised of a prime mover for power generation and waste heat recovery system which is linked to heater for space or water heating and absorption chiller for space cooling. For this study, I analyze two types of prime movers: fuel cell (FC) and microturbine (MT) powered by natural gas (NG). Both prime movers are used for topping cycle, as opposed to bottoming cycle for waste heat-based power generation. Oxidation is a common underlying electricity generation mechanism of FC and MT, but FC is based on electrochemical process whereas MT is based on combustion, resulting in different electrical and thermal characteristics. Previous studies evaluated various aspects of the CHP/CCHP systems and decentralized power generation. By and large, they all can be categorized into four groups: Comparison of different prime mover technologies, evaluation of system operation control strategies, system design, and assessment of geographical and building type suitability for CHP/CCHP. Table 4.1

summarizes and characterizes the scope and some of the key aspects analyzed in previous CHP/CCHP literatures.

I address the key factors that previous studies identified as important in evaluating CHP/CCHP systems, including system design, building energy demand characteristics, system operating strategy, variations in local conditions, etc. Compared to previous researches, however, my focus is to demonstrate a different way of looking at the economic and environmental tradeoffs of the CHP/CCHP systems. More specifically, previous CHP/CCHP literatures indicate that overall performances vary, but few studies show why and how much results vary in a systematic way, particularly from the life cycle perspective. I propose a systematic way of explaining and predicting economic and environmental performances of CHP/CCHP. In addition, to my knowledge, holistic LCA of CHP/CCHP for decentralized building energy systems is scant, especially in the U.S. context. Only few studies (Staffell et al. 2012; Balcombe et al. 2015a, 2015b) conducted life-cycle assessment (LCA) of the CHP/CCHP systems or technologies. Most studies focus on on-site and electric grid energy consumption, air emissions, or water consumption. In selecting the best possible technology for distributed building energy systems, indirect energy use and environmental impact from the CHP/CCHP system production and upstream fuel supply-chain can be significant. Not only that, it is hard to find research results that are based on detailed analysis of "avoided" electricity. Most of the existing studies rely on average numbers for electric grid. Average electric grid conditions can be misleading in determining true benefits of the CHP/CCHP system – energy consumption and/or environmental impact that are displaced or reduced by adopting CHP/CCHP system. Focusing on more holistic life cycle tradeoffs (i.e., energy consumption, air emissions, and water intensity) and displaced electric grid characteristics as such, I attempt to answer the following two research questions: What are the life cycle trade-offs, more importantly, avoided environmental impacts, of

CHP/CCHP for buildings? What explains the variability of the LCA results for CHP/CCHP systems?

In the following sections, I propose a parametric life cycle assessment (LCA) approach to systematically predict the life cycle trade-offs of CHP/CCHP systems with functions of input factors or variables. This differs from conventional approaches that present generalized or case-specific results. For the parametric LCA approach, I first qualitatively and quantitatively assess the governing equations that define life cycle results (Section 4.3). I then evaluate the typology of variables and develop a strategy to deal with different types of variables in the parametric LCA (Section 4.4). To account for non-linear characteristics and collect samples for statistical analysis, I run building energy simulations and construct a sample space (Section 4.5). I also characterize the electricity that is avoided and displaced as buildings generate their electricity using CHP/CCHP technologies (Section 4.6). Based on the sample data collected from building energy simulation as such and the data for avoided electricity, I develop functional forms of identify underlying relationships between input and output parameters and develop a parametric LCA model that can systematically predict the output as a function of input variables (Section 4.7).

Table 4.1. Summary of CHP/CCHP literatures

	Geographical context	Building type	Prime mover[a]	Operation strategy[b]
Mago and Chamra (2009)	USA (Columbus, MS)	Office	-	FEL, FTL, HETS and others
Mago et al. (2009); Cho et al. (2009)	USA (multiple states and cities)	Office	-	FEL, FTL, and LP
Fumo et al. (2009)	USA (For Worth, TX; Minneapolis, MN)	Office	-	Others
Kavvadias and Maroulis (2010)	Greece	350-bed hospital complex	ICE	FEL
Mago and Hueffed (2010)	USA (Chicago, IL)	Office	-	FSS
Shaneb et al. (2011)	England	House	ICE, SE, SOFC, and PEMFC	LP
TeymouriHamzehkolaei and Sattari (2011)	Iran (multiple cities)	Residential (various sizes)	SE	-
Mago and Smith (2012)	USA (Chicago, IL)	Commercial	-	BL
Staffell et al. (2012)	UK	House	SOFC	-
Magri et al. (2012)	Italy (Milan)	House	SE	-
Naimaster and Sleiti (2013)	USA (multiple cities)	Office	SOFC	-
Pruitt et al. (2013)	USA (California and Wisconsin)	Hotel and office	SOFC	BL and FEL
Wu et al. (2014)	Japan (multiple cities)	Hotels, hospitals, stores, and offices	ICE	MRM
Li et al. (2015)	China (Dalian)	Residential and commercial	ICE	FEL, FTL, HETL, FSS, and FBL
Angrisani et al. (2015)	Italy (Napoli and Torino)	House	ICE	CL
Cappa et al. (2015)	Italy	Residential	ICE and PEMFC	-
Balcombe et al. (2015a; 2015b)	UK	House	SE	-
Shimizu et al. (2015)	Japan (Tokyo, Sapporo, and Naha)	Office, house, and hospital	Fuel cell	-
James et al. (2015)	USA (Atlanta, GA)	Office and house	MT	FTL and others

[a] Prime movers: ICE – internal combustion engine, SE – Stirling engine, SOFC – solid oxide fuel cell, PEMFC – proton exchange membrane fuel cell, MT – microturbine

[b] Control strategies: FEL – following the electric load, FTL – following the thermal load, HETL – hybrid electric-thermal load following, FSS – following the seasonal operation strategy, FBL – following the electric-thermal load, CL – constant load, LP – linear programming, MRM – maximum rectangular method, BL – baseload

4.3 Governing Equations

Parametric LCA starts with the evaluation of governing equations that determine all or part of the life cycle results. Governing equations provides theoretical foundation when characterizing and parameterizing life cycle results as functions of the input variables. For CHP/CCHP systems shown with a schematic in Figure 4.1, thermodynamic relationships between key components can be written as follows:

$$P_{Elec} = \eta_{DC/AC} \cdot P_{PM}\left(f_{CS,PM}\right) + P_{EG} \tag{4.1}$$

$$\dot{Q}_{Cooling} = C_{\frac{CHP}{CCHP}} \cdot f_{CS,cooling} \cdot \frac{\dot{Q}_{Cooling}}{COP_{CCHP,Chiller}} + (1 - C_{CHP/CCHP}) \cdot f_{CS,cooling,A/C} \cdot \frac{\dot{Q}_{Cooling}}{COP_{A/C}}$$

$$\dot{Q}_{Heating} = f_{CS,heating} \cdot \frac{\dot{Q}_{Heating}}{\eta_{CCHP,Heater}} + C_{Heater,E/NG} \cdot f_{CS,heating,Heater,E} \cdot \frac{\dot{Q}_{Heating}}{\eta_{E,Heater}} + (1 - C_{Heater,E/NG}) \cdot f_{CS,heating,Heater,NG} \cdot \frac{\dot{Q}_{Heating}}{\eta_{NG,Heater}} \tag{4.3}$$

where P stands for power, η efficiency, f_{CS} control factors, $\dot{Q}$ thermal energy flow rate, COP coefficient of performance, and C binary constant parameter for system configuration. System components in Figure 4.1 and Eqs. (4.1) – (4.3) include prime mover (PM), inverter (DC/AC), electric grid (EG), natural gas (NG), electric or NG heater, absorption chiller (or simply chiller), and air conditioner (A/C). $\dot{Q}_{Cooling}$, $\dot{Q}_{Heating}$, and P_{Elec} can be determined from the building energy demand profiles archived in OpenEI database (OpenEI 2015). Operating characteristics of electrical and thermal products, for example, nonlinear efficiency of prime movers, can be found from manufacturers' product specifications and test data. I use Capstone microturbines and Bloom Energy's solid oxide fuel cell (SOFC) as baseline products (Capstone 2016; Bloom Energy 2016). For any given moment, control strategy (represented by f factors) contributes to calculating the output values of each electrical and thermal components. Note that Eqs. (4.1) – (4.3) are generic and applicable to any types of CHP/CCHP

systems or technologies. Taking integral of Eqs. (4.1) – (4.3) over the time horizon T (e.g., day, month, season, year, or product lifetime) produces the following electrical and natural gas energy consumption for building energy systems depicted in Figure 4.1:

$$E_{EG} = \int_0^T \left[P_{Elec} - \eta_{DC/AC} \cdot P_{PM}(f_{CS,PM})\right] dt \tag{4.4}$$

$$E_{NG} = \int_0^T \left\{ \begin{array}{l} \dfrac{1}{\eta_{FP}\eta_{CCHP,WHR}(1-\eta_{CCHP,PM})} \left[\begin{array}{c} C_{CHP/CCHP} \cdot f_{CS,Cooling} \cdot \dfrac{\dot{Q}_{Cool}}{COP_{CCHP,Chiller}} \\ + (1 - C_{CHP/CCHP}) \cdot f_{CS,Cooling,A/C} \cdot \dfrac{\dot{Q}_{Cool}}{COP_{A/C}} \\ + f_{CS,Heating,CCHP} \cdot \dfrac{\dot{Q}_{Heat}}{\eta_{CCHP,Heater}} \end{array} \right] \\ + f_{CS,PM} \cdot \dfrac{P_{PM}}{\eta_{FP} \cdot \eta_{CCHP,PM}} + (1 - C_{Heater,E/NG}) \cdot f_{CS,Heating,Heater,NG} \cdot \dfrac{\dot{Q}_{Heat}}{\eta_{NG,Heater}} \end{array} \right\} dt \tag{4.5}$$

Similar equations can be developed for air emissions and water consumption. Due to nonlinear terms and interaction between variables as well as complex control strategies, it is not easy to derive analytic solutions for Eqs. (4.4) and (4.5). Therefore, I conduct building energy and emissions simulation as discussed in Section 4.5 below.

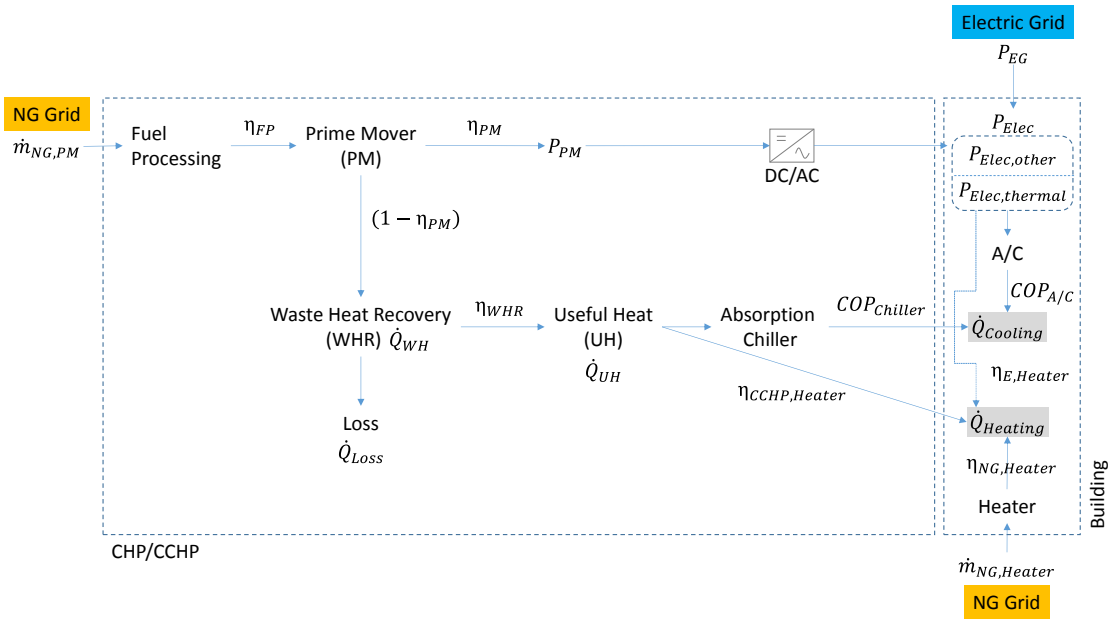

Figure 4.1. CHP/CCHP system schematic diagram.

4.4 Typology of Variables and Treatment Strategy

Regarding the simplified governing equations shown in previous section, three types of variables represent most of the thermodynamic relationships and resulting economic and environmental performances: product attributes, operating conditions, and environmental factors. To deal with those three types of variables in the parametric modeling approach, I adopt characterization, simulation-based, and decoupled modeling strategies. Industrial products such as heaters, prime movers, chillers, and air conditioners all have unique performance characteristics, and their behavior is mostly predictable once product operating conditions are known. From the life cycle perspective, overall end results rather than instantaneous changing behavior of the product components will be important and useful. In other words, product attributes will be embedded in the overall life cycle results and thus I don't treat them separately. Nevertheless, it is crucial to account for their nonlinear and varying performances based on detailed building energy and emissions simulation (Section 4.5). Second type of variables is related to operating conditions, including building energy demand characteristics and control strategies. I consider building energy demand profiles as known variables which will appear in my parametric LCA model as inputs. I test a variety of control strategies proposed by previous studies (Table 4.1), more specifically, providing base electric or thermal load (BEL or BTL), following electric or thermal load (FEL or FTL), and hybrid electric-thermal load (HETL). Because of the complexity involved in control strategies and their impact on life cycle results, I develop a separate parametric LCA model for each of the control strategies. Third type of variables includes environmental factors such as local climate and built-in systems (e.g., electric grid) that individual building operators or owners cannot change or control. Climatic conditions affect product efficiency and other components in the CHP/CCHP systems. Climate is decoupled from the building energy demand characteristics, because I am primarily interested in characterizing life cycle results as a function of input variables such as building energy demand profiles. Once I

develop the baseline parametric model (or functions of those characterization variables), I incorporate the climatic condition as an additional correction factor. Like climatic condition, I also take a decoupled modeling approach for electric grid and on-site results. I develop two separate (one for on-site and the other for electric grid) models for each life cycle inventory or impact result (see Section 4.6).

4.5 Building Energy and Emissions Simulation

As a bridge from the governing equations and the input variables in those equations in Section 4.2 to a parameterized LCA model, I conduct building energy and emissions simulation and construct sample space which is a set of the results collected from the simulation. Those samples are used later for a statistical analysis to develop a parametric LCA model. For building simulation, I take hourly energy demand profiles from the OpenEI database (OpenEI 2015) as an input. For a baseline case, I choose a building in the largest city for each state in the continental U.S., which leads to 48 cases in total.

With the hourly energy demand profiles, I first conduct a system design (component sizing and configuration) for each control strategy and each prime mover. I determine the size (or capacity) of prime mover, heater, chiller, and air conditioner based on the energy demand characteristics and control strategies. For example, for base electric load (BEL) control strategy for microturbine (MT), I pick a prime mover that can provide up to 50^{th} percentile of the electrical power demand during the off-peak (March – May, and October) period. The CHP/CCHP system performance and competitiveness are very sensitive to the utilization level of prime mover. To run and use the prime mover as much as possible, the 50^{th} percentile of off-peak demand is a reasonable choice of threshold. Above the 50-th percentile threshold, CHP/CCHP is likely to operate more frequently but with more energy not fully utilized and thus wasted. Below the threshold, the system is going to operate less frequently, but the use value of CHP/CCHP will become limited. Finding optimal level of threshold could be investigated further in future research, but it is not the focus of my study. When the electrical power demand is above the threshold, the prime mover runs at its full capacity and the deficit power is provided from the electric grid. When the power demand is lower than the prime mover capacity, prime mover output is lowered and switches to following the electric load (FEL) mode. In addition to the component sizing, I simultaneously determine the system configuration

– single or tandem. Because it is difficult to always match the building energy demand and the output energy from the CHP/CCHP system, prime movers are likely to run at part load most of the time. Therefore, it is important to consider part load characteristics. In case of fuel cell (FC), because of the high efficiency at lower power level (Figure 4.2 – b)

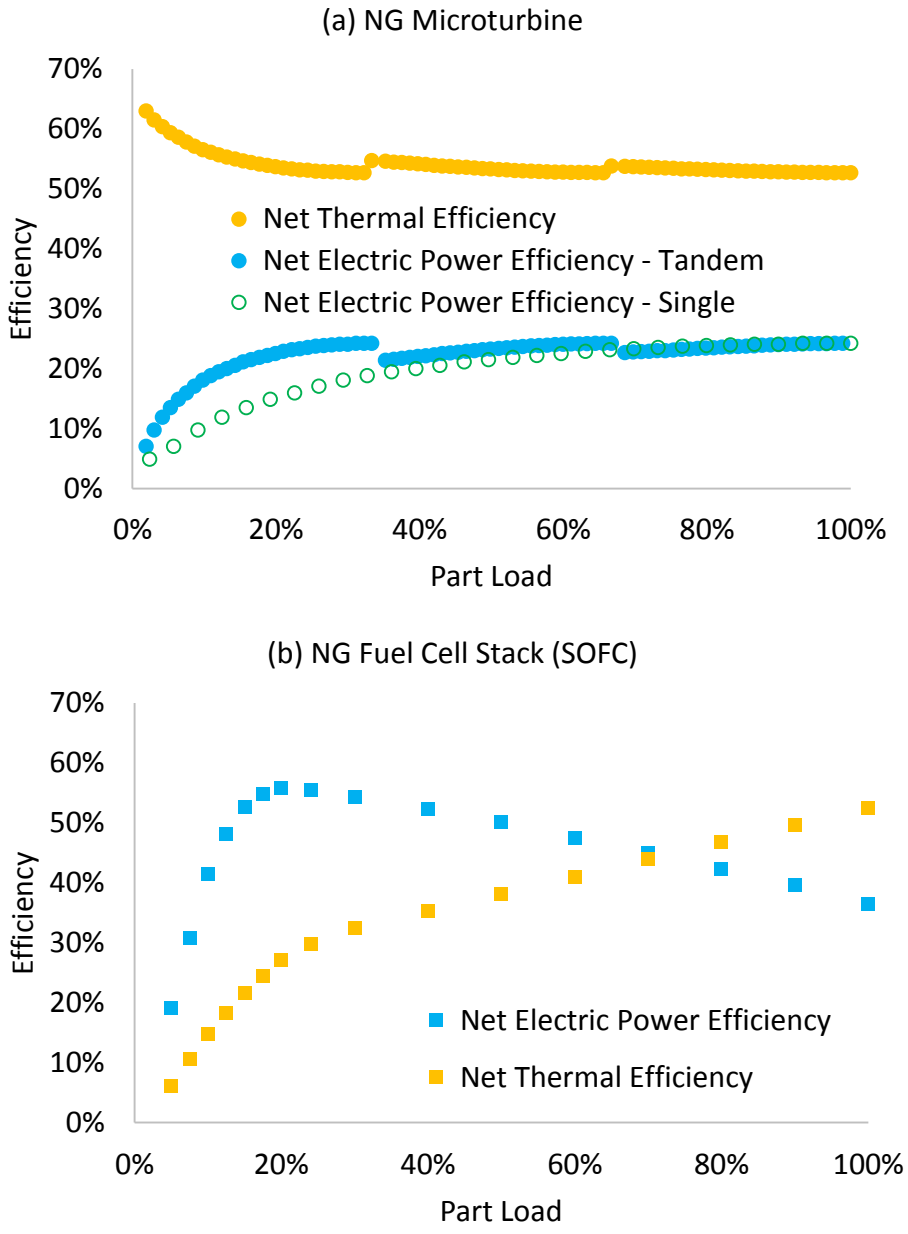

Figure 4.2. Electric and thermal efficiency of prime movers – microturbine and solid oxide fuel cell.

which is the advantage of electrochemical prime mover, single configuration will suffice. However, for microturbine (MT), tandem configuration provides higher efficiency at low power region in comparison with single configuration, but the choice between single and tandem configuration is also constrained by the available MT models in the market and the building energy demand characteristics. Whenever possible, I design the system in tandem configuration to compare the best MT and FC technologies.

Once the size and configuration of the system components are determined, I simulate hourly system operation for all the elements (i.e., prime mover, chiller, heater, etc.) shown in Figure 4.1. I consider part load operating characteristics for both energy, water, and emissions, based on the product specifications, emissions certification data, and experimental test data (BNL 2009; EPA 2014; Capstone 2016; Bloom Energy 2016). The building energy simulation only provides on-site and direct energy consumption, air emissions, and water use. Sections 4.6 and 4.7 below discuss the upstream and fuel supply chain parts.

4.6 Electric Grid

In addition to CHP/CCHP analysis described in previous section, a fair assessment of potential benefits and drawbacks of decentralized energy production for buildings also requires accurate evaluation of the centralized electric grid characteristics. For example, "avoided" environmental impacts from the centralized electric grid by adopting CHP/CCHP technology is secondary and consequential benefit of decentralized building energy systems. If the analysis is solely based on average or typical electric grid conditions on an attributional basis, the comparison may lead to biases, i.e., under- or over-estimation of true environmental impacts. To more accurately reflect the avoided and displaced electricity and its environmental impacts, I adopt the following accounting method for net emissions of avoided power generation in centralized electric grid:

$$EM_{EG,Net} = \int_0^T \{(P_{Elec} \cdot EM_{EG,Average}) - [P_{Elec} - \eta_{DC/AC} \cdot P_{PM}(f_{CS,PM})] \cdot EM_{EG,Displaced}\} dt \quad (4.6)$$

where EM stands for emissions factors (e.g., grams of NOx per kW of purchased electricity), P_{Elec} electrical power demand in buildings, and P_{PM} output power from the prime mover. What most CHP/CCHP studies assume is that decentralized power generation displaces average electricity generation sources: $EM_{EG,Average}$ and $EM_{EG,Displaced}$ are equal. This simplistic average electric grid displacement assumption implies that the change in emissions due to the introduction of decentralized power generation depends solely on how much power or electricity generated from the CHP/CCHP prime mover. In reality, that is not entirely true. When all or part of the electricity demand in buildings is met by the power generated from decentralized electricity generation technologies, electricity generation sources that are displaced by the decentralized power production is not the average sources (e.g., 20% of hydroelectric, 30% coal, 25% nuclear, and 25% natural gas, hypothetically). In reality, it is more likely that the displaced or avoided electricity generation sources in centralized electric grid are

non-average sources such as natural gas, petroleum, and others used for peak loads or ramping-up/down. Therefore, it is crucial to distinguish emission factors for typical or average electric grid ($EM_{EG,Average}$) and those for avoided or displaced electric grid ($EM_{EG,Displaced}$), which Eq. (4.6) accounts for. Not only that, electricity consumed in one state may have not been generated within the state boundary and could have been imported from the neighboring states or regions. This requires the distinction between power generation and consumption. Using the life cycle energy efficiency, air emissions, and water intensity data for marginal (or avoided/displaced) power consumption developed by Lee and Thomas (2016a, 2016b), I estimate net environmental impacts of CHP/CCHP technologies, as shown in Eq. (4.6). Regardless of electricity generation or consumption, I assume 7% loss for transmission and distribution (EIA 2016).

4.7 Parametric Life Cycle Assessment

For economic and environmental life cycle assessment (LCA) of CHP/CCHP technologies, as shown in Figure 4.3, I include two sub-systems such as fuel (i.e., natural gas and electricity) and CHP/CCHP-related products as well as natural gas heaters and air conditioners for conventional buildings. I exclude components related to building construction and operation, assuming CHP/CCHP will make only changes in energy consumption without significant changes in baseline buildings. The goal of my LCA is to compare CHP/CCHP-based decentralized power generation technologies and conventional building energy systems in terms of primary energy consumption, water intensity, and air emissions (greenhouse gases such as CO2, CH4, and N2O, and air pollutants including CO, NOx, PM2.5, PM10, SO2, and VOC). As Figure 4.3 indicates, I calculate social life cycle cost for impact assessment and draw implications from both life cycle inventory and social life cycle cost results. The intended audience of my LCA includes policy-makers, analysts, and researchers interested in the trade-offs of CHP/CCHP technologies or decentralized building energy systems. The target industrial products are solid oxide fuel cell (SOFC) and microturbine (MT) combined with absorption chiller, which is used for midrise (4-story) apartment buildings of 34,000 square feet across the country over 20 years of lifetime between 2016 and 2036. The functional units are energy throughput or end-use energy use (thermal or electrical). Our

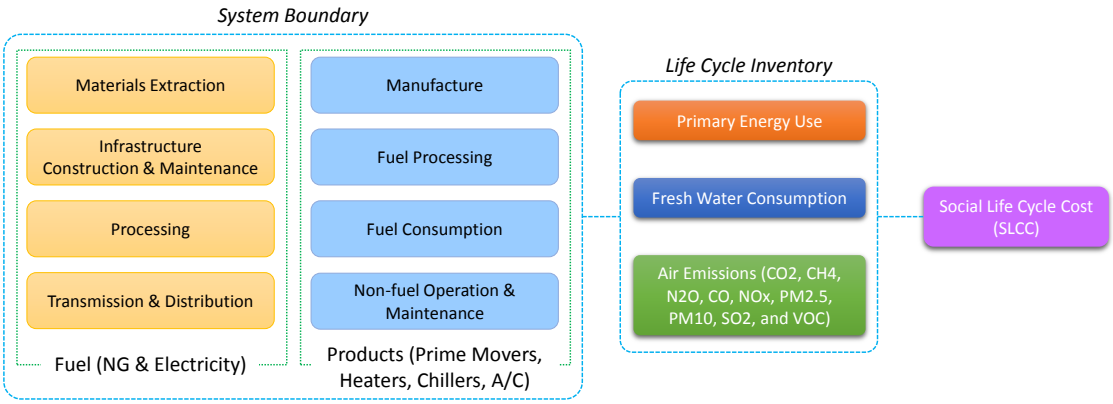

Figure 4.3. System boundary diagram.

modeling approach shares some elements of consequential LCA, as I incorporate the changes (avoided and displaced resources) in electric grid caused by adopting CHP/CCHP technologies as discussed in previous section. I adopt a hybrid LCA framework, integrating process-based and input-output-based data and methods. I use process-based data (ANL 2015) for fuel supply chain for natural gas and electricity and product use (on-site power generation) (BNL 2009; EPA 2014b; Capstone 2016; Bloom Energy 2016). Input-output-based data set (CMU GDI 2008) is used for product manufacture and non-fuel operation and maintenance. Every cost in my analysis is in constant 2015 dollars in net present value over 20 years of CHP/CCHP system lifetime, at 7% of discount rate. I use Nick Muller's APEEP model to estimate ecological damage costs of air emissions (Muller 2011), based on the state-by-state average damage costs for each of ground-level and smoke stack emissions. Despite various potential benefits, CHP/CCHP-based decentralized building energy systems are capital-intensive investment and may move emissions sources closer to population centers from rural/suburban areas where utility-scale power plants are typically located. Having said that, the air pollution damage cost estimation can provide useful insights as to overall and monetized trade-offs of CHP/CCHP technologies.

Most importantly, my LCA is oriented towards developing a parametric life cycle assessment (LCA) model to systematically explain and predict life cycle trade-offs of CHP/CCHP systems in comparison with conventional building energy systems. For this, I adopt ordinary least squares (OLS) linear regression method. I characterize building energy use profiles with hundreds of variables (e.g., annual mean heating demand, standard deviation of summer electricity use, etc.) and evaluate overall relationship between those statistical characterization variables and life cycle results. For variable selection, I rely on least absolute shrinkage and selection operator (LASSO) and correlation coefficients. However, to make my model more intuitive, I choose annual average statistics whenever possible, instead of standard deviation and others. Annual

average values are relatively more readily available compared to standard deviation and other measures for building energy demand statistics. To compare the best CHP/CCHP technology and system design for each state with conventional building systems, I run simulations for all the possible combinations of prime mover (microturbine or SOFC), control strategy (base electric load, following the thermal load, etc.), and system configurations (single vs. tandem or CHP vs. CCHP) discussed above. Based on the simulations and social life cycle cost estimation for each combination, I pick the least cost technology and configuration and compare with the conventional building energy system. Although I use sequential optimization for the ease of presentation and analysis as such, performances of individual technology and configuration can also be parameterized using the same method. In addition to the sequential optimization based on social life cycle cost, another strategy I adopt is to decouple life cycle results related to on-site energy consumption and those for electric grid. Life cycle results for on-site components will be directly estimated by the parametric LCA method. On the other hand, due to the heterogeneity of electric grid, I estimate on-site electricity consumption separately so that those parameterized electricity use data can be applied to any local or regional electric grid.

4.8 Results

CHP/CCHP technologies such as microturbine (MT) and solid oxide fuel cell (SOFC) do reduce some of the life cycle air pollutants emissions, as shown in Figure 4.4. For example, in the state of Michigan, both MT and SOFC for CHP/CCHP systems create less life cycle NOx, PM2.5, and SO2 emissions. Also, MT reduces fresh water consumption by around 20% compared to conventional building energy system, but SOFC shows higher water intensity than the conventional system. MT and SOFC emit higher greenhouse gases (GHG) and VOC. In particular, MT creates significantly higher CO emissions than conventional or SOFC technologies. However, the life cycle inventory results of air emissions will vary from state to state and from one building energy profile to another. Therefore, here I demonstrate a systematic way of predicting or describing the air emissions reduction potential of CHP/CCHP technologies. As an example, here I show annual life cycle GHG emissions savings as a function of natural gas load portion of overall building energy demand, annual total electricity consumption, and the natural gas load ration over electricity (Table 4.2). Note that I take a log transformation of the dependent variable to comply with the normality assumption of OLS linear regression. As indicated in Table 4.2, my parametric life cycle inventory model explains 99% of variability in the GHG emissions savings potential. This shows why parametric LCA can be an effective way of dealing with the variability in LCA. As mentioned earlier, I take a decoupled modeling approach and present a model for annual net electricity consumption separately. As in the case of GHG emissions savings, Table 4.2 shows 91% variability is explainable by the parametric LCA model. With this net electricity demand prediction model, any LCA researchers or practitioners can estimate electricity consumption using the building energy demand characteristics and then multiply with the electric grid energy efficiency, air emissions, and water intensity data to get life cycle results. This result can then be combined with the on-site life cycle results (e.g., GHG savings potential in Table 4.2) to produce overall life cycle results.

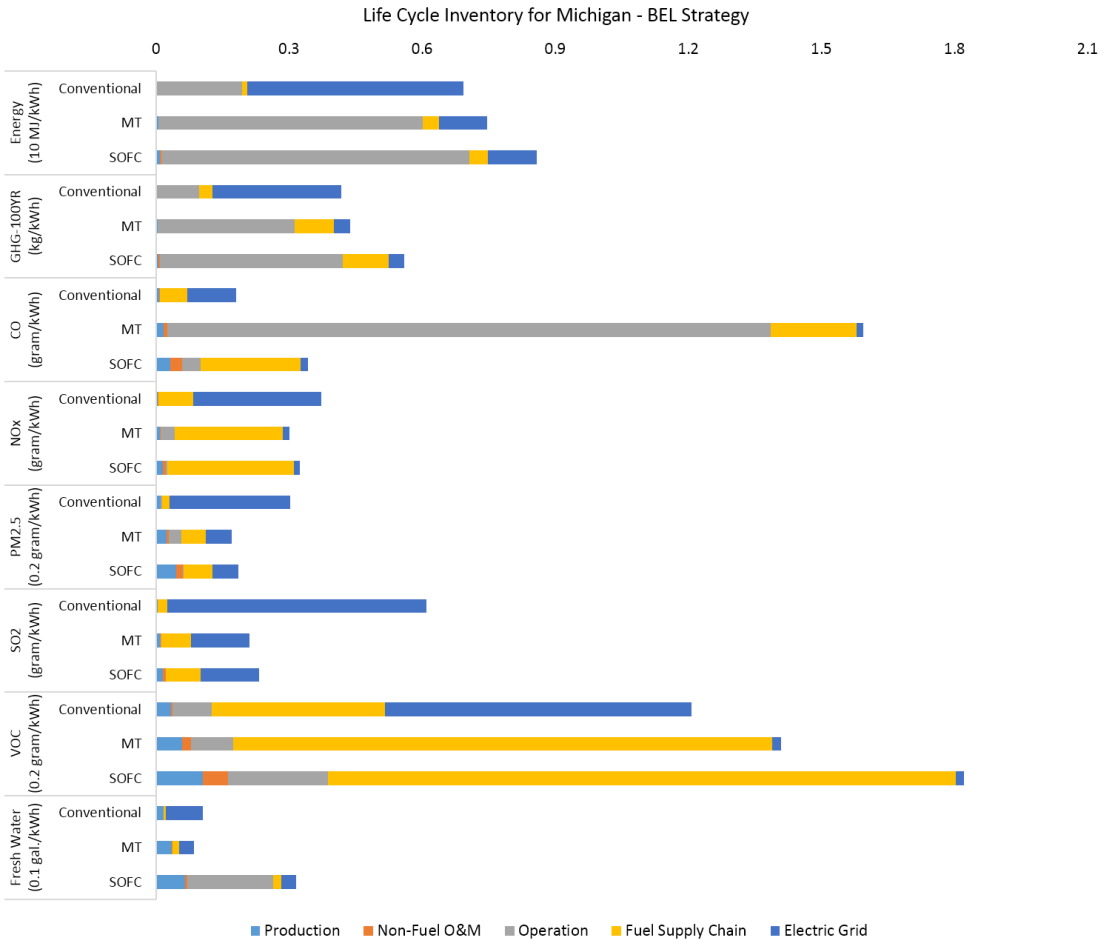

Figure 4.4. Life cycle inventory results – Michigan as an example.

Despite that MT or SOFC CHP/CCHP systems provide emissions and water consumption savings potential as discussed above, MT or SOFC is not cost-competitive in comparison with conventional building energy systems. In state of Michigan, social life cycle of MT-based CHP system with base electric load (BEL) control strategy is slightly lower than conventional system, but generally my analysis indicates that MT and particularly SOFC don't have cost competitiveness. The air emissions reduction potentials and their damage cost reduction effect are not sufficient to make the CHP/CCHP systems cost-competitive. Also, as in the case of air emissions and water consumption above, social life cycle cost comparison varies from one area to another. For instance, MT-BHTL system shows the lowest social life cycle cost among CHP/CCHP

Table 4.2. Parametric life cycle assessment model, based on decoupled modeling approach – greenhouse gas emissions savings example

Parameters	**(On-site) Annual Life Cycle GHG Emissions Savings** **log(metric ton of CO2e)**	**Annual Net Electricity Consumption (MWh) for CHP/CCHP System** **log(E_{MWhe})**
Intercept	5.14 (111)	0.69 (2.1)
NG Load Portion	-1.29 (-34.4)	2.58 (4.5)
Total Electricity Consumption	0.01 (7.67)	0.105 (12.9)
NG/Electricity Load Ratio		-0.28 (-3.3)
F-stat.	3240	163
Adj. R2	0.99	0.91

(Values in parentheses are t-statistic.)

technologies in Georgia, but SOFC-BHTL is the least-expensive CHP/CCHP system in California. Dealing with each scenario on a case-by-case manner is time-consuming and not very efficient way of analyzing life cycle trade-offs of CHP/CCHP technologies. I demonstrate that the social life cycle cost differential can be predicted in a systematic way with the parametric LCA. Figure 4.6 shows the social life cycle cost (SLCC) results from building energy and emissions simulation (Section 4.5) and SLCC results from a parametric SLCC model which explains 92% variability of SLCC. As can be seen in Figure 4.6, parametric LCA approach is a very effective way of explaining and predicting life cycle results whether life cycle inventory or impact assessment. Previous studies have shown that spark spread (or fuel prices ratio or differences between natural gas and electricity) can explain the cost-effectiveness of CHP/CCHP systems. However, as shown in Figure 4.6, the spark spread does not sufficiently explain the changing pattern of

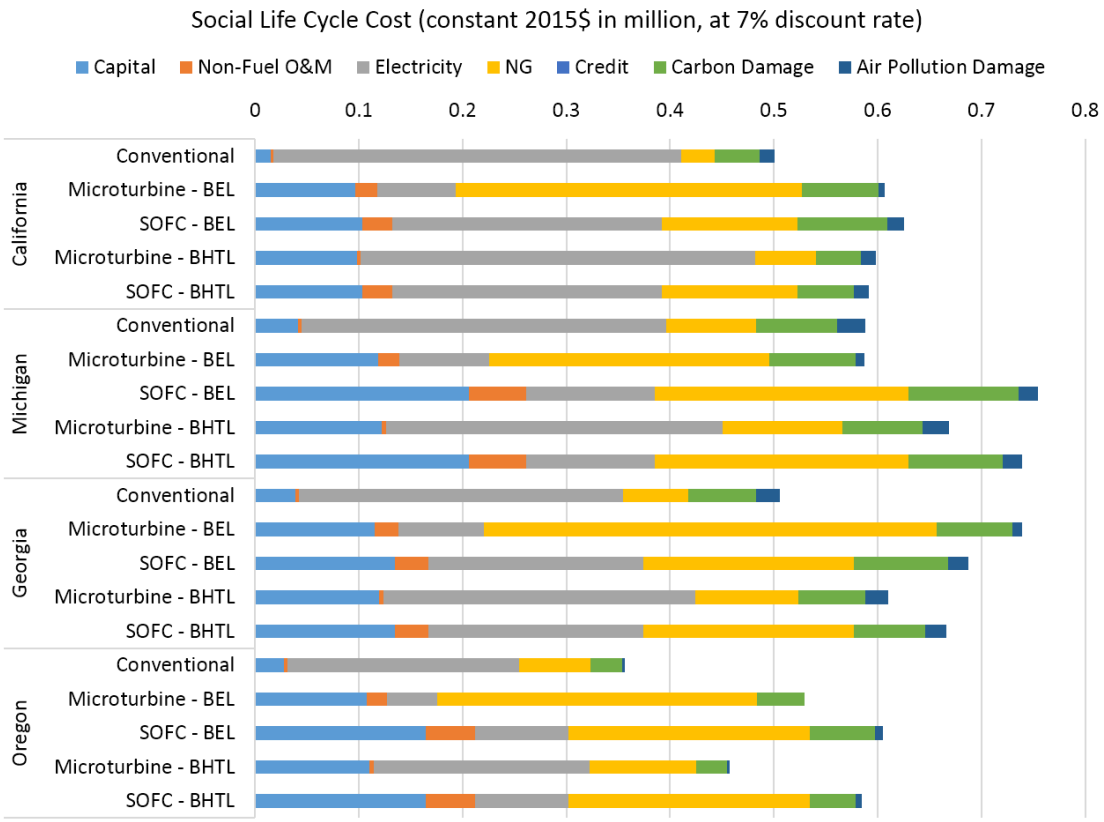

Figure 4.5. Social life cycle cost results for four select states. Control strategies: BEL – base electric load; BHTL – base heating thermal load.

SLCC, which is why my parametric modeling approach produces better descriptive and predictive power.

Lastly, Figure 4.7 shows social life cycle cost results for all the cases that I simulated and evaluated for the 48 states in the continental U.S. As can be seen in black diamonds, currently the electric grid independence (or the reliance on natural gas over electricity) is 40% for typical midrise apartment buildings in the U.S. Whether energy concern, power outage, environmental protection, or some other reasons, if building operators or owners want to adopt CHP/CCHP technologies and achieve 100% electric grid independence (EGI), the additional cost to pay is about 50% for microturbine-based CHP/CCHP and much higher for fuel cell-based system. As such, even when the

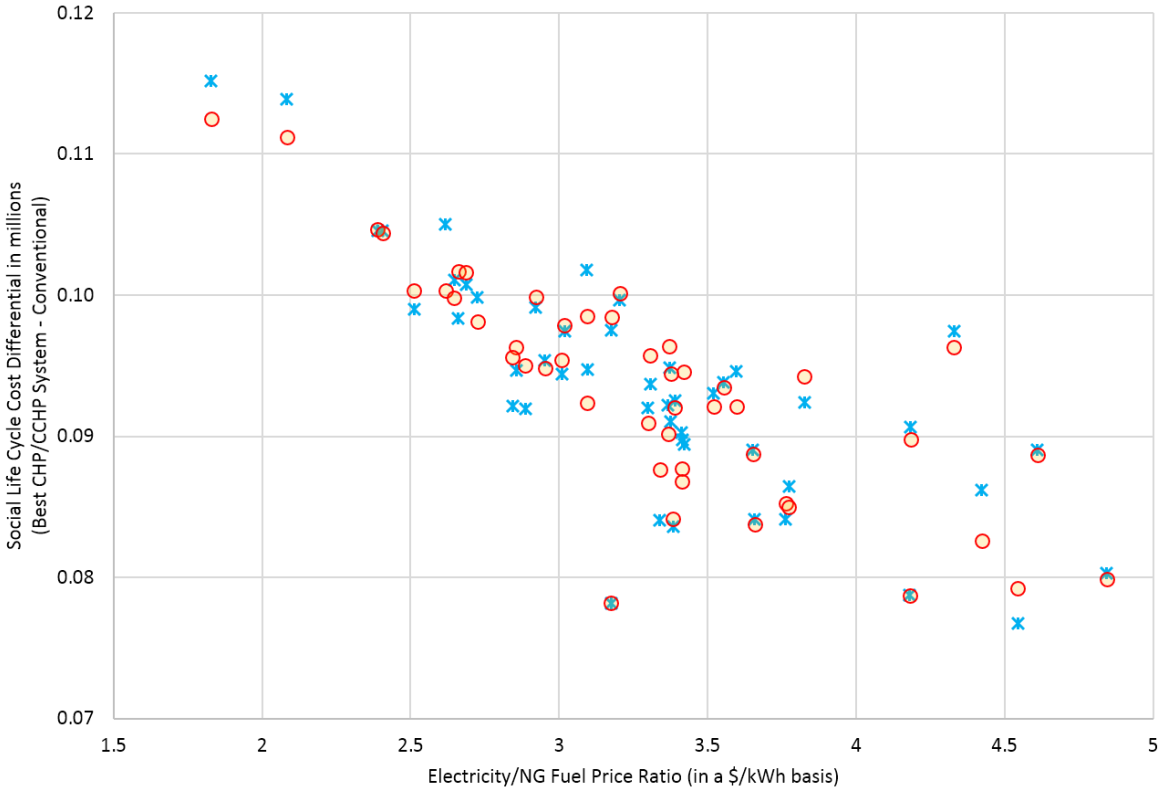

Figure 4.6. Social life cycle cost differential in constant million 2015$ for each state considered. The result is based on sequential optimization by running all possible combinations of system configuration and control strategies and pick the most cost-effective CHP/CCHP technology and calculate the cost differential against conventional building system without CHP/CCHP. The parametric SLCC model is based on 6 different variables (total electricity demand, total natural gas demand, electricity vs. total load ratio, natural gas vs. electricity load ratio, electricity vs. natural gas fuel prices differential, and electricity vs. natural gas fuel prices ratio) in the same form as the one shown in Table 4.2.

environmental impacts are internalized, microturbine or fuel cell-based CHP/CCHP is not currently cost-effective approach for reaching 100% EGI.

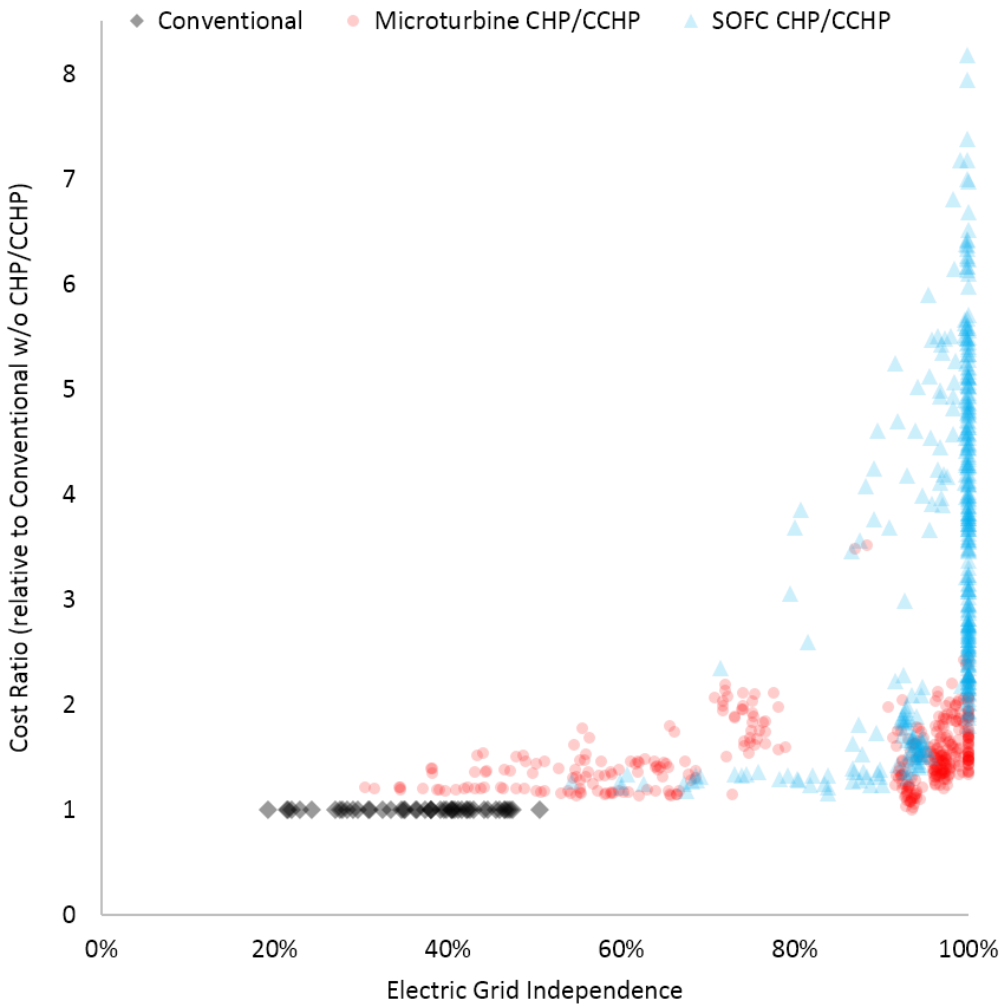

Figure 4.7. Cost for electric grid independence (EGI) – all cases (or system design and configuration variations) analyzed in this study for 48 states in the continental U.S.

4.9 Conclusion

I developed and demonstrated how parametric life cycle assessment approach can be utilized for analyzing economic and environmental life cycle trade-offs of microturbine and SOFC-based CHP/CCHP systems compared to conventional building energy systems. I showed that the parametric life cycle assessment can be successfully applied to evaluating varying trade-offs of the CHP/CCHP technologies. And the same methodology can be used for any types of energy systems modeling or analysis. I find that microturbine and SOFC-based CHP/CCHP systems provide life cycle air emissions and water consumption reduction benefits but currently lack cost-effectiveness and can use more life cycle energy for the same level of energy service. Internalizing the potential air emissions and water consumption benefits does not significantly improve cost barriers. This study is focused on current technologies and two prime movers (i.e., fuel cell and microturbine). Future research would evaluate future technological advances as well as the interaction between technologies and market evolutions for more diverse prime movers and fuel types.

CHAPTER 5

CONCLUSION

As demonstrated in previous chapters, the parametric LCA approach can be applied to numerous industrial products and systems, particularly to deal with the variability issue in LCA. More specifically, the parametric LCA explains and predicts why and how much LCA results change. As input parameters are operationalized in functional forms, adjustable levels of specificity become feasible, for example, meeting the needs of case-specific, local, regional, or national scale analysis. Not only that, the parametric LCA alleviates the issues related to functional units, because the functional unit-related parameters are included in functional forms of parametric LCA models. The parametric LCA can also help reduce the burden of data availability or unknowns, as it provides the capability of sweeping through the spectra of input variables, even when exact input conditions are not known. Despite the potential benefits, the parametric LCA has limitations. Among others, the parametric LCA relies on the existence of converging and distinct relationship or pattern between input variables and outputs. In case that there are no discernible relationship or pattern, it will be difficult to develop a parametric LCA model.

Although the parametric LCA approach can help deal with the variability issue in LCA, the framework and case studies presented in this dissertation will need to be enhanced further to develop a general theory that can be applicable to any LCA study. In particular, a unified methodological framework would be needed to help and guide full

parameterization and corresponding explanatory/predictive model development throughout LCA.

APPENDIX A

APPENDIX FOR CHAPTER 1: MEDIUM-DUTY VEHICLE ELECTRIFICATION

A.1 Integration of Vehicle Dynamic Simulator and VSP-based Emissions Model

EPA MOVES (EPA 2014a) is a modal emissions model based on statistical stratification and/or binning method using the concept of vehicle specific power (VSP) proposed by Jimenez (1999). That is, vehicle operation modes (or their bins) and corresponding emissions rates are determined sequentially based on VSP. VSP for heavy-duty vehicles is often called specific tractive power (STP), but VSP and STP are essentially the same concepts. As shown in Eq. (A1), VSP is a function of vehicle dynamics-related parameters such as speed, acceleration, etc.

$$VSP_t = \frac{1}{f_{scale}} \times \left[A \times V_t + B \times V_t^2 + C \times V_t^3 + (m_{curb} + m_{payload}) \times (a_t + g \times sin\theta_t) \times V_t\right] \quad \text{(A1)}$$

, where VSP_t is vehicle-specific power (kW) at time t; f_{scale} is a mass factor (17.1 for medium-duty trucks); m_{curb} is curb mass of individual test vehicle in metric ton; $m_{payload}$ is mass of cargo loaded in vehicle in metric ton; A is the rolling resistance coefficient ($0.0785 \times 10^{-3} \times \left[m_{curb} + m_{payload}\right]$) in kW·sec/meter; B is the rotational resistance coefficient (0 by MOVES definition) in kW·sec^2/meter^2; C is the aerodynamic drag coefficient (2.091×10^{-3}) in kW·sec^3/meter^3; V_t is instantaneous vehicle speed in meter/sec; a_t instantaneous vehicle acceleration in meter/sec^2; g is gravitational acceleration (9.81 meter/sec^2); and $sin\theta_t$ is the fractional road grade. For each moment of time t, MOVES calculates VSP as in Eq. (A1), determines the so called operating mode bin, and then produces corresponding emissions rates (gram/sec or gram/mile) which

constitute generic emissions data in my analysis. Depending on the vehicle specifications modeled/tested, customized values instead of MOVES default can be used for A, B, and C.

The statistical stratification of operating mode(s) in MOVES is solely based on high level variables such as vehicle speed and acceleration as in Eq. (A1). The basic output of MOVES is mean base rate (MBR) which is re-scaled for final output, based on other types of inputs and/or specifications (e.g., fuel properties, climate condition, etc.) in MOVES. MBR data are directly available from the MOVES MySQL database and retrievable without running simulations. The relationship between the input and final output which is a function of VSP can be summarized by the following generic equation:

$$MBR_i = C_{i0} + C_{i\alpha}V\alpha + \sum_{j=1}^{J} C_{ij}V^j + \sum_{k=1}^{K} C_{ik}a^k + \sum_{m=1}^{M}\sum_{n=1}^{N} C_{im}C_{in}V^m a^n \qquad \text{(A2)}$$

, where MBR_i is mean base rate (gram/sec) for the i-th pollutant; V is instantaneous vehicle speed; and a is acceleration. Here the coefficients (C_{i0}, $C_{i\alpha}$, C_{ij}, C_{im}, C_{im}, and C_{in}) are functions of vehicle characteristics (e.g., vehicle mass, drag coefficient, and etc.) and other factors including road grade α, which are embedded in MOVES, along with the specific values of J, K, M, and N. This approach is convenient and efficient when measuring and modeling real-world vehicle emissions and/or when integrating with traffic simulators/models, because the only information needed is vehicle speed and acceleration. However, this dependency on high-level information sacrifices the functionality of detailed vehicle dynamic and emissions simulation, testing, and/or modeling, which requires low level data, including engine torque, engine speed, gear selection, etc. This issue becomes even more significant when it comes to emissions modeling for hybrid-electric vehicles.

Here I integrate the VSP-based emissions model (MOVES) and vehicle dynamic simulator (ADVISOR) for a more detailed analysis, based on the vehicle dynamics principles. In conventional internal combustion engine vehicles, engine output torque and

speed (or rpm) has the following relationships with overall power demand for moving vehicles and providing accessory loads (e.g., air conditioning, etc.):

$$N_{Engine_{out}}[rpm] = \frac{63{,}360}{2\times\pi\times 60} \times \left(\frac{GR_i \times \xi_{axle} \times V[mph]}{r_{wheel}[inch]}\right) \quad \text{(A3)}$$

$$T_{Engine_{out}}[N\cdot m] = \frac{\left\{\left(\frac{1}{\eta_{DT}}\times f_{scale}\times VSP\right) + P_{acc}\right\}}{\left(N_{Engine_{out}}[rpm]\times\frac{2\times\pi}{60}\right)[\frac{rad}{sec}]} \quad \text{(A4)}$$

, where $N_{Engine_{out}}$ and $T_{Engine_{out}}$ are engine output speed and torque; V is vehicle speed in miles/hour; ξ_{axle} is axle ratio; GR_i is the i-th gear ratio; r_{wheel} is wheel radius; P_{acc} is accessory load; and η_{DT} is drive-train efficiency which is non-linear. As discussed earlier, once drive or duty cycle as well as vehicle specifications are known, f_{scale}, V, a, and VSP are determined, and then engine output torque and speed can be estimated. In doing so, a certain level of approximation can be done, for example, assuming some parameters to be constant, but here I take advantage of the ADVISOR for a very detailed simulation of non-linear vehicle dynamic behavior, including gear selection, engine control, etc. Above all, what Eqs. (A1 – A4) tell us is that emissions rates information (i.e., MBR) from MOVES can be populated in the engine output torque and speed domain, because of the vehicle dynamic relationships shown in those equations. Also, since the "mean" base rate (MBR), by definition, is the expected value of emissions for the given vehicle operating condition, a large number of simulations are to be run to comply with the "expected" value concept of MBR. For this, I run thousands of vehicle dynamic simulations in ADVISOR and populate the MOVES MBR in engine operating domain. In the end, the expected emission rate will be drawn from the constructed sample space of MBR in engine torque and speed domain.

Figure A1 shows the comparison of direct results for diesel truck emissions from MOVES and those from ADVISOR implemented with MOVES MBR. Most of the data points lie close to the diagonal parity line, and thus the emissions map implemented in ADVISOR provides almost the same result as MOVES. The emissions maps built in this

way based off MOVES MBR can also be used for hybrid-electric truck modeling in ADVISOR, taking advantage of the hybrid-electric truck's engine operating data from ADVISOR. Using the vehicle dynamic simulator such as ADVISOR also minimizes the biases of more simplistic tractive energy-based modeling approach.

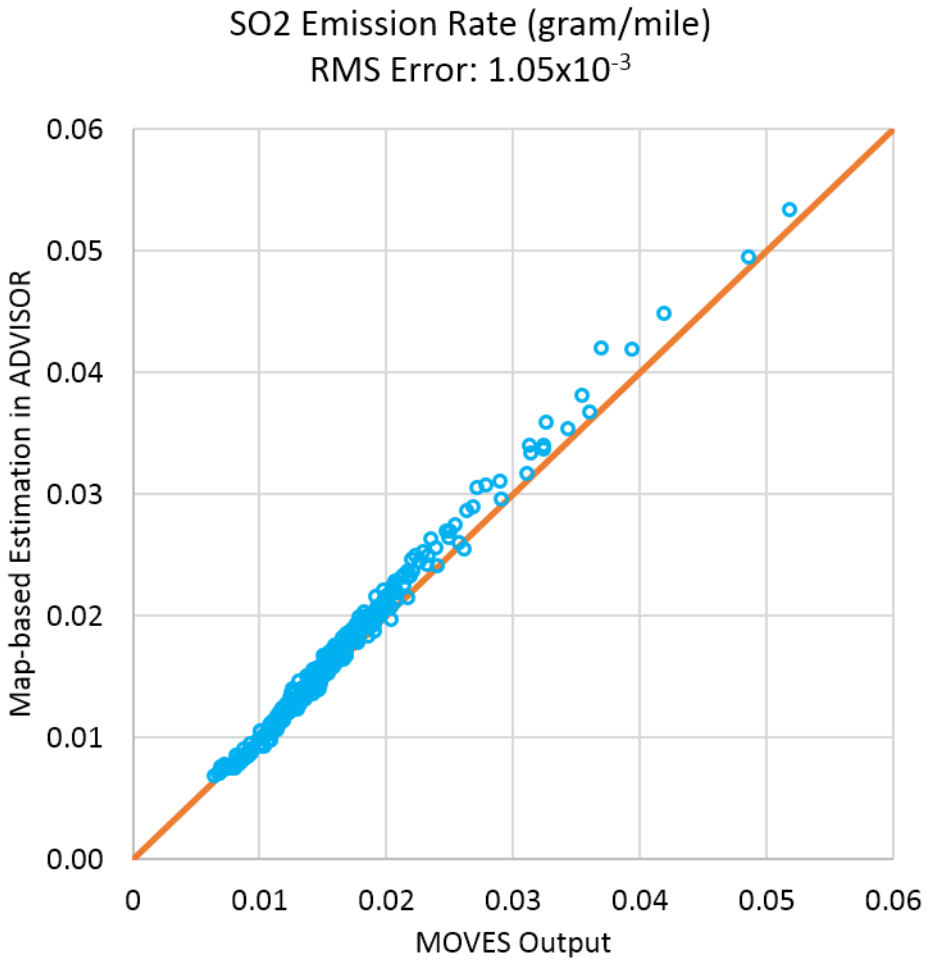

Figure A1. Comparison of SO2 emissions results between direct output from MOVES (x-axis) and engine map-based output from ADVISOR populated with MOVES rates. Data points align well with the diagonal parity line, resulting in a very low root mean square (RMS) error value.

A.2 Vehicle Dynamic and Emissions Simulation for WVU-HD City Driving Schedule

In addition to the example (for HTUF-6PDDS driving schedule) shown in Figure 2.4 in main text, here I present another example for West Virginia University Heavy Duty City (WVU-HD City) driving schedule and provide more detailed discussion of the simulation results.

The first chart in Figure A2 shows the driving schedule of WVU-HD City. The second chart from the top shows internal combustion engine power for conventional diesel, compressed natural gas (CNG), and diesel hybrid-electric trucks. Note that engine power for hybrid trucks (blue dashed lines) are sometimes 0, mostly when vehicle speed is 0, whereas diesel and CNG trucks' engine power stay in idle (above 0) at the same condition. Although the same diesel engine is used for both conventional diesel and

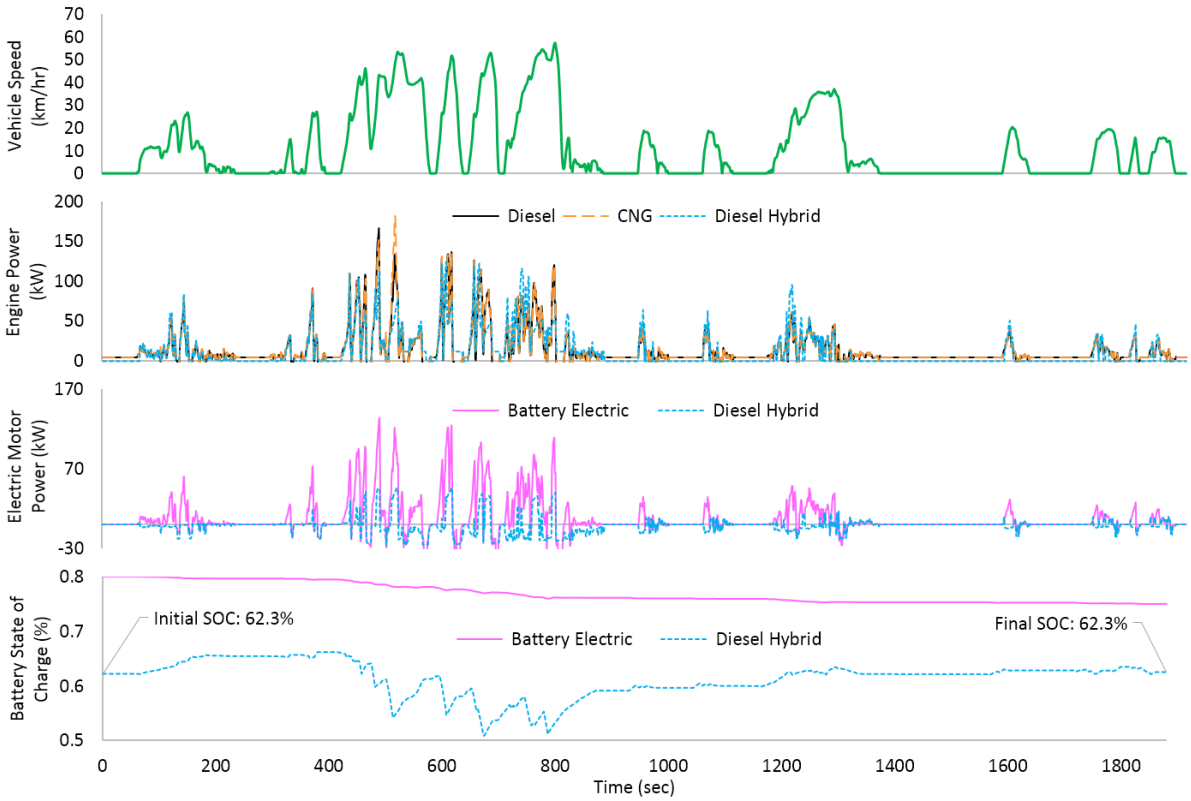

Figure A2. Vehicle dynamic and emissions simulation result for WVU-HD City drive cycle, tested at 11.8 metric ton of total vehicle weight – Part I (driving schedule and energy-related output).

hybrid-electric trucks, engine power of hybrid trucks is sometimes higher than diesel trucks for the same condition, because the additional engine power is used to charge the traction battery, increasing the state of charge, as can be seen around 1,200 second in the second and third charts from the top. Whenever the electric motor is used for generating electrical energy to charge the battery, the electric motor power becomes negative, because the internal combustion engine and/or vehicle inertia (when braking) rotates the electric motor in those cases. When the electric motor is providing tractive energy (directly propelling the vehicle), the power becomes positive. Also, note that the final state of charge (SOC) of hybrid-electric truck battery at the end of the test is the same as the initial SOC value at the beginning, which is needed to avoid biases, as discussed in main text. This requirement, however, doesn't apply to battery electric vehicles, because the battery recharging consumes energy exclusively from the wall plugs rather than on-board generator like automotive internal combustion engine.

Figure A3 shows tail-pipe emissions result. Battery electric trucks do create tire- and brake-wear particulate matters, but those emissions are not shown here for combustion-related "tail-pipe" emissions. These non-tail-pipe particulate emissions are all accounted for in overall life-cycle emissions calculations. As can be seen in the first chart in Figure A3, CNG trucks emit much higher tail-pipe methane emissions, mainly because of the unburned fuel (methane). CNG trucks used to emit even higher methane emissions (more than a few thousand times higher than diesel). This in turn has resulted in overall higher tail-pipe greenhouse gas emissions of CNG trucks than diesel trucks, negating the lower carbon intensity of CNG fuel than petroleum diesel, because methane is 25 or more powerful greenhouse gas than carbon dioxide in terms of global warming potential. However, owing to recent CNG truck engine and aftertreatment technology advances, relative methane emissions level in comparison with that of diesel engine has become lower. Also, the new heavy-duty vehicles regulations require the tail-pipe methane emissions of CNG buses and trucks to be the same (0.1 gram/bhp-hr for FTP

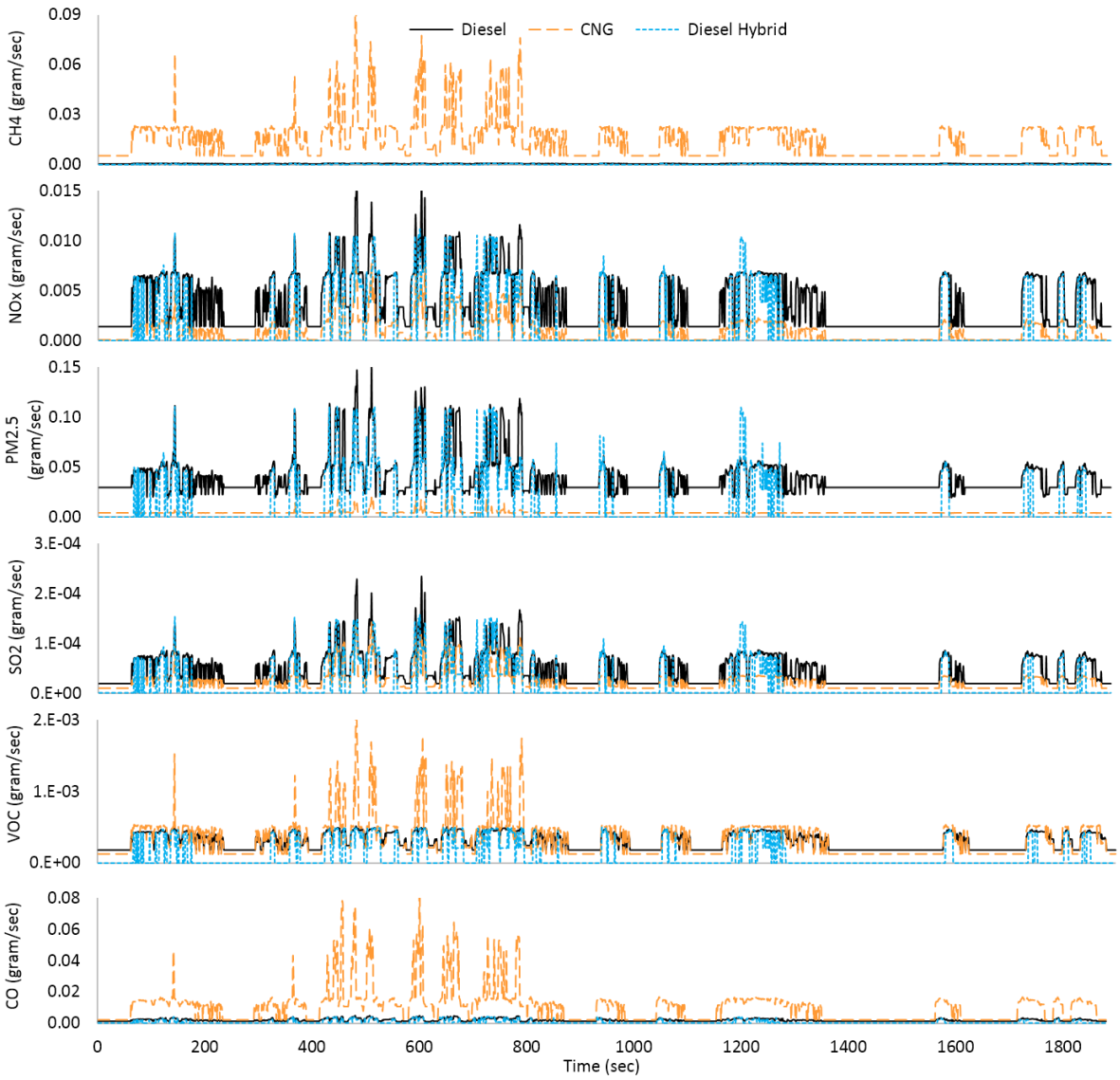

Figure A3. Vehicle dynamic and emissions simulation result for WVU-HD City drive cycle, tested at 11.8 metric ton of total vehicle weight – Part II (tail-pipe emissions).

duty cycle) as diesel vehicles, which can contribute the tail-pipe greenhouse gas emissions advantage of CNG trucks over diesel counterparts. CNG trucks emit lower NOx, in part due to the stoichiometric engine + three-way catalyst system, however, CNG trucks don't show definitive advantage in terms of SO2 emissions. CNG trucks emit much higher VOC and CO than diesel trucks, which together contribute to the ground-level ozone (smog) formation with NOx and ultraviolet radiation from the sun, among other factors.

A.3 State-by-State Energy-Water Intensity for Average and Marginal Power Consumption

Here I provide state-by-state energy efficiency and water intensity for average and marginal power consumption (per unit electricity purchased at wall plugs). The detailed estimation method is presented in the main text. I only show energy (Table A1) and water (Tables A2 and A3) data. For state-by-state air emissions for average and marginal power consumption, please see (Lee and Thomas 2015).

As can be seen in Table A1, in most of the states, marginal energy efficiency is lower than average efficiency. This is because of the effect of the higher efficiency of renewable power generation that is included in average electric grid. Except nuclear and biomass, thermal efficiency of renewables are approximately doubly higher than that of fossil fuels. In some states (e.g., New Jersey and Massachusetts), however, marginal efficiency is higher than average electric grid. In those states, coal and nuclear together accounts for about half of average power consumption mix. And in both states, marginal electricity generation is primarily based on natural gas which has higher thermal efficiency than petroleum, coal, and/or nuclear. This contributes to the higher marginal life cycle power consumption efficiency.

Table A2 shows life cycle fresh water withdrawal for power consumption in each state in the U.S. Unlike energy efficiency, I don't see a distinctive general pattern for (fresh) water withdrawal between average and marginal electricity consumption. This is not surprising, given the complexity and heterogeneity of cooling systems for thermo-electric power generation between regions and generating units, as briefly discussed in main text.

Table A3 shows fresh water consumption. Considering the dominance of natural gas as a marginal fuel and the high portion of recirculating cooling system type for natural gas power plants in the U.S., water consumption is expected to increase from average to marginal grid. However, in some cases (e.g., Georgia), marginal power consumption

leads to lower (fresh) water intensity, because nuclear power that accounts for significant portion of average electric grid tends to be very water-intensive.

Table A1. Consumption-based Life Cycle Energy Efficiency for Purchased Electricity (Year 2014)

State	AVERAGE	MARGINAL	State	AVERAGE	MARGINAL
AL	0.352	0.340	NC	0.333	0.363
AR	0.333	0.329	ND	0.423	0.291
AZ	0.346	0.339	NE	0.350	0.285
CA	0.457	0.453	NH	0.345	0.335
CO	0.388	0.361	NJ	0.342	0.416
CT	0.343	0.320	NM	0.352	0.304
DC	0.340	0.305	NV	0.426	0.342
DE	0.322	0.338	NY	0.419	0.385
FL	0.334	0.321	OH	0.331	0.361
GA	0.347	0.395	OK	0.415	0.309
IA	0.480	0.312	OR	0.752	0.362
ID	0.683	0.411	PA	0.338	0.309
IL	0.338	0.307	RI	0.341	0.345
IN	0.343	0.314	SC	0.321	0.321
KS	0.418	0.264	SD	0.735	0.278
KY	0.315	0.292	TN	0.361	0.365
LA	0.336	0.320	TX	0.388	0.341
MA	0.353	0.376	UT	0.347	0.346
MD	0.330	0.319	VA	0.326	0.355
ME	0.564	0.369	VT	0.391	0.391
MI	0.347	0.335	WA	0.768	0.325
MN	0.404	0.312	WI	0.331	0.316
MO	0.318	0.317	WV	0.340	0.304
MS	0.324	0.314	WY	0.353	0.310
MT	0.547	0.302	US-AVG	0.383	0.339

Table A2. Consumption-based Life Cycle Fresh Water *Withdrawal* (gal/kWh) for Purchased Electricity (Year 2014)

State	AVERAGE	MARGINAL	State	AVERAGE	MARGINAL
AL	16.30	12.45	NC	15.59	17.52
AR	4.79	3.12	ND	7.83	9.93
AZ	0.29	0.40	NE	22.77	29.57
CA	0.53	0.77	NH	1.64	5.26
CO	0.40	0.39	NJ	3.11	50.72
CT	0.93	9.50	NM	0.54	0.55
DC	7.98	8.74	NV	1.28	1.53
DE	13.66	128.25	NY	5.86	28.66
FL	0.34	0.48	OH	9.61	8.73
GA	4.42	5.20	OK	3.68	4.87
IA	10.03	12.07	OR	0.68	2.66
ID	0.67	2.02	PA	14.51	369.09
IL	23.14	18.69	RI	0.27	0.04
IN	12.41	11.75	SC	12.49	10.74
KS	4.05	3.09	SD	0.46	3.49
KY	9.95	10.34	TN	31.95	35.37
LA	15.32	14.89	TX	20.44	22.36
MA	5.28	125.25	UT	0.49	0.39
MD	4.08	34.96	VA	8.27	6.14
ME	0.47	0.30	VT	23.73	23.73
MI	23.39	24.57	WA	0.24	0.40
MN	22.35	30.68	WI	20.89	28.07
MO	31.33	27.67	WV	7.96	8.73
MS	6.99	8.10	WY	0.78	0.94
MT	1.21	6.50	US-AVG	11.15	34.05

Table A3. Consumption-based Life Cycle Fresh Water *Consumption* (gal/kWh) for Purchased Electricity (Year 2014)

State	AVERAGE	MARGINAL	State	AVERAGE	MARGINAL
AL	0.36	0.33	NC	0.23	0.28
AR	0.44	0.42	ND	0.30	0.36
AZ	0.26	0.35	NE	0.17	0.17
CA	0.31	0.44	NH	0.08	0.07
CO	0.35	0.34	NJ	0.21	0.30
CT	0.12	0.17	NM	0.50	0.52
DC	0.38	0.41	NV	0.13	0.15
DE	0.31	0.31	NY	0.34	0.45
FL	0.17	0.25	OH	0.43	0.38
GA	0.50	0.39	OK	0.19	0.19
IA	0.31	0.44	OR	0.07	0.19
ID	0.19	0.48	PA	0.45	0.50
IL	0.35	0.25	RI	0.04	0.04
IN	0.27	0.25	SC	0.37	0.53
KS	0.18	0.22	SD	0.38	1.05
KY	0.76	0.71	TN	0.25	0.19
LA	0.43	0.46	TX	0.54	0.68
MA	0.20	0.22	UT	0.47	0.39
MD	0.20	0.22	VA	0.29	0.40
ME	0.14	0.27	VT	0.21	0.21
MI	0.18	0.14	WA	0.12	0.29
MN	0.47	0.32	WI	0.34	0.29
MO	0.16	0.12	WV	0.37	0.41
MS	0.43	0.28	WY	0.23	0.23
MT	0.35	0.53	US-AVG	0.34	0.38

A.4 Vehicle and Parts Production Inventory

Table A4. Energy and Air Emissions – **Conventional Diesel (& Biodiesel, B20)** Truck

	Energy (MJ)	CH4 (kg)	N2O (kg)	CO2 (kg)	CO2e (kg)	CO (gram)
Body, Chassis, & Support Structure	3.56E+05	5.24E+01	4.56E-01	2.37E+04	4.06E+04	1.01E+05
Engine & Transmission	7.07E+04	1.01E+01	8.33E-02	4.09E+03	7.33E+03	1.45E+04
Electric Motor & Controller	0.00E+00	0.00E+00	0.00E+00	0.00E+00	0.00E+00	0.00E+00
Traction Battery Pack	0.00E+00	0.00E+00	0.00E+00	0.00E+00	0.00E+00	0.00E+00
CNG Cylinders	0.00E+00	0.00E+00	0.00E+00	0.00E+00	0.00E+00	0.00E+00
Engine & Transmission Fluids	3.48E+04	3.83E+00	2.46E-02	2.85E+03	4.03E+03	1.14E+03
Other Fluids	5.83E+03	1.28E+00	1.35E-02	2.76E+02	6.45E+02	3.54E+02
Tires	6.05E+04	8.51E+00	8.71E-02	4.29E+03	7.01E+03	1.14E+04
Painting & Assembly	1.62E+05	2.62E+01	2.49E-01	1.04E+04	1.79E+04	4.41E+03
Disposal	4.49E+04	5.59E+00	5.01E-02	3.23E+03	4.95E+03	8.68E+02
Total	7.35E+05	1.08E+02	9.63E-01	4.88E+04	8.25E+04	1.34E+05
	NH3 (gram)	**NOx (gram)**	**PM2.5 (gram)**	**PM10 (gram)**	**SO2 (gram)**	**VOC (gram)**
Body, Chassis, & Support Structure	2.65E+03	3.10E+04	9.45E+03	1.88E+04	1.11E+05	2.11E+04
Engine & Transmission	5.27E+02	5.45E+03	2.08E+03	4.17E+03	1.97E+04	3.33E+03
Electric Motor & Controller	0.00E+00	0.00E+00	0.00E+00	0.00E+00	0.00E+00	0.00E+00
Traction Battery Pack	0.00E+00	0.00E+00	0.00E+00	0.00E+00	0.00E+00	0.00E+00
CNG Cylinders	0.00E+00	0.00E+00	0.00E+00	0.00E+00	0.00E+00	0.00E+00
Engine & Transmission Fluids	2.59E+02	4.82E+03	1.41E+03	1.98E+03	5.99E+03	3.27E+03
Other Fluids	4.35E+01	5.06E+02	8.54E+01	1.57E+02	1.10E+03	8.22E+01
Tires	4.51E+02	6.02E+03	8.42E+02	1.60E+03	1.66E+04	6.15E+03
Painting & Assembly	1.21E+03	1.48E+04	1.77E+03	2.95E+03	1.73E+04	2.15E+04
Disposal	3.35E+02	4.14E+03	6.12E+02	1.04E+03	8.80E+03	3.31E+02
Total	5.48E+03	6.67E+04	1.62E+04	3.07E+04	1.80E+05	5.58E+04

Table A5. Energy and Air Emissions – **CNG** Truck

	Energy (MJ)	CH4 (kg)	N2O (kg)	CO2 (kg)	CO2e (kg)	CO (gram)
Body, Chassis, & Support Structure	3.64E+05	5.34E+01	4.63E-01	2.43E+04	4.16E+04	1.05E+05
Engine & Transmission	7.57E+04	1.09E+01	8.95E-02	4.37E+03	7.85E+03	1.57E+04
Electric Motor & Controller	0.00E+00	0.00E+00	0.00E+00	0.00E+00	0.00E+00	0.00E+00
Traction Battery Pack	0.00E+00	0.00E+00	0.00E+00	0.00E+00	0.00E+00	0.00E+00
CNG Cylinders	5.93E+03	6.83E-01	6.62E-03	3.81E+02	6.04E+02	2.31E+02
Engine & Transmission Fluids	3.59E+04	3.96E+00	2.54E-02	2.94E+03	4.17E+03	1.18E+03
Other Fluids	6.03E+03	1.32E+00	1.40E-02	2.85E+02	6.66E+02	3.66E+02
Tires	6.05E+04	8.51E+00	8.71E-02	4.29E+03	7.01E+03	1.14E+04
Painting & Assembly	1.70E+05	2.75E+01	2.61E-01	1.09E+04	1.87E+04	4.62E+03
Disposal	4.71E+04	5.87E+00	5.26E-02	3.38E+03	5.20E+03	9.10E+02
Total	7.65E+05	1.12E+02	9.99E-01	5.09E+04	8.58E+04	1.39E+05
	NH3 (gram)	**NOx (gram)**	**PM2.5 (gram)**	**PM10 (gram)**	**SO2 (gram)**	**VOC (gram)**
Body, Chassis, & Support Structure	2.71E+03	3.17E+04	9.64E+03	1.92E+04	1.13E+05	2.16E+04
Engine & Transmission	5.64E+02	5.84E+03	2.19E+03	4.38E+03	2.12E+04	3.58E+03
Electric Motor & Controller	0.00E+00	0.00E+00	0.00E+00	0.00E+00	0.00E+00	0.00E+00
Traction Battery Pack	0.00E+00	0.00E+00	0.00E+00	0.00E+00	0.00E+00	0.00E+00
CNG Cylinders	4.42E+01	1.04E+03	3.12E+02	6.08E+02	1.50E+03	7.80E+01
Engine & Transmission Fluids	2.68E+02	4.98E+03	1.45E+03	2.05E+03	6.19E+03	3.38E+03
Other Fluids	4.49E+01	5.23E+02	8.82E+01	1.63E+02	1.13E+03	8.50E+01
Tires	4.51E+02	6.02E+03	8.42E+02	1.60E+03	1.66E+04	6.15E+03
Painting & Assembly	1.27E+03	1.55E+04	1.86E+03	3.09E+03	1.81E+04	2.26E+04
Disposal	3.51E+02	4.34E+03	6.42E+02	1.09E+03	9.23E+03	3.47E+02
Total	5.70E+03	7.00E+04	1.70E+04	3.22E+04	1.87E+05	5.78E+04

Table A6. Energy and Air Emissions – **Diesel Hybrid** Truck

	Energy (MJ)	CH4 (kg)	N2O (kg)	CO2 (kg)	CO2e (kg)	CO (gram)
Body, Chassis, & Support Structure	3.61E+05	5.30E+01	4.60E-01	2.40E+04	4.12E+04	1.03E+05
Engine & Transmission	7.51E+04	1.07E+01	8.78E-02	4.36E+03	7.76E+03	1.51E+04
Electric Motor & Controller	4.04E+03	6.24E-01	6.11E-03	2.46E+02	4.99E+02	6.45E+02
Traction Battery Pack	1.03E+04	1.33E+00	1.07E-02	6.38E+02	1.10E+03	4.85E+02
CNG Cylinders	0.00E+00	0.00E+00	0.00E+00	0.00E+00	0.00E+00	0.00E+00
Engine & Transmission Fluids	3.48E+04	3.83E+00	2.46E-02	2.85E+03	4.03E+03	1.14E+03
Other Fluids	5.83E+03	1.28E+00	1.35E-02	2.76E+02	6.45E+02	3.54E+02
Tires	6.05E+04	8.51E+00	8.71E-02	4.29E+03	7.01E+03	1.14E+04
Painting & Assembly	1.68E+05	2.72E+01	2.58E-01	1.08E+04	1.85E+04	4.57E+03
Disposal	4.66E+04	5.81E+00	5.20E-02	3.35E+03	5.14E+03	9.01E+02
Total	7.66E+05	1.12E+02	1.00E+00	5.09E+04	8.59E+04	1.38E+05
	NH3 (gram)	**NOx (gram)**	**PM2.5 (gram)**	**PM10 (gram)**	**SO2 (gram)**	**VOC (gram)**
Body, Chassis, & Support Structure	2.69E+03	3.14E+04	9.56E+03	1.90E+04	1.12E+05	2.14E+04
Engine & Transmission	5.60E+02	5.78E+03	2.29E+03	4.58E+03	2.06E+04	3.49E+03
Electric Motor & Controller	3.01E+01	3.75E+02	1.02E+02	2.00E+02	3.13E+03	1.14E+02
Traction Battery Pack	7.65E+01	1.07E+03	4.52E+02	7.90E+02	4.09E+03	2.22E+02
CNG Cylinders	0.00E+00	0.00E+00	0.00E+00	0.00E+00	0.00E+00	0.00E+00
Engine & Transmission Fluids	2.59E+02	4.82E+03	1.41E+03	1.98E+03	5.99E+03	3.27E+03
Other Fluids	4.35E+01	5.06E+02	8.54E+01	1.57E+02	1.10E+03	8.22E+01
Tires	4.51E+02	6.02E+03	8.42E+02	1.60E+03	1.66E+04	6.15E+03
Painting & Assembly	1.25E+03	1.54E+04	1.84E+03	3.06E+03	1.79E+04	2.24E+04
Disposal	3.47E+02	4.30E+03	6.35E+02	1.08E+03	9.14E+03	3.44E+02
Total	5.71E+03	6.96E+04	1.72E+04	3.25E+04	1.90E+05	5.74E+04

Table A7. Energy and Air Emissions – **CNG Hybrid** Truck

	Energy (MJ)	CH4 (kg)	N2O (kg)	CO2 (kg)	CO2e (kg)	CO (gram)
Body, Chassis, & Support Structure	3.72E+05	5.46E+01	4.72E-01	2.50E+04	4.27E+04	1.09E+05
Engine & Transmission	8.01E+04	1.14E+01	9.41E-02	4.64E+03	8.29E+03	1.63E+04
Electric Motor & Controller	4.04E+03	6.24E-01	6.11E-03	2.46E+02	4.99E+02	6.45E+02
Traction Battery Pack	1.03E+04	1.33E+00	1.07E-02	6.38E+02	1.10E+03	4.85E+02
CNG Cylinders	5.93E+03	6.83E-01	6.62E-03	3.81E+02	6.04E+02	2.31E+02
Engine & Transmission Fluids	3.56E+04	3.92E+00	2.52E-02	2.91E+03	4.13E+03	1.17E+03
Other Fluids	6.03E+03	1.32E+00	1.40E-02	2.85E+02	6.66E+02	3.66E+02
Tires	6.05E+04	8.51E+00	8.71E-02	4.29E+03	7.01E+03	1.14E+04
Painting & Assembly	1.76E+05	2.85E+01	2.70E-01	1.13E+04	1.94E+04	4.79E+03
Disposal	4.88E+04	6.08E+00	5.45E-02	3.50E+03	5.38E+03	9.43E+02
Total	8.00E+05	1.17E+02	1.04E+00	5.32E+04	8.98E+04	1.45E+05
	NH3 (gram)	**NOx (gram)**	**PM2.5 (gram)**	**PM10 (gram)**	**SO2 (gram)**	**VOC (gram)**
Body, Chassis, & Support Structure	2.78E+03	3.25E+04	9.85E+03	1.96E+04	1.15E+05	2.22E+04
Engine & Transmission	5.97E+02	6.17E+03	2.39E+03	4.80E+03	2.22E+04	3.75E+03
Electric Motor & Controller	3.01E+01	3.75E+02	1.02E+02	2.00E+02	3.13E+03	1.14E+02
Traction Battery Pack	7.65E+01	1.07E+03	4.52E+02	7.90E+02	4.09E+03	2.22E+02
CNG Cylinders	4.42E+01	1.04E+03	3.12E+02	6.08E+02	1.50E+03	7.80E+01
Engine & Transmission Fluids	2.65E+02	4.93E+03	1.44E+03	2.03E+03	6.12E+03	3.37E+03
Other Fluids	4.49E+01	5.23E+02	8.82E+01	1.63E+02	1.13E+03	8.50E+01
Tires	4.51E+02	6.02E+03	8.42E+02	1.60E+03	1.66E+04	6.15E+03
Painting & Assembly	1.31E+03	1.61E+04	1.92E+03	3.20E+03	1.88E+04	2.34E+04
Disposal	3.64E+02	4.50E+03	6.65E+02	1.13E+03	9.57E+03	3.60E+02
Total	5.96E+03	7.32E+04	1.81E+04	3.41E+04	1.98E+05	5.97E+04

Table A8. Energy and Air Emissions – **Battery Electric** Truck

	Energy (MJ)	CH4 (kg)	N2O (kg)	CO2 (kg)	CO2e (kg)	CO (gram)
Body, Chassis, & Support Structure	2.32E+05	3.40E+01	2.96E-01	1.54E+04	2.64E+04	6.56E+04
Engine & Transmission	0.00E+00	0.00E+00	0.00E+00	0.00E+00	0.00E+00	0.00E+00
Electric Motor & Controller	1.10E+04	1.70E+00	1.67E-02	6.71E+02	1.36E+03	1.76E+03
Traction Battery Pack	4.75E+05	6.14E+01	4.94E-01	2.95E+04	5.11E+04	2.24E+04
CNG Cylinders	0.00E+00	0.00E+00	0.00E+00	0.00E+00	0.00E+00	0.00E+00
Engine & Transmission Fluids	0.00E+00	0.00E+00	0.00E+00	0.00E+00	0.00E+00	0.00E+00
Other Fluids	5.83E+03	1.28E+00	1.35E-02	2.76E+02	6.45E+02	3.54E+02
Tires	6.05E+04	8.51E+00	8.71E-02	4.29E+03	7.01E+03	1.14E+04
Painting & Assembly	1.62E+05	2.62E+01	2.49E-01	1.04E+04	1.79E+04	4.41E+03
Disposal	4.49E+04	5.59E+00	5.01E-02	3.23E+03	4.95E+03	8.68E+02
Total	9.91E+05	1.39E+02	1.21E+00	6.38E+04	1.09E+05	1.07E+05
	NH3 (gram)	**NOx (gram)**	**PM2.5 (gram)**	**PM10 (gram)**	**SO2 (gram)**	**VOC (gram)**
Body, Chassis, & Support Structure	1.73E+03	2.01E+04	6.14E+03	1.22E+04	7.19E+04	1.37E+04
Engine & Transmission	0.00E+00	0.00E+00	0.00E+00	0.00E+00	0.00E+00	0.00E+00
Electric Motor & Controller	8.21E+01	1.02E+03	2.79E+02	5.47E+02	8.52E+03	3.11E+02
Traction Battery Pack	3.54E+03	4.95E+04	2.09E+04	3.66E+04	1.90E+05	1.03E+04
CNG Cylinders	0.00E+00	0.00E+00	0.00E+00	0.00E+00	0.00E+00	0.00E+00
Engine & Transmission Fluids	0.00E+00	0.00E+00	0.00E+00	0.00E+00	0.00E+00	0.00E+00
Other Fluids	4.35E+01	5.06E+02	8.54E+01	1.57E+02	1.10E+03	8.22E+01
Tires	4.51E+02	6.02E+03	8.42E+02	1.60E+03	1.66E+04	6.15E+03
Painting & Assembly	1.21E+03	1.48E+04	1.77E+03	2.95E+03	1.73E+04	2.15E+04
Disposal	3.35E+02	4.14E+03	6.12E+02	1.04E+03	8.80E+03	3.31E+02
Total	7.39E+03	9.61E+04	3.07E+04	5.51E+04	3.14E+05	5.24E+04

Table A9. Fresh Water Consumption (gallons)

	Diesel	CNG	Diesel Hybrid	CNG Hybrid	Electric
Body, Chassis, & Support Structure	1.11E+05	1.13E+05	1.12E+05	1.16E+05	7.23E+04
Engine & Transmission	2.55E+04	2.67E+04	2.83E+04	2.95E+04	0.00E+00
Electric Motor & Controller	0.00E+00	0.00E+00	1.44E+03	1.44E+03	3.93E+03
Traction Battery Pack	0.00E+00	0.00E+00	5.25E+03	5.25E+03	2.43E+05
CNG Cylinders	0.00E+00	5.08E+03	0.00E+00	5.08E+03	0.00E+00
Engine & Transmission Fluids	1.85E+03	1.91E+03	1.85E+03	1.89E+03	0.00E+00
Other Fluids	4.35E+02	4.50E+02	4.35E+02	4.50E+02	4.35E+02
Tires	4.68E+03	4.68E+03	4.68E+03	4.68E+03	4.68E+03
Painting & Assembly	4.39E+04	4.60E+04	4.55E+04	4.77E+04	4.39E+04
Disposal	1.22E+04	1.28E+04	1.26E+04	1.32E+04	1.22E+04
Total	2.00E+05	2.11E+05	2.13E+05	2.25E+05	3.81E+05

A.5 Life Cycle Inventory (LCI) Prediction Models

Table A10. CO Emissions LCI Prediction

Predictors	Dependent variable: $\hat{Y}$, Life cycle CO emissions (gram/km) per truck							
	$\log(\hat{Y}) = \hat{\beta}_0 + \hat{\beta}_1 m_p + \hat{\beta}_2 WPKE + \hat{\beta}_3 \bar{V}_{trip} + \hat{\beta}_4 \bar{V}_{trip}^{-1} + \hat{\beta}_5 \log(\bar{V}_{trip}) + \hat{\beta}_6 \bar{V}_{trip}^{2}$							
	Conventional ICE			Hybrid Electric			Battery Electric	
	Diesel	BD20	CNG	Diesel	BD20	CNG	VA	NV
	Coefficients $\hat{\beta}_i$ and t-statistic (in parenthesis)							
$\hat{\beta}_0$	0.887 (34.7)	0.951 (35.1)	3.202 (101)	-0.115 (-3.98)	0.099 (3.42)	2.7 (32)	-1.415 (-441)	-0.372 (-42.6)
$\hat{\beta}_1$	$9.01\text{x}10^{-3}$ (20.4)	$9.61\text{x}10^{-3}$ (20.5)	$1.16\text{x}10^{-2}$ (6.86)	$1.08\text{x}10^{-2}$ (11.31)	$1.19\text{x}10^{-2}$ (12.5)	$4.43\text{x}10^{-2}$ (11.2)	$1.28\text{x}10^{-2}$ (32.7)	$3.29\text{x}10^{-2}$ (30.7)
$\hat{\beta}_2$	$1.81\text{x}10^{-2}$ (23.6)	$3.06\text{x}10^{-2}$ (65.9)	$7.9\text{x}10^{-2}$ (25.7)	$7.41\text{x}10^{-2}$ (43.5)	$8.52\text{x}10^{-2}$ (50)	0.207 (31.8)	$7.91\text{x}10^{-2}$ (69.3)	0.206 (66.3)
$\hat{\beta}_3$			$-2.86\text{x}10^{-2}$ (-24.9)	$1.91\text{x}10^{-2}$ (14.62)	$2.03\text{x}10^{-2}$ (15.5)	$1.17\text{x}10^{-2}$ (11.48)		
$\hat{\beta}_4$	1.146 (14.6)	1.151 (13.8)	2.43 (14.5)					
$\hat{\beta}_5$	-0.436 (-61.7)	-0.433 (-57.8)		-0.386 (-23.3)	-0.435 (-26.2)	-0.343 (-10.9)		
$\hat{\beta}_6$	$3.98\text{x}10^{-5}$ (27.3)	$4.34\text{x}10^{-5}$ (28.1)	$2.2\text{x}10^{-4}$ (19.5)	$-8.89\text{x}10^{-5}$ (-8.88)	$-8.95\text{x}10^{-5}$ (-8.9)		$3.06\text{x}10^{-5}$ (28.8)	$8.27\text{x}10^{-5}$ (28.5)
Adj. R^2	0.99	0.99	0.95	0.91	0.93	0.8	0.94	0.93
F-stat.	20300	19080	2803	1298	1787	614	2547	2302
N_{obs}	725	725	680	624	624	645	489	489

m: total vehicle weight (metric ton) – sum of curb weight m_c (metric ton) and payload m_p (metric ton), $\bar{V}_{trip}$: average trip speed (km/hour) – total distance traveled divided by total trip time taken, $WPKE$: $(m \cdot PKE)$ weighted positive kinetic energy (ton·meter/sec^2), and N_{obs}: the number of observations (or samples).

For battery electric, I here show the results for two select cases – minimum (daytime charging in Virginia (VA) and nighttime charging in Nevada (NV), based on consumption-based marginal electric grid. Other states fall between the two (minimum and maximum).

On top of this generic prediction equation, correction factors may be applied (multiplied) for road grade (Figure 2.7) and/or temperature (Figure 2.8).

Table A11. NH3 Emissions LCI Prediction

Predictors	Dependent variable: $\hat{Y}$, Life cycle NH3 emissions (gram/km) per truck							
	$\log(\hat{Y}) = \hat{\beta}_0 + \hat{\beta}_1 m_p + \hat{\beta}_2 WPKE + \hat{\beta}_3 \bar{V}_{trip} + \hat{\beta}_4 \bar{V}_{trip}^{-1} + \hat{\beta}_5 \log(\bar{V}_{trip}) + \hat{\beta}_6 \bar{V}_{trip}^{2}$							
	Conventional ICE			Hybrid Electric			Battery Electric	
	Diesel	BD20	CNG	Diesel	BD20	CNG	MT	DE
	Coefficients $\hat{\beta}_i$ and t-statistic (in parenthesis)							
$\hat{\beta}_0$	-2.88 (-189.2)	-2.57 (-147.8)	-0.61 (-32.6)	-3.82 (-591)	-3.47 (-453)	-2.3 (-54.5)	-4.303 (-13323)	-3.25 (-388)
$\hat{\beta}_1$	6.27×10^{-3} (7.87)	9.29×10^{-3} (10.19)	5.47×10^{-3} (5.7)	1.64×10^{-2} (15.05)	1.8×10^{-2} (13.88)	2.66×10^{-2} (13.49)	1.28×10^{-3} (32.3)	3.17×10^{-2} (30.9)
$\hat{\beta}_2$	6.44×10^{-2} (46.8)	8.71×10^{-2} (55.3)	5.29×10^{-2} (30.9)	0.1045 (57.2)	0.1305 (60.2)	0.103 (31.8)	7.82×10^{-3} (68)	0.198 (66.6)
$\hat{\beta}_3$	-2.49×10^{-2} (-44.2)	-2.27×10^{-2} (-35.4)				1.32×10^{-2} (26)		
$\hat{\beta}_4$	3.91 (47.2)	3.72 (39.3)		2.57 (38.7)	3.28 (41.5)			
$\hat{\beta}_5$			-0.712 (-128)			-0.457 (-29.1)		
$\hat{\beta}_6$	2.24×10^{-4} (39.8)	2.09×10^{-4} (32.5)	1.09×10^{-4} (54.4)	2.3×10^{-5} (12.5)	3×10^{-5} (13.8)		2.97×10^{-6} (27.7)	7.95×10^{-5} (28.6)
Adj. R^2	0.99	0.98	0.98	0.95	0.95	0.87	0.94	0.93
F-stat.	9899	7819	10160	2703	2973	1040	2466	2327
N_{obs}	725	725	680	624	624	645	489	489

m: total vehicle weight (metric ton) – sum of curb weight m_c (metric ton) and payload m_p (metric ton), $\bar{V}_{trip}$: average trip speed (km/hour) – total distance traveled divided by total trip time taken, $WPKE$: $(m \cdot PKE)$ weighted positive kinetic energy (ton·meter/sec^2), and N_{obs}: the number of observations (or samples).

For battery electric, I here show the results for two select cases – minimum (daytime charging in Montana (MT) and nighttime charging in Delaware (DE), based on consumption-based marginal electric grid. Other states fall between the two (minimum and maximum).

On top of this generic prediction equation, correction factors may be applied (multiplied) for road grade (Figure 2.7) and/or temperature (Figure 2.8).

Table A12. NOx Emissions LCI Prediction

Predictors	Dependent variable: $\hat{Y}$, Life cycle NOx emissions (gram/km) per truck							
	$\log(\hat{Y}) = \hat{\beta}_0 + \hat{\beta}_1 m_p + \hat{\beta}_2 WPKE + \hat{\beta}_3 \bar{V}_{trip} + \hat{\beta}_4 \bar{V}_{trip}^{-1} + \hat{\beta}_5 \log(\bar{V}_{trip}) + \hat{\beta}_6 \bar{V}_{trip}^{2}$							
	Conventional ICE			Hybrid Electric			Battery Electric	
	Diesel	BD20	CNG	Diesel	BD20	CNG	CO	RI
	Coefficients $\hat{\beta}_i$ and t-statistic (in parenthesis)							
$\hat{\beta}_0$	0.372 (22.9)	0.393 (24.6)	0.848 (18.2)	0.167 (4.12)	-0.756 (-71)	0.364 (9.9)	-1.681 (-1642)	-0.1712 (-18.26)
$\hat{\beta}_1$	1.57×10^{-2} (18.5)	1.57×10^{-2} (18.8)	1.23×10^{-2} (14.75)	2.06×10^{-2} (11.2)	1.97×10^{-2} (10.96)	3.22×10^{-2} (16.29)	4.07×10^{-3} (32.5)	3.49×10^{-2} (30.4)
$\hat{\beta}_2$	2.83×10^{-2} (19.27)	3.23×10^{-2} (22.3)	8.37×10^{-2} (55)	0.101 (31.2)	0.1081 (35.9)	0.1153 (35.3)	2.5×10^{-2} (68.5)	0.219 (65.7)
$\hat{\beta}_3$	-2.53×10^{-2} (-42.1)	-2.51×10^{-2} (-42.4)		9.11×10^{-3} (17.11)				
$\hat{\beta}_4$	3.31 (37.4)	3.3 (37.9)	1.194 (8.46)		2.48 (22.6)			
$\hat{\beta}_5$			-0.378 (-29.5)	-0.332 (-21.4)		-0.322 (-29.9)		
$\hat{\beta}_6$	1.68×10^{-4} (28.1)	1.69×10^{-4} (28.7)	6.34×10^{-5} (24.6)		2.68×10^{-5} (8.9)	8.85×10^{-5} (23.1)	9.54×10^{-6} (28)	8.83×10^{-5} (28.3)
Adj. R^2	0.98	0.98	0.98	0.86	0.87	0.9	0.94	0.93
F-stat.	9107	9373	6989	927	1020	1444	2502	2257
N_{obs}	725	725	680	624	624	645	489	489

m: total vehicle weight (metric ton) – sum of curb weight m_c (metric ton) and payload m_p (metric ton), $\bar{V}_{trip}$: average trip speed (km/hour) – total distance traveled divided by total trip time taken, $WPKE$: $(m \cdot PKE)$ weighted positive kinetic energy (ton·meter/sec^2), and N_{obs}: the number of observations (or samples).

For battery electric, I here show the results for two select cases – minimum (daytime charging in Colorado (CO) and nighttime charging in Rhode Island (RI), based on consumption-based marginal electric grid. Other states fall between the two (minimum and maximum).

On top of this generic prediction equation, correction factors may be applied (multiplied) for road grade (Figure 2.7) and/or temperature (Figure 2.8).

Table A13. PM2.5 Emissions LCI Prediction

Predictors	**Dependent variable: $\hat{Y}$, Life cycle PM2.5 emissions (gram/km) per truck**							
	$\log(\hat{Y}) = \hat{\beta}_0 + \hat{\beta}_1 m_p + \hat{\beta}_2 WPKE + \hat{\beta}_3 \bar{V}_{trip} + \hat{\beta}_4 \bar{V}_{trip}^{-1} + \hat{\beta}_5 \log(\bar{V}_{trip}) + \hat{\beta}_6 \bar{V}_{trip}^{2}$							
	Conventional ICE			**Hybrid Electric**			**Battery Electric**	
	Diesel	BD20	CNG	Diesel	BD20	CNG	VT	OH
	Coefficients $\hat{\beta}_i$ and t-statistic (in parenthesis)							
$\hat{\beta}_0$	-1.002 (-41)	-0.976 (-41.2)	-1.003 (-47)	-3.35 (-1138)	-3.33 (-993)	-2.26 (-234)	-2.77 (-409)	-1.63 (-64.9)
$\hat{\beta}_1$				6.81×10^{-3} (13.66)	7.6×10^{-3} (13.43)	6.63×10^{-3} (14.62)	1.96×10^{-3} (33.1)	2.88×10^{-2} (34)
$\hat{\beta}_2$	4.76×10^{-2} (24.4)	5.2×10^{-2} (27.5)	3.25×10^{-2} (20.4)	5.52×10^{-2} (66.2)	6.27×10^{-2} (66.2)	2.26×10^{-2} (30.2)	1.12×10^{-2} (61.9)	0.172 (67.2)
$\hat{\beta}_3$			5.95×10^{-3} (22.4)			3.08×10^{-3} (26.3)	1.1×10^{-3} (20.7)	1.13×10^{-2} (28.7)
$\hat{\beta}_4$				1.513 (49.8)	1.732 (50.2)		0.9002 (50.9)	
$\hat{\beta}_5$	-0.555 (-75.4)	-0.553 (-77.5)	-0.458 (-56.6)			-0.124 (-34.5)	-3.62×10^{-2} (-15.9)	-0.211 (-20.5)
$\hat{\beta}_6$	4.5×10^{-5} (16.2)	4.72×10^{-5} (17.55)		1.85×10^{-5} (22.1)	2.05×10^{-5} (21.5)			
Adj. R^2	0.96	0.96	0.95	0.96	0.96	0.9	0.99	0.95
F-stat.	6110	6558	4779	3552	3588	1363	20670	2132
N_{obs}	725	725	680	624	624	645	489	489

m: total vehicle weight (metric ton) – sum of curb weight m_c (metric ton) and payload m_p (metric ton), $\bar{V}_{trip}$: average trip speed (km/hour) – total distance traveled divided by total trip time taken, $WPKE$: $(m \cdot PKE)$ weighted positive kinetic energy (ton·meter/sec^2), and N_{obs}: the number of observations (or samples).

For battery electric, I here show the results for two select cases – minimum (daytime charging in Vermont (VT) and nighttime charging in Ohio (OH), based on consumption-based marginal electric grid. Other states fall between the two (minimum and maximum).

On top of this generic prediction equation, correction factors may be applied (multiplied) for road grade (Figure 2.7) and/or temperature (Figure 2.8).

Table A14. PM10 Emissions LCI Prediction

Predictors	Dependent variable: $\hat{Y}$, Life cycle PM10 emissions (gram/km) per truck							
	$\log(\hat{Y}) = \hat{\beta}_0 + \hat{\beta}_1 m_p + \hat{\beta}_2 WPKE + \hat{\beta}_3 \bar{V}_{trip} + \hat{\beta}_4 \bar{V}_{trip}^{-1} + \hat{\beta}_5 \log(\bar{V}_{trip}) + \hat{\beta}_6 \bar{V}_{trip}^{2}$							
	Conventional ICE			Hybrid Electric			Battery Electric	
	Diesel	BD20	CNG	Diesel	BD20	CNG	VT	SC
	Coefficients $\hat{\beta}_i$ and t-statistic (in parenthesis)							
$\hat{\beta}_0$	-0.565 (-11.03)	-0.564 (-11.17)	0.725 (22.9)	-2.76 (-1164)	-2.74 (-1027)	-1.1 (-198)	-1.758 (-158)	-1.66 (-253)
$\hat{\beta}_1$			-5.27×10^{-3} (-3.24)	5.52×10^{-3} (13.78)	6.15×10^{-3} (13.63)	2.73×10^{-3} (14.24)	1.44×10^{-3} (14.85)	2.45×10^{-2} (33.7)
$\hat{\beta}_2$	5.19×10^{-2} (12.14)	5.34×10^{-2} (12.7)	3.53×10^{-2} (12.2)	4.41×10^{-2} (65.8)	5.01×10^{-2} (66.4)	9.8×10^{-3} (30.3)	8.02×10^{-3} (27)	0.146 (68.3)
$\hat{\beta}_3$	-4.67×10^{-2} (-24.7)	-4.63×10^{-2} (-24.9)				3.02×10^{-3} (12.56)	2.55×10^{-3} (29.3)	
$\hat{\beta}_4$	1.91 (6.82)	1.93 (7.01)		1.205 (49.4)	1.389 (50.5)		1.867 (64.5)	1.829 (30.8)
$\hat{\beta}_5$			-0.487 (-52)			-7.32×10^{-2} (-23.4)	-0.1506 (-40.4)	
$\hat{\beta}_6$	3.04×10^{-4} (16.1)	3.03×10^{-4} (16.3)	3.52×10^{-5} (10.42)	1.53×10^{-5} (22.7)	1.7×10^{-5} (22.4)	-1.3×10^{-5} (-7.2)		6.33×10^{-5} (29.4)
Adj. R^2	0.93	0.93	0.93	0.96	0.96	0.9	0.99	0.95
F-stat.	2443	2486	2218	3483	3595	1086	54580	2581
N_{obs}	725	725	680	624	624	645	489	489

m: total vehicle weight (metric ton) – sum of curb weight m_c (metric ton) and payload m_p (metric ton), $\bar{V}_{trip}$: average trip speed (km/hour) – total distance traveled divided by total trip time taken, $WPKE$: $(m \cdot PKE)$ weighted positive kinetic energy (ton·meter/sec^2), and N_{obs}: the number of observations (or samples).

For battery electric, I here show the results for two select cases – minimum (daytime charging in Vermont (VT) and nighttime charging in South Carolina (SC), based on consumption-based marginal electric grid. Other states fall between the two (minimum and maximum).

On top of this generic prediction equation, correction factors may be applied (multiplied) for road grade (Figure 2.7) and/or temperature (Figure 2.8).

Table A15. SO2 Emissions LCI Prediction

Predictors	Dependent variable: $\hat{Y}$, Life cycle SO2 emissions (gram/km) per truck							
	$\log(\hat{Y}) = \hat{\beta}_0 + \hat{\beta}_1 m_p + \hat{\beta}_2 WPKE + \hat{\beta}_3 \bar{V}_{trip} + \hat{\beta}_4 \bar{V}_{trip}^{-1} + \hat{\beta}_5 \log(\bar{V}_{trip}) + \hat{\beta}_6 \bar{V}_{trip}^{2}$							
	Conventional ICE			Hybrid Electric			Battery Electric	
	Diesel	BD20	CNG	Diesel	BD20	CNG	VT	MS
	Coefficients $\hat{\beta}_i$ and t-statistic (in parenthesis)							
$\hat{\beta}_0$	-0.902 (-169.4)	-0.83 (-130)	-0.273 (-11.28)	-1 (-387)	-0.97 (-311)	-0.098 (-5.24)	-0.549 (-1083)	0.492 (59)
$\hat{\beta}_1$	4.4×10^{-3} (15.8)	5.19×10^{-3} (15.5)	5.38×10^{-3} (12.44)	5.25×10^{-3} (12)	6.26×10^{-3} (11.89)	1.53×10^{-2} (15.2)	2.01×10^{-3} (32.3)	3.16×10^{-2} (30.9)
$\hat{\beta}_2$	4.4×10^{-2} (91.4)	5.18×10^{-2} (89.6)	5.27×10^{-2} (66.5)	4.75×10^{-2} (64.8)	5.67×10^{-2} (64.3)	5.02×10^{-2} (30.2)	1.23×10^{-2} (68.2)	0.198 (66.6)
$\hat{\beta}_3$	-3.7×10^{-3} (-18.7)	-4.62×10^{-3} (-19.54)						
$\hat{\beta}_4$	1.972 (68.1)	2.19 (63)	1.95 (26.6)	1.471 (55.2)	1.727 (53.8)			
$\hat{\beta}_5$			-0.1315 (-19.8)			-0.185 (-33.7)		
$\hat{\beta}_6$	4.18×10^{-5} (21.3)	5.13×10^{-5} (21.8)	3.1×10^{-5} (23.1)	1.54×10^{-5} (20.9)	1.79×10^{-5} (20.2)	4.54×10^{-5} (23.2)	4.68×10^{-6} (27.7)	7.93×10^{-5} (28.6)
Adj. R^2	0.99	0.99	0.99	0.96	0.96	0.9	0.94	0.94
F-stat.	11860	11050	8874	3765	3671	1406	2476	2328
N_{obs}	725	725	680	624	624	645	489	489

m: total vehicle weight (metric ton) – sum of curb weight m_c (metric ton) and payload m_p (metric ton), $\bar{V}_{trip}$: average trip speed (km/hour) – total distance traveled divided by total trip time taken, $WPKE$: $(m \cdot PKE)$ weighted positive kinetic energy (ton·meter/sec^2), and N_{obs}: the number of observations (or samples).

For battery electric, I here show the results for two select cases – minimum (daytime charging in Vermont (VT) and nighttime charging in Mississippi (MS), based on consumption-based marginal electric grid. Other states fall between the two (minimum and maximum).

On top of this generic prediction equation, correction factors may be applied (multiplied) for road grade (Figure 2.7) and/or temperature (Figure 2.8).

Table A16. VOC Emissions LCI Prediction

Predictors	Dependent variable: $\hat{Y}$, Life cycle VOC emissions (gram/km) per truck							
	$\log(\hat{Y}) = \hat{\beta}_0 + \hat{\beta}_1 m_p + \hat{\beta}_2 WPKE + \hat{\beta}_3 \bar{V}_{trip} + \hat{\beta}_4 \bar{V}_{trip}^{-1} + \hat{\beta}_5 \log(\bar{V}_{trip}) + \hat{\beta}_6 \bar{V}_{trip}^{2}$							
	Conventional ICE			Hybrid Electric			Battery Electric	
	Diesel	BD20	CNG	Diesel	BD20	CNG	VT	WA
	Coefficients $\hat{\beta}_i$ and t-statistic (in parenthesis)							
$\hat{\beta}_0$	0.1166 (5.87)	-2.66x10^{-2} (-1.38)	-0.505 (-17.16)	-0.631 (-63.2)	-0.767 (-78.9)	-0.812 (-30.6)	-2.318 (-3223)	-1.963 (-373)
$\hat{\beta}_1$	1.37x10^{-2} (13.2)	1.35x10^{-2} (13.3)	8.57x10^{-3} (16.3)	1.86x10^{-2} (11.03)	1.83x10^{-2} (11.12)	2.16x10^{-2} (15.12)	2.86x10^{-3} (32.4)	2.08x10^{-2} (32.2)
$\hat{\beta}_2$	0.115 (63.9)	0.112 (64.1)	5.71x10^{-2} (59.4)	0.1558 (55.1)	0.1527 (55.5)	7.35x10^{-2} (31.3)	1.75x10^{-2} (68.3)	0.129 (68.8)
$\hat{\beta}_3$	-1.78x10^{-2} (-24.3)	-1.77x10^{-2} (-24.7)						
$\hat{\beta}_4$	3.33 (30.8)	3.33 (31.6)	1.78 (19.98)	3.98 (38.7)	3.92 (39.2)			
$\hat{\beta}_5$			-0.269 (-33.3)			-0.23 (-29.6)		
$\hat{\beta}_6$	1.69x10^{-4} (23.1)	1.67x10^{-4} (23.4)	3.14x10^{-5} (19.3)	3.72x10^{-5} (13.1)	3.66x10^{-5} (13.3)	5.44x10^{-5} (19.67)	6.66x10^{-6} (27.8)	5.07x10^{-5} (28.9)
Adj. R^2	0.98	0.98	0.99	0.94	0.94	0.9	0.94	0.94
F-stat.	5826	6020	12700	2475	2517	1325	2486	2500
N_{obs}	725	725	680	624	624	645	489	489

m: total vehicle weight (metric ton) – sum of curb weight m_c (metric ton) and payload m_p (metric ton), $\bar{V}_{trip}$: average trip speed (km/hour) – total distance traveled divided by total trip time taken, $WPKE$: ($m \cdot PKE$) weighted positive kinetic energy (ton·meter/sec^2), and N_{obs}: the number of observations (or samples).

For battery electric, I here show the results for two select cases – minimum (daytime charging in Vermont (VT) and nighttime charging in Washington (WA), based on consumption-based marginal electric grid. Other states fall between the two (minimum and maximum).

On top of this generic prediction equation, correction factors may be applied (multiplied) for road grade (Figure 2.7) and/or temperature (Figure 2.8).

A.6 Life Cycle Impact Assessment (LCIA) Prediction Models

Table A17. GHG (GWP20) LCIA Prediction

Predictors	Dependent variable: $\hat{Y}$, Life cycle GHG-20YR emissions (gram/km) per truck							
	$\log(\hat{Y}) = \hat{\beta}_0 + \hat{\beta}_1 m_p + \hat{\beta}_2 WPKE + \hat{\beta}_3 \bar{V}_{trip} + \hat{\beta}_4 \bar{V}_{trip}^{-1} + \hat{\beta}_5 \log(\bar{V}_{trip}) + \hat{\beta}_6 \bar{V}_{trip}^{2}$							
	Conventional ICE			Hybrid Electric			Battery Electric	
	Diesel	BD20	CNG	Diesel	BD20	CNG	VT	ND
	Coefficients $\hat{\beta}_i$ and t-statistic (in parenthesis)							
$\hat{\beta}_0$	6.76 (340)	6.74 (340)	8.24 (167)	6.1 (617)	6.1 (617)	7.68 (192)	4.98 (4133)	6.3 (695)
$\hat{\beta}_1$	1.35×10^{-2} (12.9)	1.34×10^{-2} (13)	1.33×10^{-2} (15.1)	1.8×10^{-2} (10.8)	1.81×10^{-2} (10.8)	3.61×10^{-2} (16.8)	4.8×10^{-3} (32.5)	3.4×10^{-2} (30.5)
$\hat{\beta}_2$	0.1186 (65.9)	0.1184 (66)	0.0941 (58.3)	0.154 (55.1)	0.154 (55.1)	0.123 (34.7)	0.0294 (68.6)	0.213 (66)
$\hat{\beta}_3$	-1.62×10^{-2} (-22.1)	-1.62×10^{-2} (-22.1)						
$\hat{\beta}_4$	3.28 (30.3)	3.28 (30.4)	1.446 (9.67)	3.93 (38.7)	3.93 (38.6)			
$\hat{\beta}_5$			-0.44 (-32.4)			-0.372 (-31.7)		
$\hat{\beta}_6$	1.59×10^{-4} (21.7)	1.59×10^{-4} (21.7)	5.55×10^{-5} (20.3)	3.74×10^{-5} (13.3)	3.74×10^{-5} (13.3)	8.61×10^{-5} (20.6)	1.12×10^{-5} (28.1)	8.56×10^{-5} (28.4)
Adj. R^2	0.97	0.97	0.99	0.94	0.94	0.91	0.94	0.93
F-stat.	5510	5524	9204	2462	2460	1602	2509	2279
N_{obs}	725	725	680	624	624	645	489	489

m: total vehicle weight (metric ton) – sum of curb weight m_c (metric ton) and payload m_p (metric ton), $\bar{V}_{trip}$: average trip speed (km/hour) – total distance traveled divided by total trip time taken, $WPKE$: $(m \cdot PKE)$ weighted positive kinetic energy (ton·meter/sec^2), and N_{obs}: the number of observations (or samples).

For battery electric, I here show the results for two select cases – minimum (daytime charging in Vermont (VT) and nighttime charging in North Dakota (ND), based on consumption-based marginal electric grid. Other states fall between the two (minimum and maximum).

On top of this generic prediction equation, correction factors may be applied (multiplied) for road grade (Figure 2.7) and/or temperature (Figure 2.8).

Table A18. Fresh Water Consumption LCIA Prediction

Predictors	Dependent variable: $\hat{Y}$, Life cycle fresh water consumption (gallon/km) per truck							
	$\log(\hat{Y}) = \hat{\beta}_0 + \hat{\beta}_1 m_p + \hat{\beta}_2 WPKE + \hat{\beta}_3 \bar{V}_{trip} + \hat{\beta}_4 \bar{V}_{trip}^{-1} + \hat{\beta}_5 \log(\bar{V}_{trip}) + \hat{\beta}_6 \bar{V}_{trip}^{2}$							
	Conventional ICE			Hybrid Electric			Battery Electric	
	Diesel	BD20	CNG	Diesel	BD20	CNG	RI	SD
	Coefficients $\hat{\beta}_i$ and t-statistic (in parenthesis)							
$\hat{\beta}_0$	-0.688 (-94.3)	0.393 (23.2)	-0.483 (-25.8)	-0.838 (-237)	-0.1487 (-17.93)	-0.262 (-18.1)	-0.369 (-796)	-9.35×10^{-2} (-20.6)
$\hat{\beta}_1$	5.63×10^{-3} (14.7)	1.18×10^{-2} (13.3)	3.99×10^{-3} (11.9)	6.89×10^{-3} (11.54)	1.54×10^{-2} (10.99)	1.14×10^{-2} (14.56)	1.84×10^{-3} (32.3)	1.08×10^{-2} (32.5)
$\hat{\beta}_2$	5.87×10^{-2} (89)	0.108 (70.3)	4.08×10^{-2} (66.8)	6.33×10^{-2} (63.3)	0.134 (57.1)	3.69×10^{-2} (28.6)	1.12×10^{-2} (68.1)	0.1117 (69.1)
$\hat{\beta}_3$	-5.01×10^{-3} (-18.57)	-1.36×10^{-2} (-21.7)						
$\hat{\beta}_4$	2.302 (58)	3.18 (34.4)	1.75 (30.9)	1.921 (52.8)	3.54 (41.5)			
$\hat{\beta}_5$			-8.54×10^{-2} (-16.61)			-0.1416 (-33.3)		
$\hat{\beta}_6$	5.68×10^{-5} (21.15)	1.37×10^{-4} (21.9)	2.27×10^{-5} (22)	1.95×10^{-5} (19.45)	3.43×10^{-5} (14.54)	3.48×10^{-5} (23)	4.28×10^{-6} (27.7)	4.37×10^{-5} (28.9)
Adj. R^2	0.99	0.98	0.99	0.96	0.95	0.9	0.94	0.94
F-stat.	10000	6165	8923	3557	2691	1308	2472	2525
N_{obs}	725	725	680	624	624	645	489	489

m: total vehicle weight (metric ton) – sum of curb weight m_c (metric ton) and payload m_p (metric ton), $\bar{V}_{trip}$: average trip speed (km/hour) – total distance traveled divided by total trip time taken, $WPKE$: $(m \cdot PKE)$ weighted positive kinetic energy (ton·meter/sec^2), and N_{obs}: the number of observations (or samples).

For battery electric, I here show the results for two select cases – minimum (daytime charging in Rhode Island (RI) and nighttime charging in South Dakota (SD), based on consumption-based marginal electric grid. Other states fall between the two (minimum and maximum).

On top of this generic prediction equation, correction factors may be applied (multiplied) for road grade (Figure 2.7) and/or temperature (Figure 2.8).

Table A19. Acidification LCIA Prediction

Predictors	Dependent variable: $\hat{Y}$, Life cycle acidification impact per km per truck							
	$\log(\hat{Y}) = \hat{\beta}_0 + \hat{\beta}_1 m_p + \hat{\beta}_2 WPKE + \hat{\beta}_3 \bar{V}_{trip}^{-1} + \hat{\beta}_4 \bar{V}_{trip} + \hat{\beta}_5 \log(\bar{V}_{trip}) + \hat{\beta}_6 \bar{V}_{trip}^{2}$							
	Conventional ICE			Hybrid Electric			Battery Electric	
	Diesel	BD20	CNG	Diesel	BD20	CNG	VT	MS
	Coefficients $\hat{\beta}_i$ and t-statistic (in parenthesis)							
$\hat{\beta}_0$	0.387 (34)	0.448 (38.9)	0.993 (28.4)	-0.326 (-52.6)	-0.273 (-44)	0.731 (26.4)	-0.299 (-341)	0.812 (94.8)
$\hat{\beta}_1$	1.1×10^{-2} (18.5)	1.13×10^{-2} (18.8)	8.59×10^{-3} (13.77)	1.3×10^{-2} (12.42)	1.36×10^{-2} (12.98)	2.38×10^{-2} (15.96)	3.49×10^{-3} (32.4)	3.23×10^{-2} (30.8)
$\hat{\beta}_2$	3.59×10^{-2} (34.9)	4.41×10^{-2} (42.4)	6.75×10^{-2} (59.2)	7.94×10^{-2} (45.3)	8.76×10^{-2} (49.9)	8.3×10^{-2} (33.7)	2.14×10^{-2} (68.4)	0.2027 (66.4)
$\hat{\beta}_3$	-1.73×10^{-2} (-41.3)	-1.74×10^{-2} (-40.9)						
$\hat{\beta}_4$	3.14 (50.7)	3.16 (50.5)	1.669 (15.78)	2.02 (31.7)	2.26 (35.4)			
$\hat{\beta}_5$			-0.286 (-29.8)			-0.257 (-31.6)		
$\hat{\beta}_6$	1.3×10^{-4} (31.1)	1.34×10^{-4} (31.7)	5.22×10^{-5} (27.1)	2.13×10^{-5} (12.1)	2.34×10^{-5} (13.3)	6.9×10^{-5} (23.8)	8.16×10^{-6} (27.9)	8.13×10^{-5} (28.5)
Adj. R^2	0.99	0.99	0.99	0.92	0.93	0.9	0.94	0.93
F-stat.	11010	11320	8850	1690	2063	1440	2494	2313
N_{obs}	725	725	680	624	624	645	489	489

m: total vehicle weight (metric ton) – sum of curb weight m_c (metric ton) and payload m_p (metric ton), $\bar{V}_{trip}$: average trip speed (km/hour) – total distance traveled divided by total trip time taken, $WPKE$: ($m \cdot PKE$) weighted positive kinetic energy (ton·meter/sec^2), and N_{obs}: the number of observations (or samples).

For battery electric, I here show the results for two select cases – minimum (daytime charging in Vermont (VT) and nighttime charging in Mississippi (MS), based on consumption-based marginal electric grid. Other states fall between the two (minimum and maximum).

On top of this generic prediction equation, correction factors may be applied (multiplied) for road grade (Figure 2.7) and/or temperature (Figure 2.8).

Table A20. Eutrophication LCIA Prediction

Predictors	**Dependent variable**: $\hat{Y}$, **Life cycle eutrophication impact per km per truck**							
	$\log(\hat{Y}) = \hat{\beta}_0 + \hat{\beta}_1 m_p + \hat{\beta}_2 WPKE + \hat{\beta}_3 \bar{V}_{trip}^{-1} + \hat{\beta}_4 \bar{V}_{trip} + \hat{\beta}_5 \log(\bar{V}_{trip}) + \hat{\beta}_6 \bar{V}_{trip}^{2}$							
	Conventional ICE			**Hybrid Electric**			**Battery Electric**	
	Diesel	BD20	CNG	Diesel	BD20	CNG	CO	NH
	Coefficients $\hat{\beta}_i$ and t-statistic (in parenthesis)							
$\hat{\beta}_0$	-2.65 (-174.9)	-2.59 (-174.4)	-1.957 (-42.1)	-3.78 (-367)	-2.43 (-50.6)	-2.615 (-71.6)	-4.59 (-2922)	-3.24 (-354.8)
$\hat{\beta}_1$	1.47×10^{-2} (18.5)	1.47×10^{-2} (18.9)	1.12×10^{-2} (13.45)	1.93×10^{-2} (11.09)	1.95×10^{-2} (12.29)	3.15×10^{-2} (16.02)	6.27×10^{-3} (32.6)	3.42×10^{-2} (30.5)
$\hat{\beta}_2$	3.23×10^{-2} (23.6)	4.06×10^{-2} (30.2)	7.9×10^{-2} (52.06)	0.1048 (35.9)	0.1107 (39)	0.113 (34.9)	3.85×10^{-2} (68.8)	0.214 (65.9)
$\hat{\beta}_3$	-2.53×10^{-2} (-45.4)	-2.48×10^{-2} (-45.2)			2.43×10^{-2} (11.16)			
$\hat{\beta}_4$	3.37 (40.9)	3.36 (41.5)	1.207 (8.58)	2.402 (22.6)				
$\hat{\beta}_5$			-0.417 (-32.7)		-0.527 (-19.12)	-0.318 (-29.7)		
$\hat{\beta}_6$	1.76×10^{-4} (31.5)	1.77×10^{-4} (32.3)	6.86×10^{-5} (26.7)	2.56×10^{-5} (8.74)	-1.14×10^{-4} (-6.81)	8.96×10^{-5} (23.5)	1.47×10^{-5} (28.2)	8.64×10^{-5} (28.4)
Adj. R^2	0.99	0.99	0.98	0.87	0.9	0.9	0.94	0.93
F-stat.	10400	10720	7606	1026	1157	1397	2522	2273
N_{obs}	725	725	680	624	624	645	489	489

m: total vehicle weight (metric ton) – sum of curb weight m_c (metric ton) and payload m_p (metric ton), $\bar{V}_{trip}$: average trip speed (km/hour) – total distance traveled divided by total trip time taken, $WPKE$: ($m \cdot PKE$) weighted positive kinetic energy (ton·meter/sec^2), and N_{obs}: the number of observations (or samples).

For battery electric, I here show the results for two select cases – minimum (daytime charging in Colorado (CO) and nighttime charging in New Hampshire (NH), based on consumption-based marginal electric grid. Other states fall between the two (minimum and maximum).

On top of this generic prediction equation, correction factors may be applied (multiplied) for road grade (Figure 2.7) and/or temperature (Figure 2.8).

Table A21. Smog Formation LCIA Prediction

Predictors	Dependent variable: $\hat{Y}$, Life cycle smog formation impact per km per truck							
	$\log(\hat{Y}) = \hat{\beta}_0 + \hat{\beta}_1 m_p + \hat{\beta}_2 WPKE + \hat{\beta}_3 \bar{V}_{trip} + \hat{\beta}_4 \bar{V}_{trip}^{-1} + \hat{\beta}_5 \log(\bar{V}_{trip}) + \hat{\beta}_6 \bar{V}_{trip}^{2}$							
	Conventional ICE			Hybrid Electric			Battery Electric	
	Diesel	BD20	CNG	Diesel	BD20	CNG	CO	RI
	Coefficients $\hat{\beta}_i$ and t-statistic (in parenthesis)							
$\hat{\beta}_0$	3.68 (239)	3.69 (240)	4.09 (89.7)	3.88 (80.2)	3.9 (81.2)	3.62 (100)	1.605 (1544)	3.061 (330)
$\hat{\beta}_1$	1.54×10^{-2} (19.2)	1.54×10^{-2} (19.22)	1.21×10^{-2} (14.86)	1.96×10^{-2} (12.26)	1.96×10^{-2} (12.36)	3.18×10^{-2} (16.27)	4.14×10^{-3} (32.5)	3.46×10^{-2} (30.4)
$\hat{\beta}_2$	4.13×10^{-2} (29.7)	4.25×10^{-2} (30.6)	8.25×10^{-2} (55.4)	0.1125 (39.4)	0.1133 (40)	0.113 (35.3)	2.53×10^{-2} (68.5)	0.217 (65.8)
$\hat{\beta}_3$	-2.43×10^{-2} (-42.8)	-2.42×10^{-2} (-42.8)		2.45×10^{-2} (11.22)	2.45×10^{-2} (11.29)			
$\hat{\beta}_4$	3.3 (36.4)	3.3 (39.5)	1.222 (8.85)					
$\hat{\beta}_5$			-0.373 (-29.7)	-0.537 (-19.38)	-0.54 (-19.6)	-0.318 (-29.9)		
$\hat{\beta}_6$	1.7×10^{-4} (30)	1.7×10^{-4} (30.1)	6.19×10^{-5} (24.6)	-1.13×10^{-4} (-6.77)	-1.13×10^{-4} (-6.76)	8.7×10^{-5} (23)	9.68×10^{-6} (28)	8.75×10^{-5} (28.3)
Adj. R^2	0.99	0.99	0.98	0.9	0.91	0.9	0.94	0.93
F-stat.	9947	9990	7199	1186	1221	1444	2502	2263
N_{obs}	725	725	680	624	624	645	489	489

m: total vehicle weight (metric ton) – sum of curb weight m_c (metric ton) and payload m_p (metric ton), $\bar{V}_{trip}$: average trip speed (km/hour) – total distance traveled divided by total trip time taken, $WPKE$: ($m \cdot PKE$) weighted positive kinetic energy (ton·meter/sec^2), and N_{obs}: the number of observations (or samples).

For battery electric, I here show the results for two select cases – minimum (daytime charging in Colorado (CO) and nighttime charging in Rhode Island (RI), based on consumption-based marginal electric grid. Other states fall between the two (minimum and maximum).

On top of this generic prediction equation, correction factors may be applied (multiplied) for road grade (Figure 2.7) and/or temperature (Figure 2.8).

Table A22. Human Health LCIA Prediction

Predictors	Dependent variable: $\hat{Y}$, Life cycle human health impact per km per truck							
	$\log(\hat{Y}) = \hat{\beta}_0 + \hat{\beta}_1 m_p + \hat{\beta}_2 WPKE + \hat{\beta}_3 \bar{V}_{trip} + \hat{\beta}_4 \bar{V}_{trip}^{-1} + \hat{\beta}_5 \log(\bar{V}_{trip}) + \hat{\beta}_6 \bar{V}_{trip}^{2}$							
	Conventional ICE			Hybrid Electric			Battery Electric	
	Diesel	BD20	CNG	Diesel	BD20	CNG	VT	OH
	Coefficients $\hat{\beta}_i$ and t-statistic (in parenthesis)							
$\hat{\beta}_0$	-0.298 (-5.19)	-1.442 (-45)	-0.1208 (-5.15)	-2.92 (-886)	-2.88 (-783)	-1.587 (-145.1)	-2.29 (-287)	-1.748 (-209)
$\hat{\beta}_1$				7.77×10^{-3} (13.95)	8.62×10^{-3} (13.86)	7.75×10^{-3} (15.1)	1.98×10^{-3} (28.4)	2.65×10^{-2} (25.9)
$\hat{\beta}_2$	4.76×10^{-2} (17.3)	5.26×10^{-2} (19.69)	3.53×10^{-2} (17.39)	5.79×10^{-2} (62.1)	6.64×10^{-2} (63.8)	2.82×10^{-2} (33.4)	1.13×10^{-2} (52.8)	0.171 (57.5)
$\hat{\beta}_3$	-1.46×10^{-2} (-6.02)	-3.37×10^{-2} (-28.5)				3.35×10^{-3} (25.2)	1.51×10^{-3} (24.1)	
$\hat{\beta}_4$		2.57 (14.68)		1.552 (45.7)	1.803 (47.6)		1.309 (62.8)	
$\hat{\beta}_5$	-0.463 (-14.4)		-0.452 (-65.1)			-0.1289 (-31.5)	-6.38×10^{-2} (-23.8)	
$\hat{\beta}_6$	1.35×10^{-4} (7.47)	2.41×10^{-4} (20.4)	4.35×10^{-5} (17.24)	1.86×10^{-5} (19.87)	2.08×10^{-5} (19.93)			5.66×10^{-5} (20.3)
Adj. R^2	0.95	0.95	0.95	0.95	0.96	0.9	0.99	0.92
F-stat.	3579	3735	4265	3128	3332	1338	34700	1757
N_{obs}	725	725	680	624	624	645	489	489

m: total vehicle weight (metric ton) – sum of curb weight m_c (metric ton) and payload m_p (metric ton), $\bar{V}_{trip}$: average trip speed (km/hour) – total distance traveled divided by total trip time taken, $WPKE$: ($m \cdot PKE$) weighted positive kinetic energy (ton·meter/sec^2), and N_{obs}: the number of observations (or samples).

For battery electric, I here show the results for two select cases – minimum (daytime charging in Vermont (VT) and nighttime charging in Ohio (OH), based on consumption-based marginal electric grid. Other states fall between the two (minimum and maximum).

On top of this generic prediction equation, correction factors may be applied (multiplied) for road grade (Figure 2.7) and/or temperature (Figure 2.8).

A.7 Additional Parameters and Results of Monte Carlo Simulation

In addition to the key input parameters presented in Table 2.1 in main text, here I discuss in more detail my Monte Carlo simulations for Figures 2.14 and 2.15 in main text. By and large, I use two different types of Monte Carlo simulation. One is for a baseline analysis (Figure 2.14 in main text) with reasonable (or commonly-agreed) ranges of input parameters that are presented in Table 2.1 in main text. The other is for robustness test and identification of necessary conditions in Figure 2.15. For this, I relax the assumptions used for a baseline Monte Carlo simulation and look at a broader range of input parameters. Note that all monetary values are in 2015 constant U.S. dollars and that I use uniform distribution for the input parameters in Monte Carlo simulations.

As can be seen in Table A23, I don't consider some input parameters in my robustness analysis, for example, CNG and electricity fuel prices and battery pack price. As shown in Figures A5 and A6, CNG and electricity fuel prices are expected to remain relatively steady. Also, my baseline analysis indicates that in average (e.g., typical local-hauling) and least severe (e.g., highway) operating conditions, conventional diesel trucks are generally the most cost-effective. In more severe (e.g., extreme city or urban) operating conditions which is believed to be a niche for electric trucks, the technology choice from the overall cost minimization standpoint is idle reduction for conventional diesel, hybrid electric diesel, or battery electric trucks. For this, Figure 2.14 in main text shows the results for niche application condition. For these reasons, I focus on conventional diesel and battery electric trucks for my robustness analysis for average operating conditions (or major market/application).

There are two reasons that I don't consider secondary battery pack price in robustness analysis. First, it is almost certain that electric vehicle battery price will decrease over time, as shown in Figure A6. Second, battery replacement costs are not significant, compared to other parameters (e.g., purchase cost). I estimate that two or three battery replacements will be needed. First of the replacements will be covered by

truck manufacture warranty, which is part of the reason why electric truck's upfront cost is significantly more expensive than diesel or other non-electric trucks. The impact of the second and third battery replacements would be not significant, not only because the battery price is declining, but also because the battery replacement cost in several or more years becomes less significant because of the concept of time value of money.

Table A23. Comparison of the ranges of input parameters for Monte Carlo simulations

Input Parameters	**Monte Carlo Simulations**	
	Baseline Analysis	**Robustness Analysis**
Diesel fuel prices	Figure A4	1 – 10 $/diesel gallon
CNG fuel prices	Figure A4	-
Electricity fuel prices	Figure A5	-
Secondary battery pack price	Figure A6	-
Purchase cost	$150,000 – 180,000	$70,000 – 180,000
Carbon price	30 – 60 $/metric ton CO2	0 – 3,000 $/metric ton CO2
Payback time	20 years	3 – 20 years
Discount rate	7.5%	5 – 20%

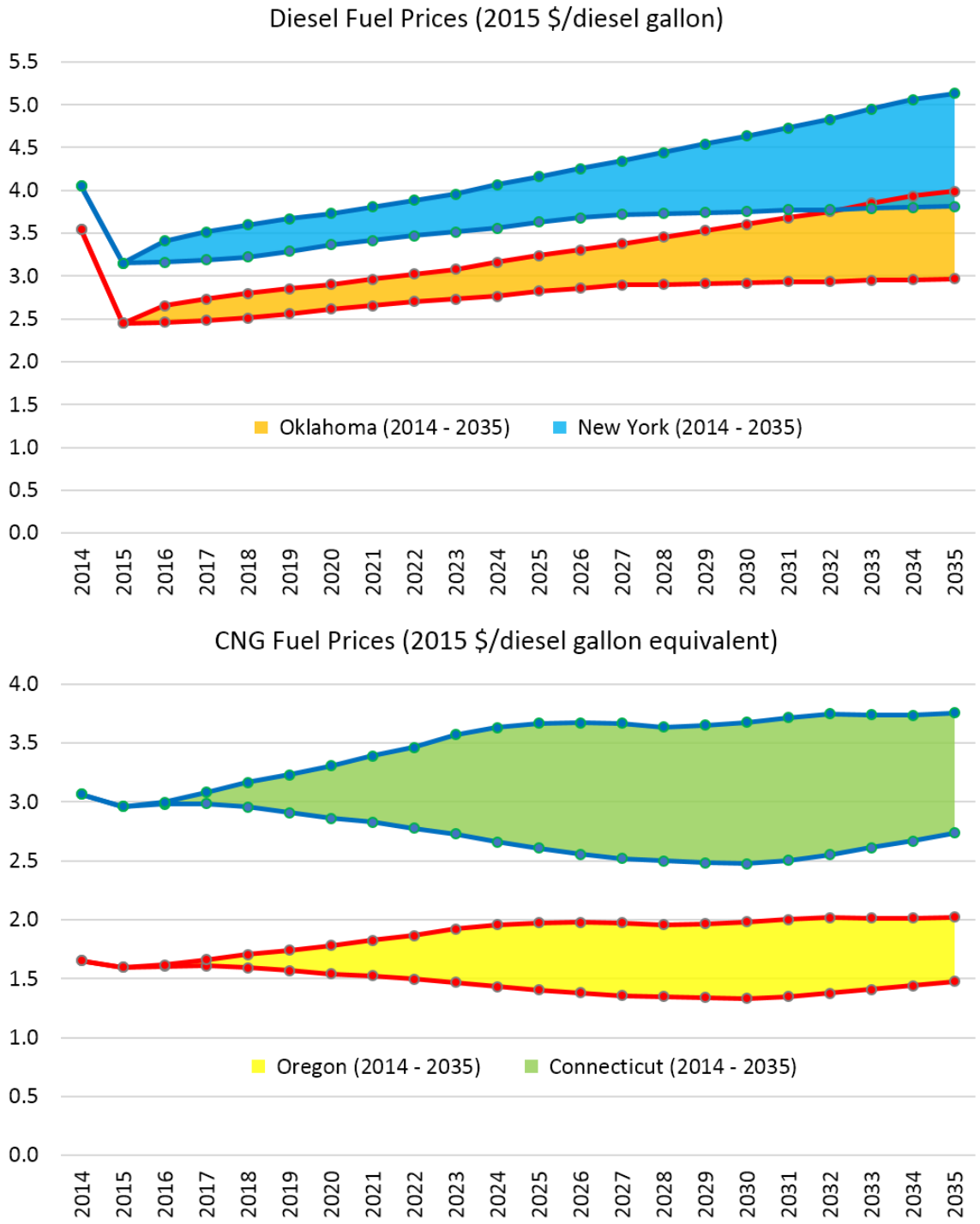

Figure A4. Actual fuel prices in two select states (min and max in continental U.S. for 2014 and 2015) and future fuel price projections – diesel (top) and CNG (bottom). The ranges shown here are used for baseline Monte Carlo simulation. For robustness test Monte Carlo simulation, future diesel fuel prices assumptions are relaxed with a wider ranges.

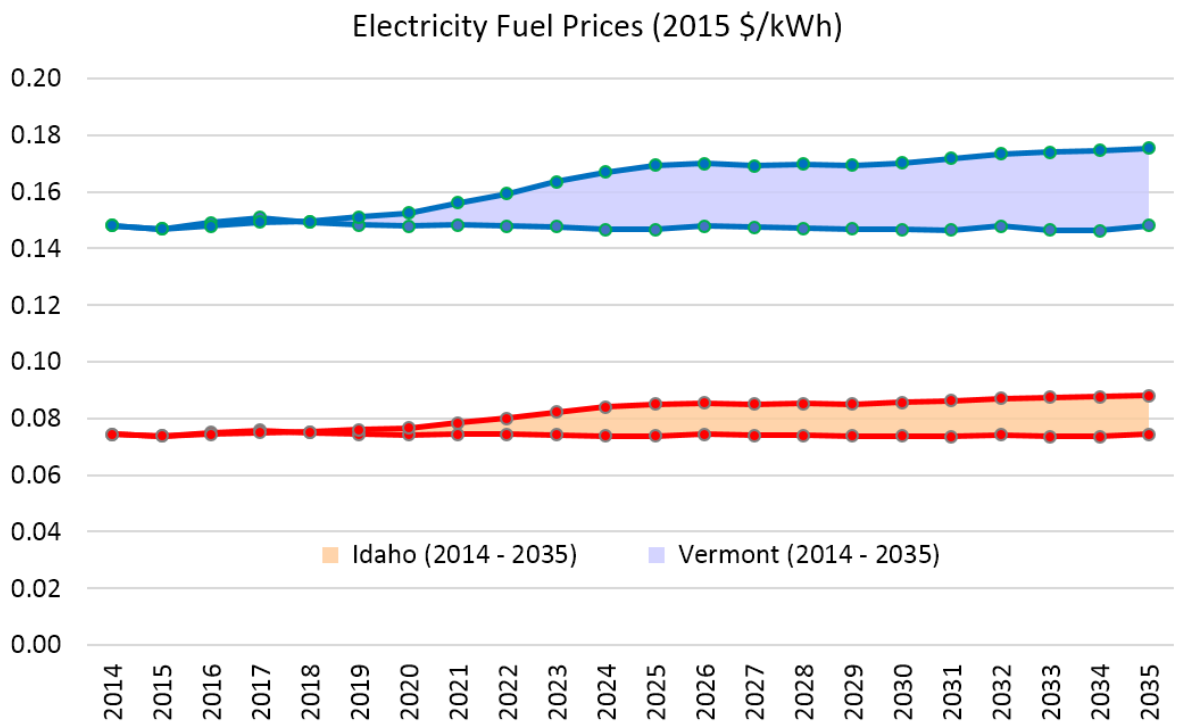

Figure A5. Actual electricity rates in two select states (min and max in continental U.S. for 2014 and 2015) and future price projections.

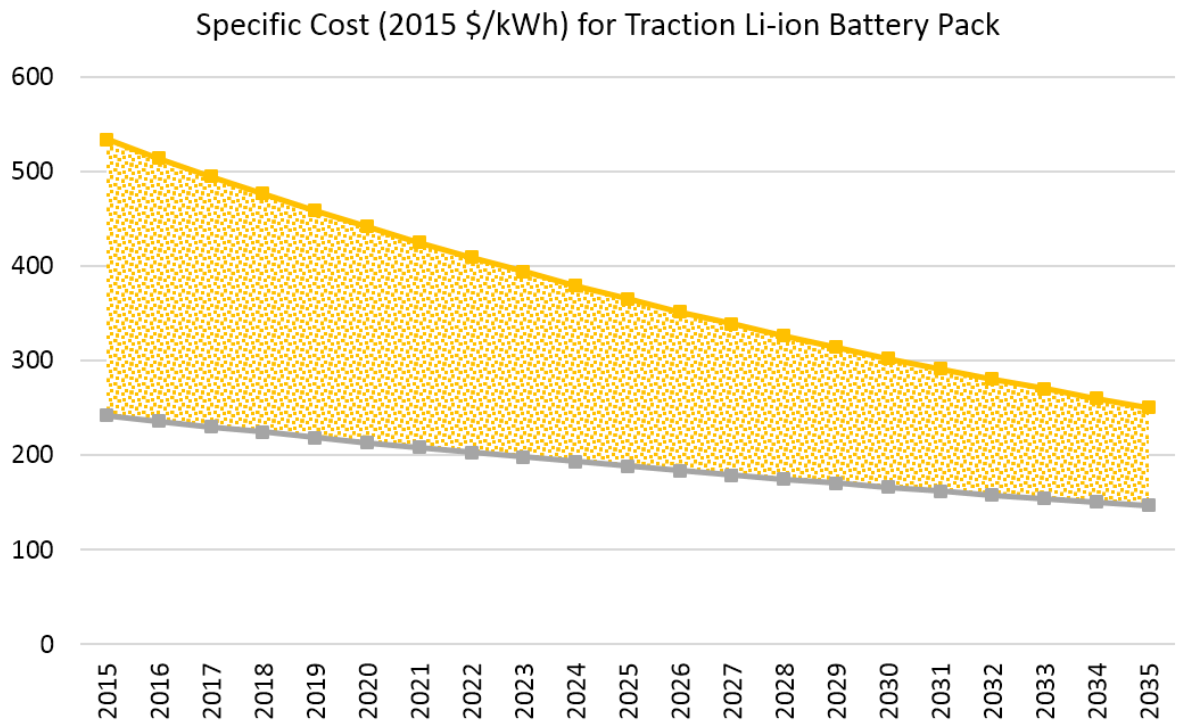

Figure A6. Secondary Li-ion battery pack cost estimation, based on (NRC 2010; Lee et al. 2013; Nykvist and Nilsson 2015).

APPENDIX B

APPENDIX FOR CHAPTER 2: HEAVY-DUTY VEHICLE ELECTRIFICATION

B.1 Vehicle Specifications

	Non-Electric			Electric				
	DB	HEB	CNGB	BEB	BEB-RF	BEB-ORC	BEB-ORC-LW	ETB
Manufacturer and model	New Flyer XD40	New Flyer XDE40	New Flyer XN40	BYD K9	CCW ZEPS	New Flyer XE40	Proterra Catalyst	New Flyer XT40
GVW (lb)	19300 kg (42600)	19300 kg (42600)	19300 kg (42600)	18500 kg (40800)	18500 kg (40800)	18700 kg (41300)	17800 kg (39300)	18700 kg (41300)
Curb weight (lb)	11800 kg (26100)	12930 kg (28600)	12930 kg (28600)	14300 kg (31600)	12700 kg (28000)	13900 kg (30700)	12400 kg (27400)	13500 kg (29800)
GVW-based passenger loading capacity [a]	83	70	70	47	63	53	60	58
Engine	Cummins ISL 9	Cummins ISB 6.7	Cummins ISL-G	-	-	-	-	-
Engine power (kW)	209	209	209	-	-	-	-	-
Drivetrain	Allison B400-R	Allison H 40 EP	Allison B400-R	In-wheel drive	Single gear reduction	Single gear reduction	Two-speed trans-mission	Single gear reduction
Traction motor power (kW)	-	160	-	360	150	160	220	240
Secondary battery type and capacity in kWh (energy density in Wh/kg)	-	Ni-MH 17 (37)	-	LFP-C Li-ion 324 (90)	LFP-C Li-ion 213 (90)	NCM-C Li-ion 120 (132)	LMO-LTO Li-ion 105 (90)	Ni-Cd 7.2 (23)
Fuel tank capacity	100 diesel gallons	100 diesel gallons	20000 SCF (6 Type-3 cylinders)	-	-	-	-	-
Tire	Michelin 305/70R22.5							
	All data were collected from the bus manufacturers' vehicle specifications, available at: http://www.newflyer.com (New Flyer); http://completecoach.com (Complete Coach Works); www.proterra.com (Proterra); http://www.byd.com/na/auto/ElectricBus.html (BYD). [a] Compared to the vehicle size- or room space-based passenger capacity calculation, using weight-based attribute (e.g., payload) enables more fair comparison between different bus technologies and the corresponding energy use and emissions performance. The same principle is adopted in the EPA and NHTSA's heavy-duty vehicle GHG and fuel efficiency standards (Federal Register 2011).							

B.2 Life-Cycle Inventory for Bus and Parts Production, Replacement, and End-of-Life

The materials composition data are created based on the transit bus specifications in Section 1 above, transit bus studies (Pusenius et al. 2005; Ally and Pryor 2008), and GREET model (ANL 2014a). Fluids (e.g., engine coolant, transmission oil, after-treatment urea, and etc.), their replacements, and corresponding material input are based on the light-duty vehicle (LDV) data in GREET but adjusted by the differences between the LDV and transit bus (e.g., engine displacement, frontal area, and etc.) as well as transit bus parts maintenance schedule specifications. The EOL inventory is considered only for new buses. It is expected that approximately the same amount of energy consumption and emissions will be caused from the retirement of in-use buses, regardless of the vehicle retirement scenarios or technology choice. As for the electric buses' traction battery and its replacement over the bus lifetime, as Cooney et al. (2013) proposed, I base my calculation on US-specific data from GREET. I estimate battery degradation and lifetime based on the battery age, duty cycle, depth of discharge, ambient temperature, voltage level, and state of health (see SI – Section 4).

$$e_{s,t,k} = \sum_i \sum_j \left\{ \left[\frac{\left(m_{curb} - m_{FL} - m_{TR} - m_{fuel}\right)_{New\ Flyer,diesel}}{\left(m_{curb} - m_{FL} - m_{TR}\right)_s} \times m_{s,j} \right.\right.$$
$$- m_{TR}\left(1 + \theta_{TR,t}\right)\varphi_{TR,j} - m_{PT}\left(1 + \theta_{PT,t}\right)\varphi_{PT,j} - m_{TX}\left(1 + \theta_{TX,t}\right)\varphi_{TX,j}$$
$$\left.\left. + m_{t,i}\left(1 + \theta_{t,i}\right)\varphi_{ij} \right] e_{jk} \right\} + \left[\frac{\left(m_{curb} - m_{BT} - m_{FL} - m_{fuel}\right)_{t,k}}{\left(m_{curb} - m_{BT} - m_{FL} - m_{fuel}\right)_{GREET\ LDV}} \right]$$
$$\times \left(\tau_{Paint,k} + \tau_{Painting,k} + \tau_{Assembly,k} + \tau_{Disposal,k}\right)$$

$e_{s,t,k}$: the k-th inventory component (energy and emissions) for the t-th technology, based on the s-th material composition data source

$\theta_{t,i}$: the number of replacements over lifetime for the i-th vehicle component (or parts) and the t-th technology

φ_{ij}: material compositions for the i-th vehicle component (or parts) and the j-th material; in case of the battery, battery assembly is included

e_{jk}: energy and emissions factors for the j-th material and the k-th inventory component from GREET (ANL 2014a)

τ_k: energy and emissions factors per vehicle for the k-th inventory component

m: mass in kg

FL: fluids (see below)

TR: tires

PT: powertrain

TX: transmission

k: inventory component (energy and emissions)

s: the bus for which material composition is based on – Volvo 8500 Low Entry (Pusenius et al. 2005) or Mercedes-Benz O LE500 (Ally and Pryor 2008)

t: technology – DB, HEB, CNGB, BEB, BEB-ORC, BEB-ORC LW, or ETB

The results are summarized in the following charts:

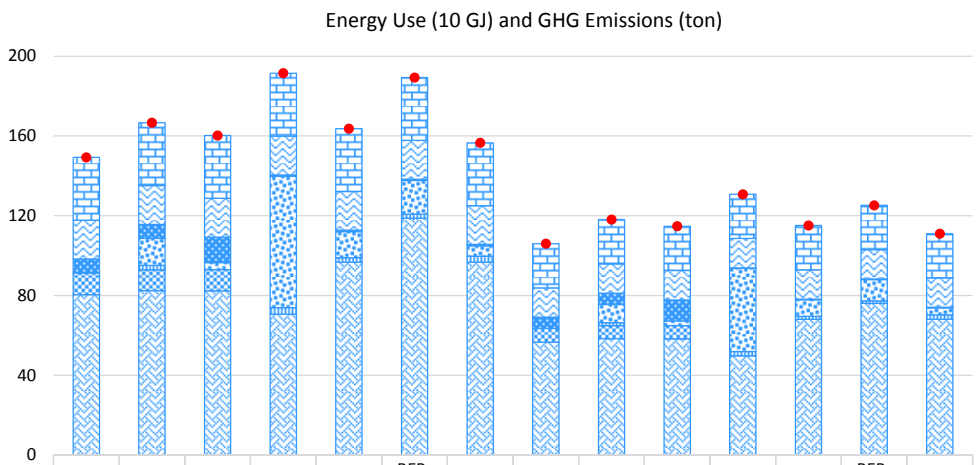

	Energy (10 GJ)							GHG (ton)						
	DB	HEB	CNGB	BEB	BEB-ORC	BEB-ORC-LW	ETB	DB	HEB	CNGB	BEB	BEB-ORC	BEB-ORC-LW	ETB
Assembly & Disposal	31.5	31.5	31.5	31.5	31.5	31.5	31.5	22.2	22.2	22.2	22.2	22.2	22.2	22.2
Tire	19.4	19.4	19.4	19.4	19.4	19.4	19.4	14.7	14.7	14.7	14.7	14.7	14.7	14.7
Fluids	7.0	7.0	12.8	0.7	0.7	0.7	0.7	5.6	5.6	10.6	0.3	0.3	0.3	0.3
ESS	0.0	13.6	3.5	65.9	13.1	16.8	5.2	0.0	9.1	2.4	41.6	8.3	10.6	3.6
EDS	0.0	2.2	0.0	3.4	2.2	2.0	3.0	0.0	1.6	0.0	2.2	1.5	1.4	2.2
PT & TX	10.9	10.4	10.6	0.0	0.0	0.0	0.0	6.8	6.5	6.6	0.0	0.0	0.0	0.0
Body & Chassis	80.4	82.5	82.3	70.6	96.7	118.8	96.7	56.6	58.3	58.2	49.7	68.1	76.0	68.1
Total	149.3	166.6	160.2	191.5	163.7	189.3	156.6	106.0	118.1	114.7	130.8	115.1	125.2	111.0

ESS: energy storage system (battery, compressed natural gas cylinders, including ESS assembly and disposal)

EDS: electric-drive system such as electric motor and controller

PT: powertrain

TX: transmission

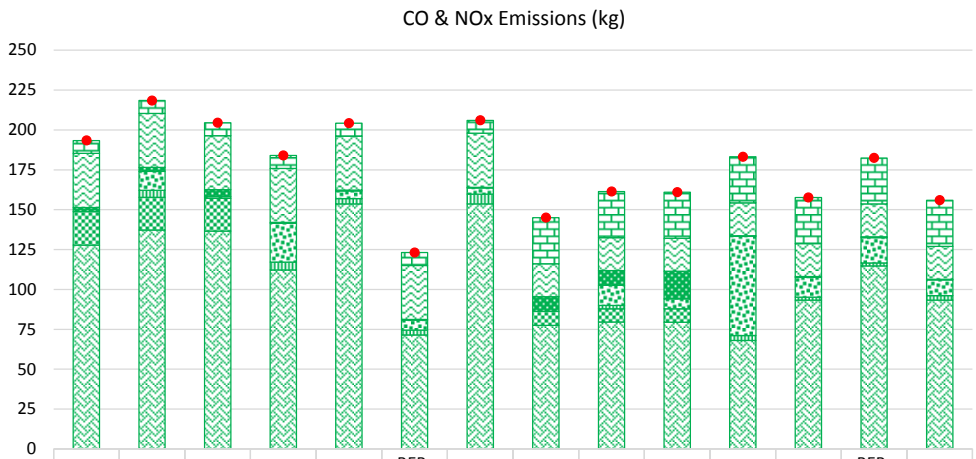

	CO (kg)							NOx (kg)						
	DB	HEB	CNGB	BEB	BEB-ORC	BEB-ORC-LW	ETB	DB	HEB	CNGB	BEB	BEB-ORC	BEB-ORC-LW	ETB
Assembly & Disposal	8.0	8.0	8.0	8.0	8.0	8.0	8.0	28.9	28.9	28.9	28.9	28.9	28.9	28.9
Tire	33.9	33.9	33.9	33.9	33.9	33.9	33.9	20.6	20.6	20.6	20.6	20.6	20.6	20.6
Fluids	2.5	2.5	4.4	0.4	0.4	0.4	0.4	9.2	9.2	17.3	0.5	0.5	0.5	0.5
ESS	0.0	11.8	1.1	24.5	4.9	6.2	3.9	0.0	12.7	6.3	62.2	12.4	15.9	9.9
EDS	0.0	4.3	0.0	4.9	3.3	3.0	6.0	0.0	2.1	0.0	3.0	2.0	1.8	2.8
PT & TX	21.1	20.5	20.4	0.0	0.0	0.0	0.0	8.7	8.3	8.5	0.0	0.0	0.0	0.0
Body & Chassis	127.8	137.3	136.6	112.2	153.7	71.5	153.7	77.5	79.6	79.4	68.1	93.2	114.8	93.2
Total	193.3	218.4	204.5	183.9	204.2	123.1	206.0	145.0	161.4	160.9	183.2	157.6	182.5	155.9

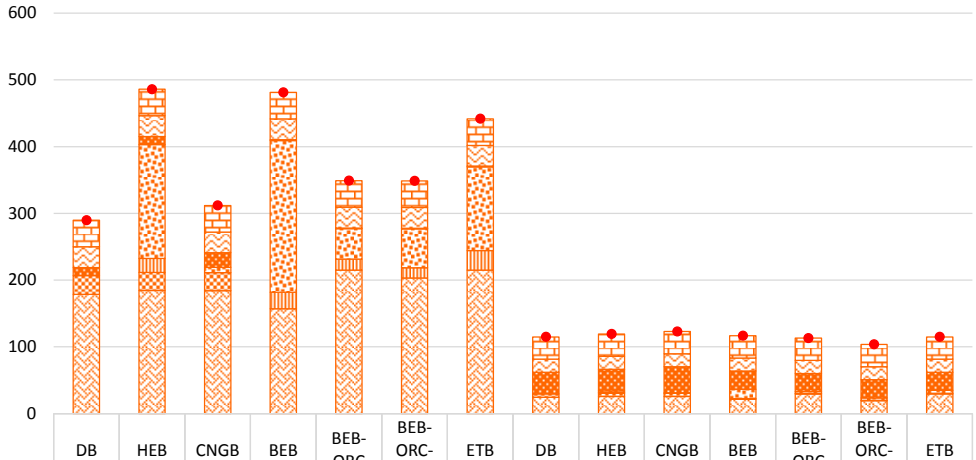

	SOx (kg)							VOC (kg)						
	DB	HEB	CNGB	BEB	BEB-ORC	BEB-ORC-LW	ETB	DB	HEB	CNGB	BEB	BEB-ORC	BEB-ORC-LW	ETB
Assembly & Disposal	39.8	39.8	39.8	39.8	39.8	39.8	39.8	33.4	33.4	33.4	33.4	33.4	33.4	33.4
Tire	31.1	31.1	31.1	31.1	31.1	31.1	31.1	19.5	19.5	19.5	19.5	19.5	19.5	19.5
Fluids	12.1	12.1	22.0	1.2	1.2	1.2	1.2	32.5	32.5	39.1	27.3	27.3	27.3	27.3
ESS	0.0	170.6	8.0	227.4	45.2	58.1	125.3	0.0	2.5	0.4	14.0	2.8	3.6	4.3
EDS	0.0	21.1	0.0	24.9	16.6	15.2	29.3	0.0	0.7	0.0	0.9	0.6	0.6	1.0
PT & TX	27.9	26.9	27.0	0.0	0.0	0.0	0.0	5.0	4.8	4.8	0.0	0.0	0.0	0.0
Body & Chassis	178.8	184.5	184.1	157.0	215.1	203.4	215.1	24.5	25.8	25.7	21.5	29.5	19.4	29.5
Total	289.7	486.0	311.9	481.3	349.0	348.7	441.7	114.9	119.2	123.0	116.6	113.1	103.7	114.9

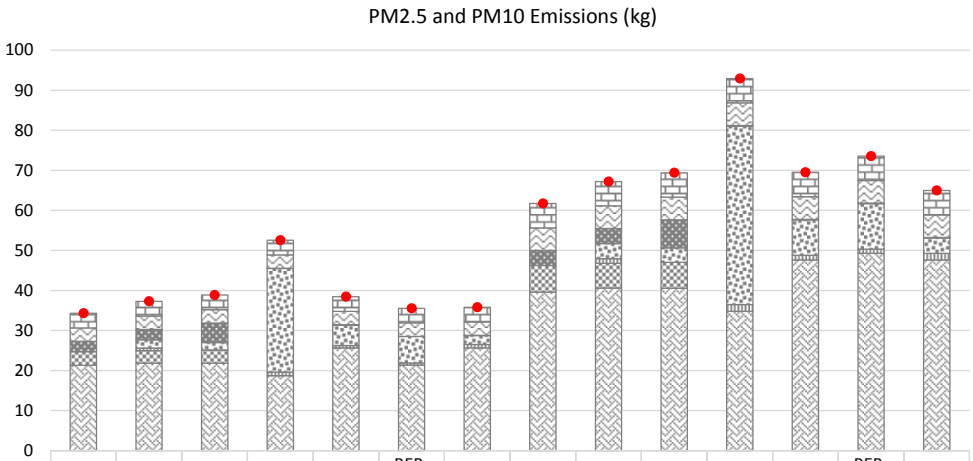

	DB	HEB	CNGB	BEB	BEB-ORC	BEB-ORC-LW	ETB	DB	HEB	CNGB	BEB	BEB-ORC	BEB-ORC-LW	ETB
	PM2.5 (kg)							PM10 (kg)						
Assembly & Disposal	3.6	3.6	3.6	3.6	3.6	3.6	3.6	6.1	6.1	6.1	6.1	6.1	6.1	6.1
Tire	3.4	3.4	3.4	3.4	3.4	3.4	3.4	5.7	5.7	5.7	5.7	5.7	5.7	5.7
Fluids	2.6	2.6	4.9	0.0	0.0	0.0	0.0	3.8	3.8	7.0	0.1	0.1	0.1	0.1
ESS	0.0	2.1	1.9	25.9	5.2	6.6	2.2	0.0	3.7	3.6	44.6	8.9	11.4	3.8
EDS	0.0	0.6	0.0	0.9	0.6	0.5	0.9	0.0	1.2	0.0	1.7	1.2	1.1	1.6
PT & TX	3.3	3.1	3.3	0.0	0.0	0.0	0.0	6.6	6.1	6.5	0.0	0.0	0.0	0.0
Body & Chassis	21.3	21.9	21.8	18.7	25.7	21.3	25.7	39.6	40.6	40.5	34.8	47.6	49.3	47.6
Total	34.3	37.3	38.9	52.5	38.4	35.5	35.8	61.7	67.2	69.4	92.9	69.5	73.5	64.9

B.3 Impact of Road Grade and Hot/Cold Conditions

Our results imply that more exposure to hilly roads will benefit the competitiveness of electric buses, whereas extreme hot or cold temperatures can disproportionally increase the energy consumption of electric buses compared to non-electric competitors. Non-electric buses are less sensitive to extremely hot or cold temperatures. As both road grade and weather conditions fluctuate over time and space, location-specific (or regional) average values would be sufficient for electric bus LCA to avoid bias of (national) averages. Getting more into details than that or focusing on specific conditions might actually result in the bias of extremes.

To see the road grade impact, I test three cases – level ground (0%), downhill driving (constant -1%), and uphill driving (constant +1%) – for all the drive cycles that I included in my study. In reality, buses experience varying road grades over the route. Also, as bus drivers experience up- or down-hill roads, it is very likely that they adjust vehicle speeds or drive differently than they would on level ground. Not only the level of road grade but also its extent affect drivers' behavior. In other words, there may be an interaction between drive cycles (speed-time profiles) and road grades. I don't consider these two aspects – varying road grades over the route and interaction between drive cycles and road grades. Our main objective here is to see the relative net impact of road grade with respect to the bus technology and its overall contribution to the energy and emissions performance. The figure below shows a sequence of two identical drive cycles with two different constant road grades. Considering that buses typically return to the depot after service, making back-to-origin trips, the overall change in energy consumption will be averages of the results at constant positive (+1%) and negative (-1%) road grades.

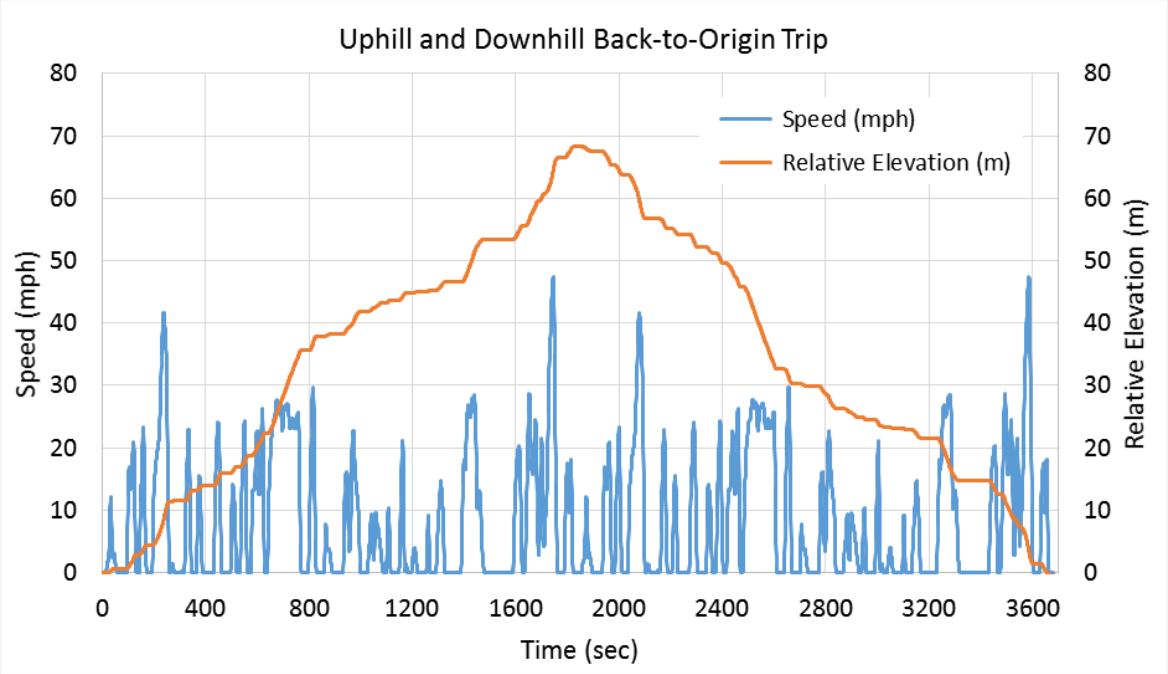

Real-world road grades can vary between -8% and +8%, with different probability distributions by location (NREL 2014b). It should be noted that the steeper the grade is, the more likely that buses having the specifications shown in Section 1 cannot follow the original drive cycles because of the mechanical constraints (e.g., maximum power). If these constraints are not considered, the energy and emissions results can be misleading, especially when the road grade assumed is high. That's why I use 1% road grade - to save original drive cycles and avoid biases by estimating the energy and emissions within the vehicle performance constraints specified in Section 1. More realistic analysis should use duty cycles, i.e., profiles of speed, road grade, passenger loading over time. Last, it is also important to not use constant road grade over the entire drive cycles or trips. It is not impossible that buses travel on uphill or downhill throughout their lifetime, but a more realistic approach is to look at combinations of uphill and downhill driving for back-to-origin trips.

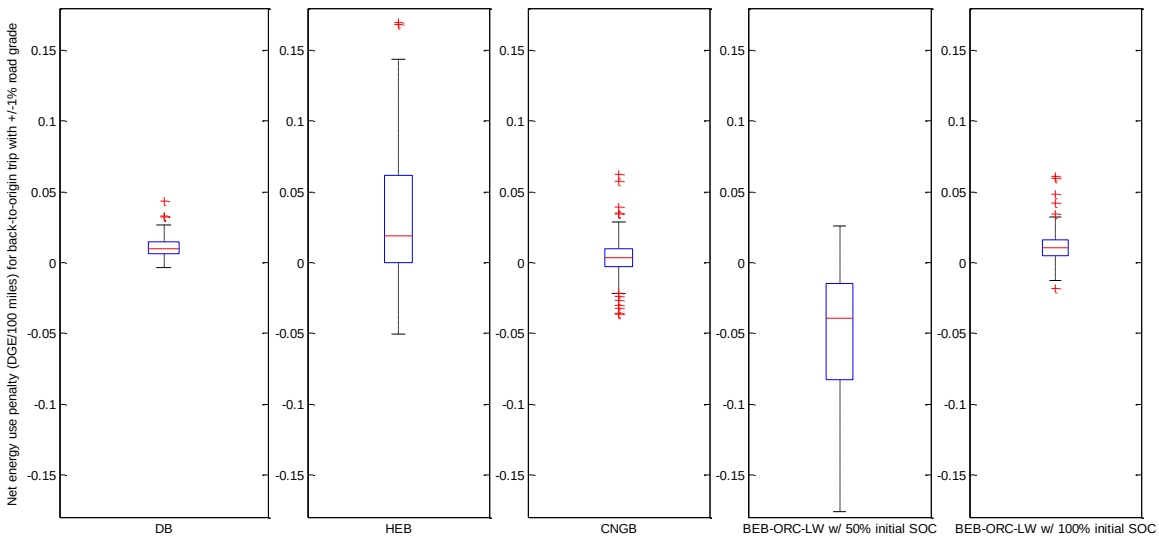

The figure above shows net change in energy consumption (DGE/100 miles) for ±1% road grade conditions, showing technology-dependent sensitivity to road grade. Also, for non-electric buses, the net change in energy consumption is not zero; the energy use reductions in downhill driving are smaller than the energy penalty in uphill driving. This phenomenon appears also in light-duty vehicles (NREL 2014b). Considering the road grade-related energy penalty tends to be linear (NREL 2014b), the factors found here can be multiplied to extrapolate to road grades steeper than 1%. However, as discussed previously, if only road grade is increased while drive cycles are fixed, there is no guarantee that vehicles can follow the given drive cycles.

Interestingly, the electric bus shows negative net energy consumption when the initial state-of-charge (SOC) is 50%, regardless of whether the bus experiences uphill first and then downhill or vice versa. However, when the initial SOC is 100% (hypothetically) and the bus operates in downhill condition followed by uphill on the way back to origin, the energy use savings potential significantly diminishes; less energy from the regenerative braking in downhill driving can be fed back to the traction battery because the battery is already full – see figure below. Overall, for back-to-origin (or roughly equal share of uphill and downhill) bus trips, electric buses have an energy advantage because of the energy recuperation potential.

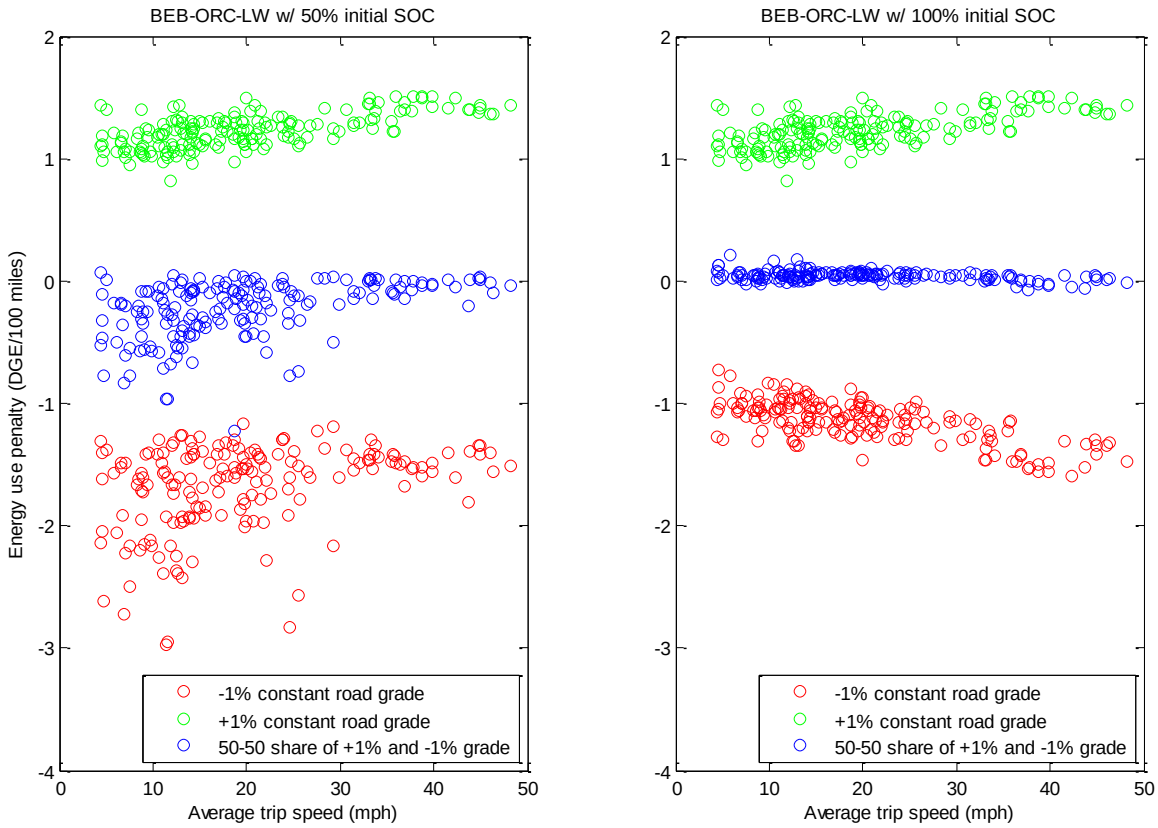

In addition to the route characteristics, driving pattern, and passenger loading cases, I incorporate the impact from the exposure to extreme climate conditions, that is, hot and cold. Using the electric vehicle's cooling and heating system performance test data (ANL 2014b) and the conventional bus technologies' heating and cooling load data (WVU 2014), I develop the following energy consumption penalty factors for a range of extreme climate conditions. For air emissions, I use climate condition-embedded emissions factors for each location (county) directly from MOVES.

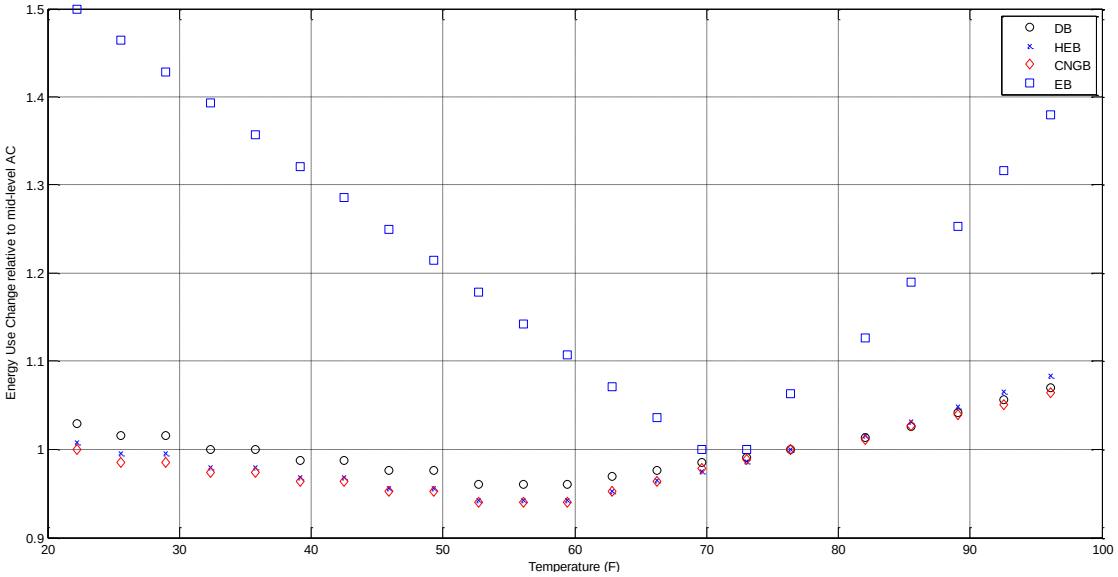

These factors are integrated with location-dependent seasonal temperature fluctuation profiles (Current Results Nexus 2014; EPA 2014) – see below for examples – to get location-specific energy consumption and emissions results. For heating (the left side of the temperature spectrum), non-electric buses have advantages because of the availability of waste heat from the internal combustion engine. For the same reason (the engine heat availability), cooling is more energy-intensive than heating in case of non-electric buses. Heating and/or cooling increases electric buses' energy consumption significantly more than non-electric counterparts, which in turn affects the electric range. For example, at the temperature of 20 ^{0}F, energy consumption of the BEB will increase by 50% and the advertised electric range of 150 miles will shrink to 100 miles.

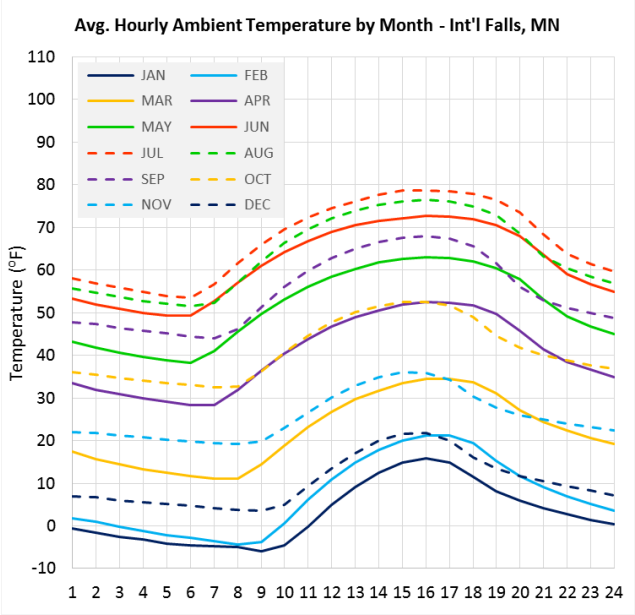
Avg. Hourly Ambient Temperature by Month - Int'l Falls, MN
Temperature (°F)
110
100
90
80
70
60
50
40
30
20
10
0
-10
1 2 3 4 5 6 7 8 9 10 11 12 13 14 15 16 17 18 19 20 21 22 23 24
JAN
FEB
MAR
APR
MAY
JUN
JUL
AUG
SEP
OCT
NOV
DEC

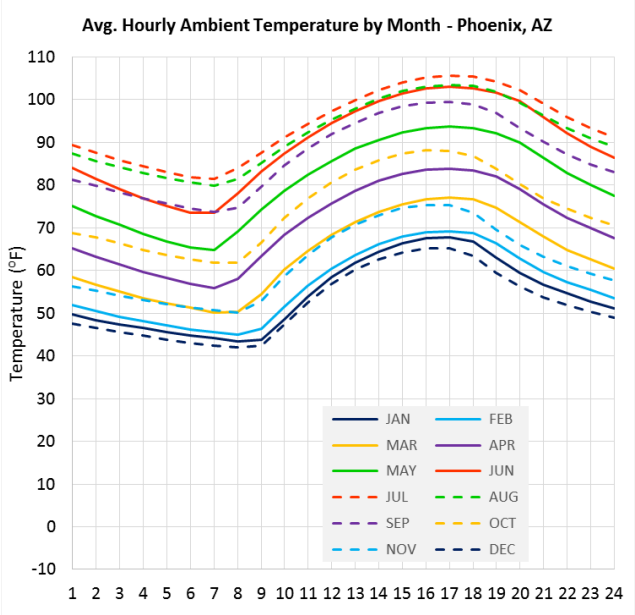
Avg. Hourly Ambient Temperature by Month - Phoenix, AZ
Temperature (°F)
110
100
90
80
70
60
50
40
30
20
10
0
-10
1 2 3 4 5 6 7 8 9 10 11 12 13 14 15 16 17 18 19 20 21 22 23 24
JAN
FEB
MAR
APR
MAY
JUN
JUL
AUG
SEP
OCT
NOV
DEC

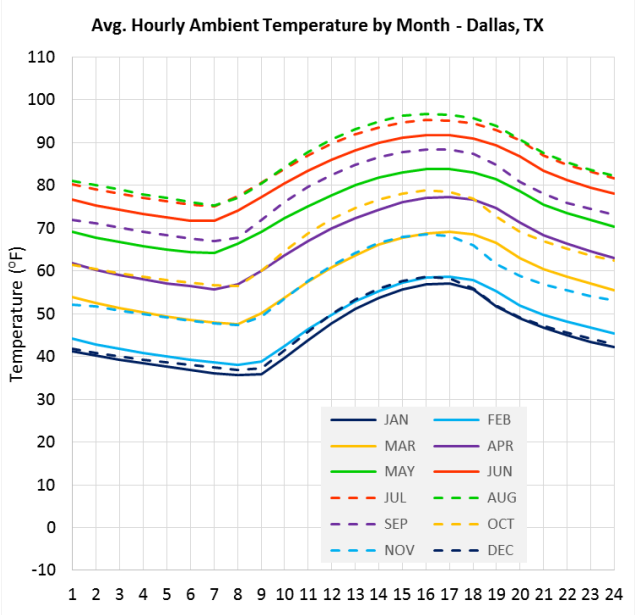
Avg. Hourly Ambient Temperature by Month - Dallas, TX
Temperature (°F)
110
100
90
80
70
60
50
40
30
20
10
0
-10
1 2 3 4 5 6 7 8 9 10 11 12 13 14 15 16 17 18 19 20 21 22 23 24
JAN
FEB
MAR
APR
MAY
JUN
JUL
AUG
SEP
OCT
NOV
DEC

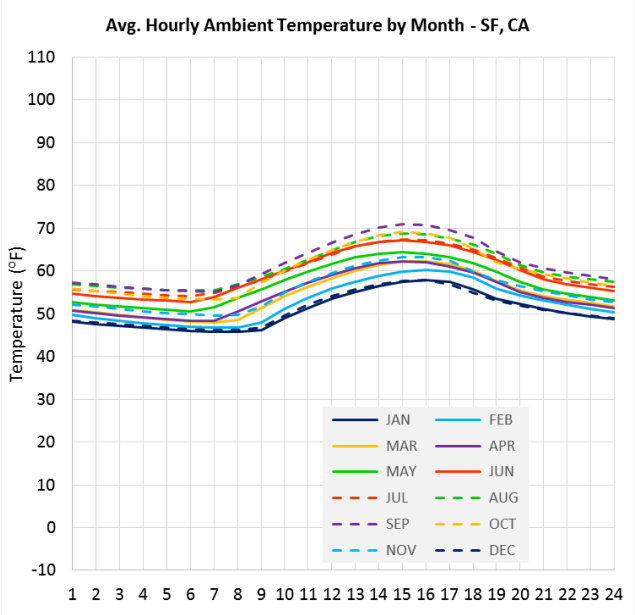
Avg. Hourly Ambient Temperature by Month - SF, CA
Temperature (°F)
110
100
90
80
70
60
50
40
30
20
10
0
-10
1 2 3 4 5 6 7 8 9 10 11 12 13 14 15 16 17 18 19 20 21 22 23 24
JAN
FEB
MAR
APR
MAY
JUN
JUL
AUG
SEP
OCT
NOV
DEC

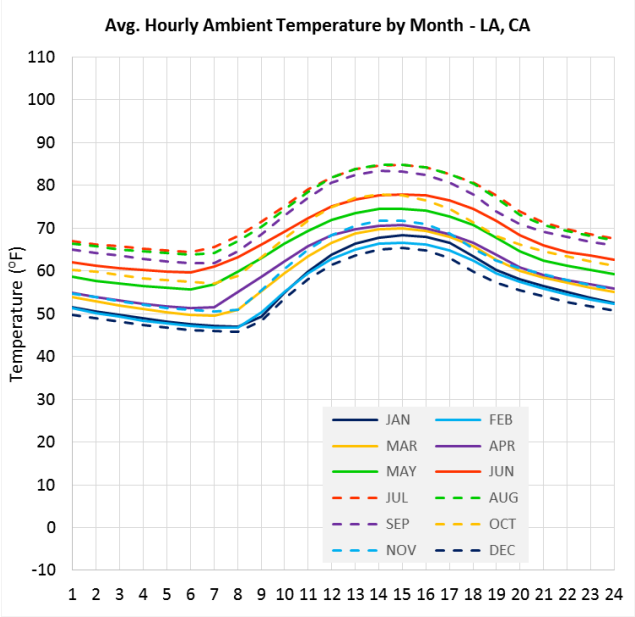
Avg. Hourly Ambient Temperature by Month - LA, CA
Temperature (°F)
110
100
90
80
70
60
50
40
30
20
10
0
-10
1 2 3 4 5 6 7 8 9 10 11 12 13 14 15 16 17 18 19 20 21 22 23 24
JAN
FEB
MAR
APR
MAY
JUN
JUL
AUG
SEP
OCT
NOV
DEC

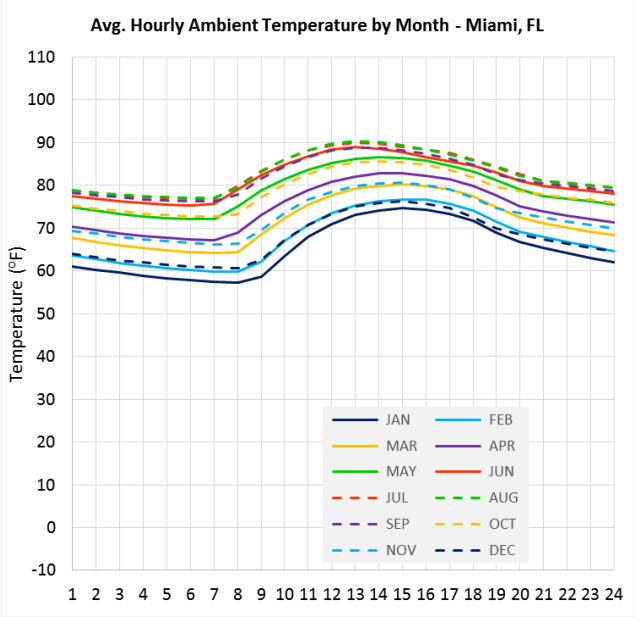
Avg. Hourly Ambient Temperature by Month - Miami, FL
Temperature (°F)
110
100
90
80
70
60
50
40
30
20
10
0
-10
1 2 3 4 5 6 7 8 9 10 11 12 13 14 15 16 17 18 19 20 21 22 23 24
JAN
FEB
MAR
APR
MAY
JUN
JUL
AUG
SEP
OCT
NOV
DEC

B.4 Traction Battery Lifetime Estimation

I use a non-linear parametric modeling approach for secondary battery degradation, based on Schmalstieg et al.'s work (2014). Depth of discharge (DOD) for each charge cycle is one of the key input variables to the battery degradation model, which varies with drive cycle and travel demand per trip or day among others. The DOD of electric buses is highly dependent on the utilization level (daily travel distance), charging strategies, and route characteristics. It should be noted that maximum daily utilization level is also dependent upon how fast the buses travel on routes. To estimate these variables, I use my cycle-dependent energy consumption results aforementioned as well as the transit bus operation statistics data from National Transit Database (FTA 2012) and American Public Transportation Association (APTA 2013).

Allowing a 20% state of charge (SOC) buffer for unaccounted energy drain and capacity loss, the 35,000 miles per year scenario corresponds to 120 miles per day for urban transit bus operation (80% x 35,000 miles a year) / 12 months x 20 days per month) I also account for the electric buses technological capability including electric range per full charge. To provide 120-mile service a day, BEB-ORC with a 120 kWh battery will need to charge once or twice during the day, totaling three times a day (including nighttime charging). Given the fact that severe DOD can decrease the battery lifetime significantly, I expect that the electric bus operators will keep the DOD around 50% so that the lifetime of expensive traction batteries can be maximized.

The figures below show the impact of DOD (per charging cycle) on the battery lifetime. As a result, BEB's battery (BYD) is expected to have 8-10 years of lifetime, and BEB-ORC's battery (NF) will have 6-7 years of lifetime at about 50-70% DOD. Considering this and the potential improvement of the next generation batteries, I expect that battery replacement is needed once or twice over the 16-year time horizon of my analysis.

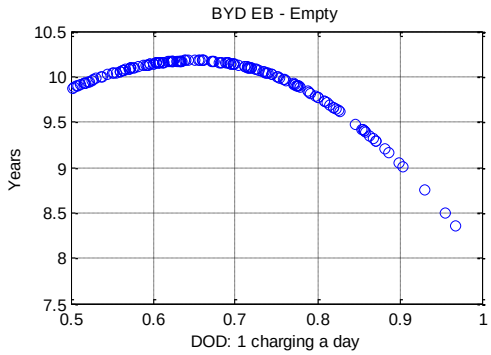
BYD EB - Empty
Years
DOD: 1 charging a day

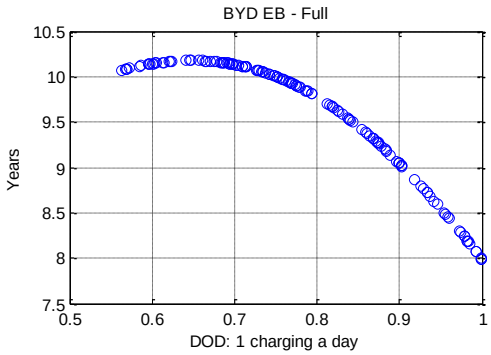
BYD EB - Full
Years
DOD: 1 charging a day

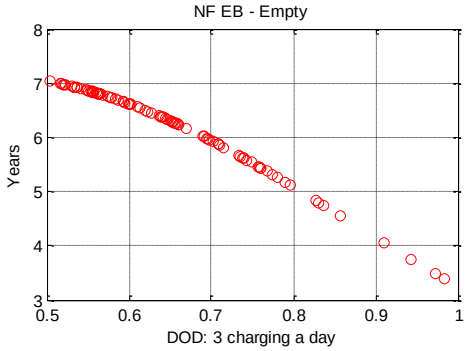
NF EB - Empty
Years
DOD: 3 charging a day

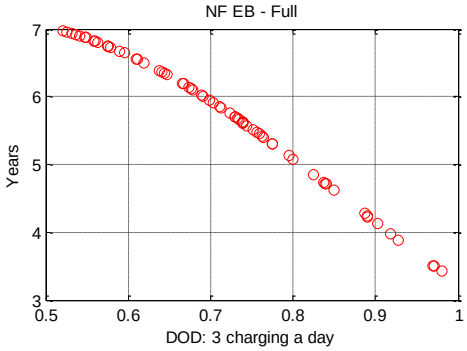
NF EB - Full
Years
DOD: 3 charging a day

B.5 Cost Parameters

	Mid-life capital investment	Repair and maintenance	Fueling station	Charger	Overhead trolley
(unit)	$	$/mile	$/vehicle	$/vehicle	$/mile/vehicle
DB	min: 65,400 max: 131,900	0.73	15,600	-	-
HEB	min: 229,000 max: 355,200	0.22 - 0.448	15,600	-	-
CNGB	min: 65,400 max: 131,900	0.84	(see the chart below)	-	-
BEB	-	0.11 - 0.22	-	(see the chart below)	-
BEB-RF	-		-		-
BEB-ORC	-		-		-
BEB-ORC-LW	-		-		-
ETB	-	1.241	-	-	26000
NAICS Code	#336300	#8111A0	#230103	#335999 and #811200	
Data sources: (FTA 2007; KCDOT 2011; Chambers 2012; Farnham 2013; Woody 2013; Boudart and Figliozzi 2012; De Filippo et al. 2014; WVU 2014)					

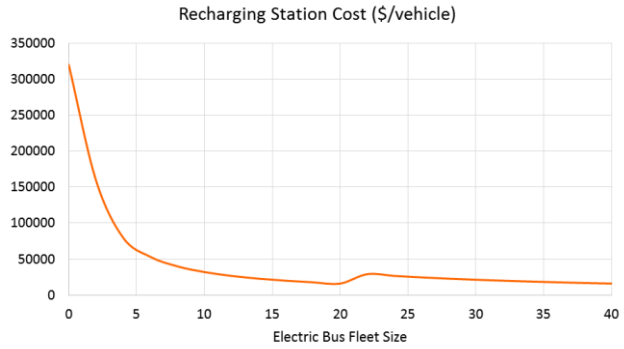

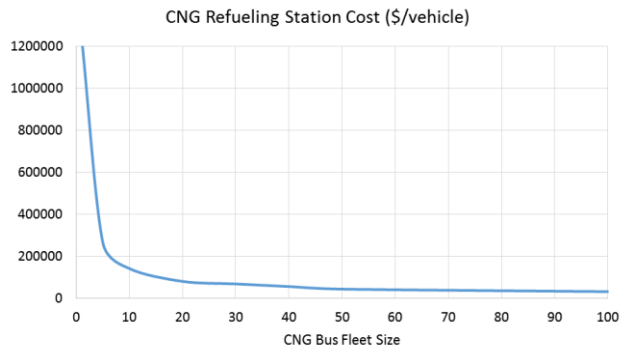

B.6 Life-Cycle Inventory (LCI) Prediction Model

In addition to life cycle energy and GHG emissions model in Table 1.1 in main text, here I provide other results which are all based on Eq. (16) in main text:

$$\hat{Y}_{i,t} = exp\left[\hat{\varphi}_{0_{i,t}} + \hat{\varphi}_{1_{i,t}}\bar{V}_{trip} + \hat{\varphi}_{2_{i,t}}\frac{1}{\bar{V}_{trip}} + \hat{\varphi}_{3_{i,t}}\, log\left(\bar{V}_{trip}\right) + \hat{\varphi}_{4_{i,t}}{\bar{V}_{trip}}^{2} + \hat{\varphi}_{5_{i,t}}\bar{m} + \hat{\varphi}_{6_{i,t}}WPKE\right]$$

As in Table 1.1 in main text, all the parameter estimates presented here are statistically significant at a 5% significance level.

Given the spatio-temporal heterogeneity of electric grid, I here provide only the results for minimum and maximum cases for BEB-ORC-LW. For example, BEB-ORC-LW based on daytime electric grid in Virginia (VA) emits the lowest life cycle CO emissions, and nighttime in Nevada (NV) the highest. These min and max cases should give the reasonable range of the life cycle results of electric buses (BEB-ORC-LW). Note that the min-max cases in main text are for average electric grid condition, whereas the min-max cases here are for marginal electric grid.

$\hat{\varphi}_j{}'s$ for CO (gram/mile)	DB	CNGB	DHEB	BEB-ORC-LW (VA-Day)	BEB-ORC-LW (NV-Night)
Intercept	1.24	4.34	1.31	-0.21	0.48
$\bar{V}_{trip}$		-7.76×10^{-2}	1.1×10^{-2}		
${\bar{V}_{trip}}^{-1}$	2.21	2.23			
$\log(\bar{V}_{trip})$	-0.153		-0.126		
${\bar{V}_{trip}}^{2}$	9.7×10^{-5}	8.75×10^{-4}	-1.07×10^{-4}	4.76×10^{-5}	1.73×10^{-4}
$\bar{m}$	3.06×10^{-3}	4.34×10^{-3}	2.3×10^{-3}	5.1×10^{-6}	1.92×10^{-5}
WPKE	1.2×10^{-2}	6.2×10^{-2}	9.5×10^{-3}	2.1×10^{-2}	7.48×10^{-2}
Adj. R^2	0.99	0.96	0.97	0.92	0.91
F-statistic	6978	1736	2563	2816	2588

$\hat{\varphi}_j's$ for NOx (gram/mile)	DB	CNGB	DHEB	BEB-ORC-LW (CO-Day)	BEB-ORC-LW (RI-Night)
Intercept	1.2	1.5	2.4	-0.32	0.55
$\bar{V}_{trip}$	-2.04x10^{-2}		1.42x10^{-2}		
$\bar{V}_{trip}^{-1}$	1.75	1.53			
log($\bar{V}_{trip}$)		-0.133	-0.39		
$\bar{V}_{trip}^{2}$	3.3x10^{-4}	7.5x10^{-5}		1.27x10^{-5}	1.83x10^{-4}
$\bar{m}$	5.9x10^{-3}	6.7x10^{-3}	8x10^{-3}	1.34x10^{-6}	2x10^{-5}
WPKE	2.5x10^{-2}	5.45x10^{-2}	1.8x10^{-2}	5.66x10^{-3}	7.86x10^{-2}
Adj. R^2	0.98	0.98	0.95	0.92	0.91
F-statistic	4410	3101	1684	2801	2559

$\hat{\varphi}_j's$ for PM2.5 (gram/mile)	DB	CNGB	DHEB	BEB-ORC-LW (VT-Day)	BEB-ORC-LW (OH-Night)
Intercept	-0.426	-0.37	-1.23	-0.98	-0.84
$\bar{V}_{trip}$		8.7x10^{-3}		9.4x10^{-3}	1.94x10^{-2}
$\bar{V}_{trip}^{-1}$			1.55		
log($\bar{V}_{trip}$)	-0.337	-0.33		-0.41	-0.3
$\bar{V}_{trip}^{2}$	2x10^{-4}		-1.88x10^{-5}		
$\bar{m}$				7.3x10^{-6}	1.93x10^{-5}
WPKE	2.5x10^{-2}	1.9x10^{-2}	1.9x10^{-2}	-1.74x10^{-2}	6.3x10^{-2}
Adj. R^2	0.96	0.95	0.92	0.78	0.91
F-statistic	2749	2505	1512	667	1859

$\hat{\varphi}_j's$ for PM10 (gram/mile)	DB	CNGB	DHEB	BEB-ORC-LW (VT-Day)	BEB-ORC-LW (SC-Night)
Intercept	0.139	1.17	-0.23	1.91	-0.754
$\bar{V}_{trip}$	-3.62x10^{-2}			2.1x10^{-2}	
$\bar{V}_{trip}^{-1}$	1.78		3.02	-1.487	2.41
log($\bar{V}_{trip}$)		-0.418		-1.1	
$\bar{V}_{trip}^{2}$	4.81x10^{-4}	1.06x10^{-4}	-1.5x10^{-4}		4.74x10^{-5}
$\bar{m}$	-4.1x10^{-3}	-2.55x10^{-3}	-2.72x10^{-3}	1.78x10^{-5}	1.677x10^{-5}
WPKE	3.5x10^{-2}	2.57x10^{-2}	3.2x10^{-2}	-5.72x10^{-2}	3.47x10^{-2}
Adj. R^2	0.92	0.92	0.9	0.75	0.74
F-statistic	887	1126	812	466	550

$\hat{\varphi}_j's$ for SO2 (gram/mile)	DB	CNGB	DHEB	BEB-ORC-LW (VT-Day)	BEB-ORC-LW (MS-Night)
Intercept	0.455	0.712	0.925	0.145	1
$\bar{V}_{trip}$	$2.3x10^{-3}$				
$\bar{V}_{trip}^{-1}$	1.27	1.55	0.33		
$\log(\bar{V}_{trip})$					
$\bar{V}_{trip}^{2}$		$7.44x10^{-6}$	$1.8x10^{-5}$	$1.17x10^{-5}$	$1.82x10^{-4}$
$\bar{m}$	$3x10^{-3}$	$3.5x10^{-3}$	$2.8x10^{-3}$	$1.23x10^{-6}$	$2x10^{-5}$
WPKE	$2.1x10^{-2}$	$2.58x10^{-2}$	$1.16x10^{-2}$	$5.2x10^{-3}$	$7.84x10^{-2}$
Adj. R^2	0.98	0.99	0.96	0.92	0.91
F-statistic	6239	6115	2657	2799	2560

$\hat{\varphi}_j's$ for VOC (gram/mile)	DB	CNGB	DHEB	BEB-ORC-LW (VT-Day)	BEB-ORC-LW (WA-Night)
Intercept	0.972	0.574	0.83	-0.76	-0.67
$\bar{V}_{trip}$					
$\bar{V}_{trip}^{-1}$	3.08	1.05	1.45		
$\log(\bar{V}_{trip})$		$-5.46x10^{-2}$			
$\bar{V}_{trip}^{2}$	$6.9x10^{-5}$	$2.7x10^{-5}$	$6.84x10^{-5}$	$7.2x10^{-6}$	$7.43x10^{-5}$
$\bar{m}$	$1x10^{-2}$	$3.33x10^{-3}$	$1.66x10^{-2}$	$7.56x10^{-7}$	$8x10^{-6}$
WPKE	$6.37x10^{-2}$	$2.38x10^{-2}$	$6.7x10^{-2}$	$3.2x10^{-3}$	$3.26x10^{-2}$
Adj. R^2	0.98	0.99	0.95	0.92	0.92
F-statistic	3916	6559	2046	2794	2802

REFERENCES

40 CFR part 1066. Vehicle Testing Procedures. Retrieved from: http://www.gpo.gov/fdsys/pkg/CFR-2012-title40-vol34/pdf/CFR-2012-title40-vol34-part1066.pdf (Accessed March 5, 2013).

AAA. (2015). Fuel Gauge Report. Retrieved from: www.FuelGaugeReport.AAA.com (Accessed October 30, 2015).

André, M. (2004). The ARTEMIS European driving cycles for measuring car pollutant emissions. Science of the Total Environment, 334-33573-84. doi:10.1016/j.scitotenv.2004.04.070.

Angrisani, G., Canelli, M., Roselli, C., & Sasso, M. (2015). Integration between electric vehicle charging and micro-cogeneration system. *Energy Conversion & Management, 98*115-126. doi:10.1016/j.enconman.2015.03.085.

Allison Transmission. (2015). Allison Transmission Parts and Service. Retrieved from: http://www.allisontransmission.com/parts-service (Accessed August 2, 2015).

Ally, J., and Pryor, T. (2008). Life Cycle Assessment (LCA) of the Hydrogen Fuel Cell, Natural Gas, and Diesel Bus Transportation Systems in Western Australia. Retrieved from: http://www.transport.wa.gov.au/mediaFiles/about-us/ACT_P_alt_LCAreport.pdf (accessed November 20, 2012).

Ang, B. W., and Fwa, T. F. (1989). A study on the fuel-consumption characteristics of public buses. *Energy, 14*797-803.

ANL (Argonne National Laboratory). (2013). Alternative Fuel Life-Cycle Environmental and Economic Transportation (AFLEET). Retrieved from: https://greet.es.anl.gov/afleet (Accessed November 3, 2014).

ANL (Argonne National Laboratory). (2014). Advanced Powertrain Research Facility - Downloadable Dynamometer Database (D3). Retrieved from: http://www.transportation.anl.gov/D3/ (accessed September 20, 2014).

ANL (Argonne National Laboratory). (2015). Greenhouse gases, Regulated Emissions, and Energy use in Transportation model (GREET). Retrieved from: http://greet.es.anl.gov (Accessed November 5, 2015).

APTA (American Public Transportation Association). (2013). *Public Transportation Fact Book.*

ARTEMIS (Assessment and Reliability of Transport Emission Models and Inventory Systems). (2006). Drive Cycles. Retrieved from: http://www.inrets.fr/ur/lte/publi-autresactions/fichesresultats/ficheartemis/road3/method31/All_Cycles_in_Artemis_BD_092006.xls (Accessed June 25, 2012).

ATRI (American Transportation Research Institute). (2013). An Analysis of the Operational Costs of Trucking: A 2013 Update. Retrieved from: www.atri-online.org (Accessed January 16, 2014).

Bachmann, C., Chingcuanco, F., MacLean, H., & Roorda, M. J. (2015). Life-Cycle Assessment of Diesel-Electric Hybrid and Conventional Diesel Trucks for Deliveries. Journal of Transportation Engineering, 141(4), -1. doi:10.1061/(ASCE)TE.1943-5436.0000761.

Balcombe, P., Rigby, D., & Azapagic, A. (2015a). Environmental impacts of microgeneration: Integrating solar PV, Stirling engine CHP and battery storage. *Applied Energy*, *139*245-259. doi:10.1016/j.apenergy.2014.11.034.

Balcombe, P., Rigby, D., & Azapagic, A. (2015b). Energy self-sufficiency, grid demand variability and consumer costs: Integrating solar PV, Stirling engine CHP and battery storage. *Applied Energy*, *155*393-408. doi:10.1016/j.apenergy.2015.06.017.

Bare, J. C., Norris, G. A., Pennington, D. W., & McKone, T. (2002). TRACI - The Tool for the Reduction and Assessment of Chemical and Other Environmental Impacts. Journal of Industrial Ecology, 6(3/4), 49.

Bare, J. (2011). TRACI 2.0: the tool for the reduction and assessment of chemical and other environmental impacts 2.0. Clean Technologies & Environmental Policy, 13(5), 687-696. doi:10.1007/s10098-010-0338-9.

Bare, J. C. (2012). Tool for the Reduction and Assessment of Chemical and other Environmental Impacts (TRACI), Software Name and Version Number: TRACI Version 2.1 - User's Manual.

Barnitt, R. (2011). Medium-and Heavy-Duty Electric Drive Vehicle Simulation and Analysis. DOE VTP Annual Merit Review. Retrieved from: http://www1.eere.energy.gov/vehiclesandfuels/pdfs/merit_review_2011/veh_sys_sim/vss043_barnitt_2011_o.pdf (Accessed December 10, 2013).

Bloom Energy. (2016). Bloom Energy, Solid Oxide Fuel Cells. Retrieved from: http://www.bloomenergy.com (Accessed September 15, 2015).

BNL (Brookhaven National Laboratory). (2009). Evaluation of Gas, Oil and Wood Pallet Fueled Residential Heating System Emissions Characteristics. BNL-91286-2009-IR.

Boudart, J., and Figliozzi, M. (2012). Key Variables Affecting Decisions of Bus Replacement Age and Total Costs. *Transportation Research Record*, *2274*(1), 109.

BTS (Bureau of Transportation Statistics). (2015). National Transportation Statistics. U.S. Department of Transportation. October 4, 2015. Retrieved from: http://www.rita.dot.gov/bts/sites/rita.dot.gov.bts/files/publications/national_transportation_statistics/index.html.

Bullis, K. (2011). Electric Buses Get a Jump Start. *MIT Technology Review*. June 16, 2011.

Burton, J., Walkowicz, K., Sindler, P., & Duran, A. (2013a). In-Use and Vehicle Dynamometer Evaluation and Comparison of Class 7 Hybrid Electric and Conventional Diesel Delivery Trucks. SAE 2013 Commercial Vehicle Engineering Congress. doi: 10.4271/2013-01-2468.

Burton, E., Gonder, J., Wood, E. (2013b). Map Matching and Real World Integrated Sensor Data Warehousing. Federal Committee on Statistical Methodology (FCSM) Research Conference. November 4-6, 2013. Washington, DC. Retrieved from: www.nrel.gov/fleet_dna (Accessed February 22, 2014).

Cappa, F., Facci, A. L., & Ubertini, S. (2015). Proton exchange membrane fuel cell for cooperating households: A convenient combined heat and power solution for residential applications. *Energy*, doi:10.1016/j.energy.2015.06.092.

Capstone. (2016). Capstone Turbine Corporation. Retrieved from: http://www.capstoneturbine.com/ (Accessed March 22, 2015).

CARB (California Air Resources Board). (2008). Staff Report: Initial Statement of Reasons for Proposed Rulemaking Proposed Regulation for In-Use On-Road Diesel Vehicles. Appendix J - Cost and Economic Analysis Methodology. Retrieved from: http://www.arb.ca.gov/regact/2008/truckbus08/appj.pdf (Accessed April 24, 2014).

Camuzeau, J. R., Alvarez, R. A., Brooks, S. A., Browne, J. B., & Sterner, T. (2015). Influence of Methane Emissions and Vehicle Efficiency on the Climate Implications of Heavy-Duty Natural Gas Trucks. Environmental Science & Technology, 49(11), 6402-6410. doi:10.1021/acs.est.5b00412.

Chambers, N. (2012). A Tale of 2 Transit Systems: Battery-Powered Buses Enter the Mainstream. *Scientific American*. June 11, 2012. Retrieved from: http://www.scientificamerican.com/article/battery-powered-electric-bus/?mobileFormat=false (accessed September 10, 2014).

Chester, M. V., and Horvath, A. A. (2009). Environmental assessment of passenger transportation should include infrastructure and supply chains. *Environmental Research Letters*, *4*(2), doi:10.1088/1748-9326/4/2/024008.

Chester, M., Horvath, A., and Madanat, S. (2010). Comparison of life-cycle energy and emissions footprints of passenger transportation in metropolitan regions. *Atmospheric Environment*, *44*(8), 1071-1079. doi:10.1016/j.atmosenv.2009.12.012.

Clark, N. N., Vora, K. A., Gautam, M., Wayne, W. S., & Thompson, G. J. (2010). Expressing Cycles and Their Emissions on the Basis of Properties and Results from Other Cycles. Environ. Sci. Technol. 2010, 44, 5986–5992.

CMU GDI (Carnegie Mellon University Green Design Institute). (2008). Economic Input-Output Life Cycle Assessment (EIO-LCA), US 2002 Industry Benchmark model. Retrieved from: http://www.eiolca.net (Accessed October 20, 2015).

Cooney, G., Hawkins, T. R., and Marriott, J. (2013). Life Cycle Assessment of Diesel and Electric Public Transportation Buses. *Journal of Industrial Ecology*, *17*(5), 689-699. doi:10.1111/jiec.12024.

Cummins. (2015). Cummins Engines and Emissions Solutions. Retrieved from: http://www.cummins.com (Accessed July 13, 2015).

Davis, B. A. & Figliozzi, M. A. (2013). A methodology to evaluate the competitiveness of electric delivery trucks. Transportation Research Part E, 498-23. doi:10.1016/j.tre.2012.07.003.

Davis, S. C. & Diegel, S. W. (2015). Transportation Energy Data Book: Edition 34. Oak Ridge National Laboratory. August 2015.

Deal, A. L. (2012). What Set of Conditions Would Make the Business Case to Convert Heavy Trucks to Natural Gas? A Case Study. National Energy Policy Institute (NEPI). Retrieved from: http://www.tagnaturalgasinfo.com/uploads/1/2/2/3/12232668/natural_gas_for_heavy_trucks.pdf (Accessed December 22, 2014).

De Filippo, G., Marano, V., and Sioshansi, R. (2014). Simulation of an electric transportation system at The Ohio State University. *Applied Energy*, *113*1686-1691. doi:10.1016/j.apenergy.2013.09.011.

Delgado, O. F., Clark, N. N., and Thompson, G. J. (2011). Modeling transit bus fuel consumption on the basis of cycle properties. *Journal of the Air and Waste Management Association*, *61*(4), 443-452. doi:10.3155/1047-3289.61.4.443.

Delorme, A. and Karbowski, D. (2010). Impact of Advanced Technologies on Medium-Duty Trucks Fuel Efficiency. SAE Technical Paper 2010-01-1929, 2010, doi:10.4271/2010-01-1929.

DOE (Department of Energy). (2014). All-Electric Vehicles (EVs). Retrieved from: http://www.fueleconomy.gov/feg/evtech.shtml#end-notes (Accessed October 5, 2014).

Duran, A. and Walkowicz, K. (2013). A Statistical Characterization of School Bus Drive Cycles Collected via Onboard Logging Systems. SAE Int. J. Commer. Veh. 6(2):400-406, 2013, doi:10.4271/2013-01-2400.

Duran, A., Ragatz, A., Prohaska, R., Kelly, K., & Walkowicz, K. (2014). Characterization of in-use medium duty electric vehicle driving and charging behavior. 2014 IEEE International Electric Vehicle Conference (IEVC), 1. doi:10.1109/IEVC.2014.7056213.

Eaton. (2014). Eaton – Hybrid Power Systems. Retrieved from: http://www.eaton.com/Eaton/ProductsServices/Vehicle/Hybrid-Power-Systems/index.htm (Accessed January 12, 2014).

EIA (Energy Information Administration). (2015a). Monthly Energy Review. Retrieved from: http://www.eia.gov/totalenergy/data/monthly (Accessed November 1, 2015).

EIA (Energy Information Administration). (2015b). Annual Energy Outlook 2015. Retrieved from: http://www.eia.gov/forecasts/aeo (Accessed August 20, 2015).

EIA (Energy Information Administration). (2015c). Electricity Data. Retrieved from: http://www.eia.gov/electricity/data.cfm (Accessed September 12, 2015).

EPA (Environmental Protection Agency). (1993). Federal Test Procedure Review Project: Preliminary Technical Report. EPA 420-R-93-007.

EPA (Environmental Protection Agency). (2003). User's Guide to MOBILE6.1 and MOBILE6.2. EPA420-R-03-010.

EPA (Environmental Protection Agency). (2011). *Final Rulemaking to Establish Greenhouse Gas Emissions Standards and Fuel Efficiency Standards for Medium- and Heavy-Duty Engines and Vehicles. Regulatory Impact Analysis*. EPA-420-R-11-901. August 2011.

EPA (Environmental Protection Agency). (2012a). Proposed Exhaust Emission Rates for Compressed Natural Gas Transit Buses in MOVES2013. MSTRS MOVES Review Work Group. September 25, 2012. Retrieved from: http://www3.epa.gov/otaq/models/moves/documents/faca-meeting-sep2012/05-cng-buses.pdf (Accessed April 16, 2013).

EPA (Environmental Protection Agency). (2012b). MOVES Work Group: Meeting Summary. Mobile Sources Technical Review Subcommittee. Retrieved from: http://www.epa.gov/otaq/models/moves/documents/faca-meeting-sep2012/meeting-summary-sep-25-2012.pdf (Accessed October 20, 2013).

EPA (Environmental Protection Agency). (2012c). *Truck Carrier Partner 2.0.12 Tool. Technical Documentation. 2012 Data Year - United States Version*. EPA-420-B-13-003. January 2013.

EPA (Environmental Protection Agency). (2014a). Motor Vehicle Emission Simulator (MOVES). Retrieved from: http://www.epa.gov/otaq/models/moves/ (Accessed December 20, 2014).

EPA (U.S. Environmental Protection Agency). (2014b). EPA's Environmental Technology Verification Program (ETV). Retrieved from: https://archive.epa.gov/nrmrl/archive-etv/web/html/ (Accessed April 4, 2015).

EPA (Environmental Protection Agency). (2015a). National Emissions Inventory (NEI). Retrieved from: http://www3.epa.gov/ttnchie1/eiinformation.html (Accessed September 22, 2015).

EPA (Environmental Protection Agency). (2015b). *SmartWay*. Retrieved from: http://www3.epa.gov/smartway/ (Accessed October 4, 2015).

EPA (Environmental Protection Agency). (2015c). *Proposed Rulemaking for Greenhouse Gas Emissions and Fuel Efficiency Standards for Medium- and Heavy-Duty Engines and Vehicles–Phase 2*. *Draft Regulatory Impact Analysis*. EPA-420-D-15-900. June 2015.

EPA (Environmental Protection Agency). (2016a). Continuous Emissions Monitoring (CEM). Retrieved from: http://www.epa.gov/airmarkt/emissions/continuous-factsheet.html (accessed January 29, 2016).

EPA (Environmental Protection Agency). (2016b). The Emissions & Generation Resource Integrated Database (eGRID). Retrieved from: http://www.epa.gov/egrid (Accessed March 1, 2016).

Fairley, P. (2011). Electric Vehicles Finally Succeed? Technology Review, February, 2011. Retrieved from: http://www.technologyreview.com/energy/26946 (Accessed July 14, 2011).

Fan, T., Jaramillo, P., & Azevedo, I. L. (2015). Comparison of Life Cycle Greenhouse Gases from Natural Gas Pathways for Medium and Heavy-Duty Vehicles. Environmental Science & Technology, 49(12), 7123-7133. doi:10.1021/es5052759.

Federal Register. (2011). *Greenhouse Gas Emissions Standards and Fuel Efficiency Standards for Medium- and Heavy-Duty Engines and Vehicles; Final Rule*. Vol. 76, No. 179. September 15, 2011.

Federal Register. (2013). *Heavy-Duty Engine and Vehicle, and Nonroad Technical Amendments; Final Rule*. Vol. 78, No. 116. June 17, 2013.

Federal Register. (2015a). *Greenhouse Gas Emissions and Fuel Efficiency Standards for Medium- and Heavy-Duty Engines and Vehicles – Phase 2; Proposed Rule*. Vol. 80, No. 133. July 13, 2015.

Federal Register. (2015b). *Carbon Pollution Emission Guidelines for Existing Stationary Sources: Electric Utility Generating Units; Final Rule*. 40 CFR Part 60. RIN 2060-AR33. August 3, 2015.

FERC (Federal Energy Regulatory Commission). (2015). FERC Forms. Retreived from: http://www.ferc.gov/docs-filing/forms.asp (Accessed September 10, 2015).

FHWA (Federal Highway Administration). (2004). The Next Generation Simulation (NGSIM) Program. Department of Transportation. Retrieved from: http://ngsim-community.org/ (Accessed September 30, 2013).

FHWA (Federal Highway Administration). (2013). Handbook for Estimating Transportation Greenhouse Gases for Integration into the Planning Process. Report no.: FHWA-HEP-13-026.

Freightliner. (2014). Freightliner Product Literature. Retrieved from: http://www.freightlinertrucks.com/Multimedia/MediaLibrary/Trucks/ (Accessed December 29, 2013).

FTA (Federal Transit Administration). (2007). *Useful Life of Transit Buses and Vans*. Report No. FTA VA-26-7229-07.1.

FTA (Federal Transit Administration). (2012). *National Transit Database (NTD) – Revenue Vehicle Inventory*. Retrieved from: http://www.ntdprogram.gov/ntdprogram (accessed April 20, 2014).

FTA (Federal Transit Administration). (2013). *Transit Vehicle Emissions Program*. FTA Report No. 0048. August 2013.

Fumo, N., Mago, P. J., & Chamra, L. M. (2009). Emission operational strategy for combined cooling, heating, and power systems. *Applied Energy, 86*2344-2350. doi:10.1016/j.apenergy.2009.03.007.

Gaines, L., Stodolsky, F., & Cuenca, R. (1998). Life-Cycle Analysis for Heavy Vehicles. Argonne National Laboratory. 1998. Retrieved from: http://www.transportation.anl.gov/pdfs/TA/102.pdf (Accessed September 25, 2012).

Gibson, B. E. & Adamson, K. (2013). Emerging Battery Technologies. Navigant Consulting, Inc. Retrieved from: http://www.navigantresearch.com/research/emerging-battery-technologies (Accessed January 3, 2014).

Hauck M., Steinmann Z. J. N., Laurenzi I. J., Karuppiah R., and Muijbregts, M. A. (2014). How to quantify uncertainty and variability in life cycle assessment: the case of greenhouse gas emissions of gas power generation in the United States. Environ. Res. Lett. 9: 074005-07011.

Howarth, R. W., Santoro, R., & Ingraffea, A. (2011). Methane and the greenhouse-gas footprint of natural gas from shale formations. Climatic Change, 106(4), 679-690. doi:10.1007/s10584-011-0061-5.

Huai, T., Shah, S., Wayne Miller, J., Chernich, D., Ayala, A., & Younglove, T. (2006). Analysis of heavy-duty diesel truck activity and emissions data. Atmospheric Environment, 40(13), 2333-2344. doi:10.1016/j.atmosenv.2005.12.006.

Huijbregts, M. J. (1998). Application of Uncertainty and Variability in LCA: Part II: Dealing With Parameter Uncertainty and Uncertainty due to Choices in Life Cycle Assessment. *International Journal of Life Cycle Assessment*, *3*(6), 343-351.

ImagineMade. (2014). Advanced Vehicle Simulator (ADVISOR). Retrieved from: http://adv-vehiclesim.sourceforge.net/ (Accessed April 16, 2014). Originally developed by NREL; license once managed by Big Ladder Software; and now an open source project.

IPCC (Intergovernmental Panel on Climate Change). (2013). Fifth Assessment Report (AR5). Retrieved from: https://www.ipcc.ch (Accessed April 5, 2014).

James, J., Thomas, V. M., Pandit, A., & Crittenden, J. C. (2015). Environmental and Economic Impacts of Air-Cooled Microturbines for Combined Cooling, Heating, and Power (CCHP) Systems: A Case Study of 5 Building Types in the Atlanta Region. Submitted for Publication.

Jimenez, J. L. (1999). Understanding and Quantifying Motor Vehicle Emissions with Vehicle Specific Power and TILDAS Remote Sensing. PhD Dissertation. Department of Mechanical Engineering, Massachusetts Institute of Technology.

Karabasoglu, O., and Michalek, J. (2013). Influence of driving patterns on life cycle cost and emissions of hybrid and plug-in electric vehicle powertrains. *Energy Policy*, *60*445-461. doi:10.1016/j.enpol.2013.03.047.

Kavvadias, K., Tosios, A., & Maroulis, Z. (2010). Design of a combined heating, cooling and power system: Sizing, operation strategy selection and parametric analysis. *Energy Conversion and Management*, *51*833-845. doi:10.1016/j.enconman.2009.11.019.

KCM (King County Metro). (2011). Trolley Bus System Evaluation. Retrieved from: http://metro.kingcounty.gov/up/projects/trolleyevaluation.html (Accessed January 5, 2014).

Kennedy, D. J., Montgomery, D. C., Rollier, D. A., and Keats, J. B. (1997). Data Quality: Assessing Input Data Uncertainty in Life Cycle Assessment Inventory Models. *International Journal of Life Cycle Assessment*, *2*(4), 229-240.

Kenworth. (2014). Medium Duty Body Builder's Manual. Retrieved from: http://www.kenworth.com/trucks (Accessed November 11, 2013).

LaClair, T. (2012). Application of a Tractive Energy Analysis to Quantify the Benefits of Advanced Efficiency Technologies for Medium- and Heavy-Duty Trucks Using Characteristic Drive Cycle Data. SAE Int. J. Commer. Veh. 5(1):141-163, 2012, doi:10.4271/2012-01-0361.

LaClair, T. J., Gao, Z., Fu, J., Calcagno, J., Yun, J. (2014). Development of a Short-Duration Drive Cycle to Represent Long-Term Measured Drive Cycle Data for the Evaluation of Truck Efficiency Technologies in Class 8 Tractor-Trailers. The 93rd Transportation Research Board Annual Meeting.

Lajunen, A. (2014). Energy consumption and cost-benefit analysis of hybrid and electric city buses. *Transportation Research, Part C: Emerging Technologies*, *38*1-15. doi:10.1016/j.trc.2013.10.008.

Lascurain, B. (2008). Class-8 Heavy Truck Duty Cycle Project Final Report. Oak Ridge National Laboratory. ORNL/TM-2008/122.

Lascurain, M. B., Franzese, O., Capps, G., Siekmann, A., Thomas, N., LaClair, T., Barker, A., Knee, H. (2012). Medium Truck Duty Cycle Data from Real-World Driving Environments: Project Final Report. Oak Ridge National Laboratory. ORNL/TM-2012/240.

Lee, D.-Y., Thomas, V. M., & Brown, M. A. (2013). Electric Urban Delivery Trucks: Energy Use, Greenhouse Gas Emissions, and Cost-Effectiveness. Environmental Science & Technology, 47(14), 8022-8030. doi:10.1021/es400179w.

Li, L., Mu, H., Li, N., & Li, M. (2015). Analysis of the integrated performance and redundant energy of CCHP systems under different operation strategies. *Energy & Buildings*, *99* 231-242. doi:10.1016/j.enbuild.2015.04.030.

Lloyd, S. M., and Ries, R. (2007). Characterizing, Propagating, and Analyzing Uncertainty in Life-Cycle Assessment. *Journal of Industrial Ecology*, *11*(1), 161-179.

LTI (The Thomas D. Larson Pennsylvania Transportation Institute). (2013). Federal Transit Administration's new model bus' reliability and in-service performance testing program, mandated by the Surface Transportation and Uniform Relocation Assistance Act (STURAA) of 1987. Retrieved from: http://www.altoonabustest.com (accessed February 20, 2014).

Luxfer. (2013). Cylinders for Natural Gas Vehicles. Retrieved from: http://www.luxfercylinders.com (Accessed February 20, 2015).

Mago, P., & Chamra, L. (2009). Analysis and optimization of CCHP systems based on energy, economical, and environmental considerations. *Energy & Buildings*, *41* 1099-1106. doi:10.1016/j.enbuild.2009.05.014.

Mago, P. J., Fumo, N., & Chamra, L. M. (2009). Performance analysis of CCHP and CHP systems operating following the thermal and electric load. *International Journal of Energy Research*, *33*(9), 852-864. doi:10.1002/er.1526.

Mago, P. J., & Hueffed, A. K. (2010). Evaluation of a turbine driven CCHP system for large office buildings under different operating strategies. *Energy & Buildings*, *42* 1628-1636. doi:10.1016/j.enbuild.2010.04.005.

Mago, P. J., & Smith, A. D. (2012). Evaluation of the potential emissions reductions from the use of CHP systems in different commercial buildings. *Building & Environment*, *53*74. doi:10.1016/j.buildenv.2012.01.006.

Magri, G., Di Perna, C., & Serenelli, G. (2012). Analysis of electric and thermal seasonal performances of a residential microCHP unit. *Applied Thermal Engineering*, *36*193-201. doi:10.1016/j.applthermaleng.2011.11.025.

Marriott, J., & Matthews, H. S. (2005). Environmental effects of interstate power trading on electricity consumption mixes. Environmental Science & Technology, 39(22), 8584-8590.

Masanet E., Chang Y., Gopal A. R., Larsen P., Morrow W. R., Sathre R., Shehabi A., and Zhai. P. (2013). Life-Cycle Assessment of Electric Power Systems. *Annual Review of Environment and Resources* 38: 107-136.

McKenzie, E. C., and Durango-Cohen, P. L. (2012). Environmental life-cycle assessment of transit buses with alternative fuel technology. *Transportation Research Part D: Transport and Environment*, *17*(1), 39-47. doi:10.1016/j.trd.2011.09.008.

Muller, N. (2011). Air Pollution Emission Experiments and Policy analysis (APEEP) Model. Retrieved from: https://sites.google.com/site/nickmullershomepage/home/ap2-apeep-model-2 (Accessed September 1, 2015).

Naimaster, E., & Sleiti, A. (2013). Potential of SOFC CHP systems for energy-efficient commercial buildings. *Energy & Buildings*, *61* 153-160. doi:10.1016/j.enbuild.2012.09.045.

NRC (National Research Council). (2010). Transitions to Alternative Transportation Technologies: Plug-in Hybrid Electric Vehicles.

NREL (National Renewable Energy Laboratory). (2014a). TSDC. Database.

NREL (National Renewable Energy Laboratory). (2014b). Contribution of Road Grade to the Energy Use of Modern Automobiles across Large Datasets of Real-World Drive Cycles. Retrieved from: http://www.nrel.gov/docs/fy14osti/61108.pdf (accessed June 20, 2014).

NREL (National Renewable Energy Laboratory). (2015). System Advisor Model (SAM). Retrieved from: https://sam.nrel.gov/ (Accessed July 30, 2015).

Nellums, R., Steffen, J., & Naito, S. (2003). Class 4 Hybrid Electric Truck for Pick Up and Delivery Applications. SAE Technical Paper 2003-01-3368, 2003, doi:10.4271/2003-01-3368.

Noel, G., J. & Wayson, R. (2012). MOVES2010a Regional Level Sensitivity Analysis. OMB No. 0704-0188. Volpe National Transportation Systems Center. Federal Highway Administration. US DOT.

Nykvist, B., & Nilsson, M. (2015). Rapidly falling costs of battery packs for electric vehicles. *Nature Climate Change*, *5*(4), 329-332. doi:10.1038/nclimate2564.

O'Keefe, M., Simpson, A., Kelly, K., & Pedersen, D. (2007). Duty Cycle Characterization and Evaluation Towards Heavy Hybrid Vehicle Applications. SAE Technical Paper 2007-01-0302, 2007, doi:10.4271/2007-01-0302.

OpenEI. (2016). Open Energy Information (OpenEI). Retrieved from: http://en.openei.org/wiki/Main_Page (Accessed June 5, 2015).

Proterra LLC. (2009). Fast Charge Battery Electric Transit Buses. *ARB ZEB Workshop*. May 2009.

Pruitt, K. A., Braun, R. J., & Newman, A. M. (2013). Establishing conditions for the economic viability of fuel cell-based, combined heat and power distributed generation systems. *Applied Energy*, *111*904-920. doi:10.1016/j.apenergy.2013.06.025.

Pusenius, K., Lettenmeier, M., and Saari, A. (2005). Natural Resource Consumption of Finnish Road Transport (Road MIPS). The Finnish Association for Nature Conservation. Retrieved from: http://www.lvm.fi/fileserver/Julkaisuja%2054_2005.pdf (accessed October 7, 2012).

Raykin, L., Roorda, M., and MacLean, H. (2012a). Impacts of driving patterns on tank-to-wheel energy use of plug-in hybrid electric vehicles. *Transportation Research, Part D (Transport and Environment), 17*(3), 243-250. doi:10.1016/j.trd.2011.12.002.

Raykin, L., MacLean, H. L., & Roorda, M. J. (2012b). Implications of driving patterns on well-to-wheel performance of plug-in hybrid electric vehicles. *Environmental Science & Technology, 46*(11), 6363-6370. doi:10.1021/es203981a.

Reap, J., Roman F., Duncan S., and Bras B. (2008a). A survey of unresolved problems in life cycle assessment. Part 1: Goal and Scope and Inventory Analysis. Int. J. Life Cycle Assessment 13 (5): 290-300.

Reap, J., Roman F., Duncan S., and Bras B. (2008b). A survey of unresolved problems in life cycle assessment. Part 2: Impact Assessment and Interpretation. Int. J. Life Cycle Assessment 13 (5): 374-388.

Sankey, P., Clark, D. T., & Micheloto, S. (2011). The End of the Oil Age. 2011 and Beyond: A Reality. Deutsche Bank Securities Inc., December 22, 2010. Retrieved from: http://gm.db.com (Accessed August 20, 2012).

Schmalstieg, J., Ka¨bitz, S., Ecker, M., and Sauer, D. (2014). A holistic aging model for Li(NiMnCo)O2 based 18650 lithium-ion batteries. *Journal of Power Sources, 257*325-334. doi:10.1016/j.jpowsour.2014.02.012.

Schwietzke, S., Griffin, W. M., Matthews, H. S., & Bruhwiler, L. P. (2014). Natural gas fugitive emissions rates constrained by global atmospheric methane and ethane. Environmental Science & Technology, 48(14), 7714-7722. doi:10.1021/es501204c.

SEV (Smith Electric Vehicles). (2014). Smith Vehicles – Models and Configurations. Retrieved from: http://www.smithelectric.com/ (Accessed August 20, 2014).

Shaneb, O., Coates, G., & Taylor, P. (2011). Sizing of residential μCHP systems. *Energy & Buildings, 43*(8), 1991-2001. doi:10.1016/j.enbuild.2011.04.005.

Shimizu, T., Kikuchi, Y., Sugiyama, H., & Hirao, M. (2015). Design method for a local energy cooperative network using distributed energy technologies. *Applied Energy, 154*781-793. doi:10.1016/j.apenergy.2015.05.032.

Siler-Evans, K., Azevedo, I. L., & Morgan, M. G. (2012). Marginal emissions factors for the U.S. electricity system. Environmental Science & Technology, 46(9), 4742-4748. doi:10.1021/es300145v.

Staffell, I., Ingram, A., & Kendall, K. (2012). Energy and carbon payback times for solid oxide fuel cell based domestic CHP. *International Journal of Hydrogen Energy*, *37*(3), 2509-2523. doi:10.1016/j.ijhydene.2011.10.060.

Steinmann, Z. N., Venkatesh, A., Hauck, M., Schipper, A. M., Karuppiah, R., Laurenzi, I. J., & Huijbregts, M. J. (2014). How to address data gaps in life cycle inventories: a case study on estimating CO2 emissions from coal-fired electricity plants on a global scale. *Environmental Science & Technology*, *48*(9), 5282-5289. doi:10.1021/es500757p.

Taptich, M. N., and Horvath, A. (2014). Bias of averages in life-cycle footprinting of infrastructure: truck and bus case studies. *Environmental Science & Technology*, *48*(22), 13045-13052. doi:10.1021/es503356c.

TeymouriHamzehkolaei, F., & Sattari, S. (2011). Technical and economic feasibility study of using Micro CHP in the different climate zones of Iran. *Energy*, *36*(8), 4790-4798. doi:10.1016/j.energy.2011.05.013.

The White House. (2013). Technical Support Document: Technical Update of the Social Cost of Carbon for Regulatory Impact Analysis under Executive Order 12866. Interagency Working Group on Social Cost of Carbon, United States Government. Retrieved from: http://www.whitehouse.gov/sites/default/files/omb/assets/inforeg/technical-update-social-cost-ofcarbon-for-regulator-impact-analysis.pdf (Accessed July 27, 2014).

Thiruvengadam, A., Besch, M. C., Thiruvengadam, P., Pradhan, S., Carder, D., Kappanna, H., Gautam, M., Oshinuga, A., Hogo, H., & Miyasato, M. (2015). Emission Rates of Regulated Pollutants from Current Technology Heavy-Duty Diesel and Natural Gas Goods Movement Vehicles. Environmental Science & Technology, 49(8), 5236-5244. doi:10.1021/acs.est.5b00943.

Venkatesh, A., Jaramillo, P., Griffin, W. M., and Matthews, H. S. (2011a). Uncertainty Analysis of Life Cycle Greenhouse Gas Emissions from Petroleum-Based Fuels and Impacts on Low Carbon Fuel Policies. *Environmental Science & Technology*, *45*(1), 125-131. doi:10.1021/es102498a.

Venkatesh, A., Jaramillo, P., Griffin, W. M., and Matthews, H. S. (2011b). Uncertainty in Life Cycle Greenhouse Gas Emissions from United States Natural Gas End-Uses and its Effects on Policy. *Environmental Science & Technology*, *45*(19), 8182-8189. doi:10.1021/es200930h.

Walkowicz, K., Kelly, K., Duran, A., & Burton, E. (2014). Fleet DNA Project Data. National Renewable Energy Laboratory. http://www.nrel.gov/fleetdna.

Wang, M., Huo, H., & Arora, S. (2011). Methods of dealing with co-products of biofuels in life-cycle analysis and consequent results within the U.S. context. Energy Policy, 39 (Sustainability of biofuels), 5726-5736. doi:10.1016/j.enpol.2010.03.052.

Watson, H., Milkins, E., Preston, M., Chittleborough, C. Alimoradian, B. (1983). Predicting Fuel Consumption and Emissions-Transferring Chassis Dynamometer Results to Real Driving Conditions. SAE Technical Paper 830435, 1983, doi:10.4271/830435.

Wayne, W. S., Clark, N. N., Nine, R. D., & Elefante, D. (2004). A Comparison of Emissions and Fuel Economy from Hybrid-Electric and Conventional-Drive Transit Buses. Energy and Fuels, 18257-270.

Wayne, W. S., Perhinschi, M. M., Clark, N. N., Tamayo, S. S., and Tu, J. J. (2011). Integrated bus information system. *Transportation Research Record*, 1 December 2011, (2233):1-10. doi:10.3141/2233-01.

Woody, T. (2013). From China to Los Angeles, Taking the Electric Bus. New York Times. October 29, 2013. Retrieved from: http://www.nytimes.com/2013/10/30/automobiles/from-china-to-los-angeles-taking-the-electric-bus.html?_r=0 (accessed September 10, 2014).

Wu, Q., Ren, H., Gao, W., & Ren, J. (2014). Multi-criteria assessment of combined cooling, heating and power systems located in different regions in Japan. *Applied Thermal Engineering*, *73*(1), 660-670. doi:10.1016/j.applthermaleng.2014.08.020.

WVU (West Virginia University). (2014). Integrated Bus Information System (IBIS): http://ibis.wvu.edu (Accessed December 15, 2014).

Yoon, S., Collins, J., Thiruvengadam, A., Gautam, M., Herner, J., & Ayala, A. (2013). Criteria pollutant and greenhouse gas emissions from CNG transit buses equipped

with three-way catalysts compared to lean-burn engines and oxidation catalyst technologies. Journal of the Air & Waste Management Association (1995), 63(8), 926-933.

Yu, Q., and Li, T. (2014). Evaluation of bus emissions generated near bus stops. *Atmospheric Environment, 85*195-203. doi:10.1016/j.atmosenv.2013.12.020.